MULTIPARAMETER SENSITIVITY OF LINEAR TIME-INVARIANT NETWORKS

MULTIPARAMETER SENSITIVITY OF LINEAR TIME-INVARIANT NETWORKS

by

WALTER J. BUTLER, B.A., B.A.I. (DUBLIN)

A Thesis

Submitted to the School of Graduate Studies

in Partial Fulfilment of the Requirements

for the Degree

Doctor of Philosophy

McMaster University

March 1970

DOCTOR OF PHILOSOPHY (1970)
(Electrical Engineering)

McMASTER UNIVERSITY
Hamilton, Ontario

TITLE: Multiparameter Sensitivity of Linear Time-invariant Networks

AUTHOR: Walter J. Butler, B.A. (Dublin)
B.A.I. (Dublin)

SUPERVISOR: Professor S. S. Haykim

NUMBER OF PAGES: 212, xv

SCOPE AND CONTENTS:

The realization of inductorless filters by means of RC-gyrator structures has been investigated, and the sensitivity of their response characteristics with respect to supply voltage variations has been measured. A critical appraisal is made of the various multiparameter sensitivity functions which have already been proposed in the literature, and the methods by which these sensitivity criteria may be computed are surveyed. A new index of performance, by which the multiparameter sensitivity of a linear, time-invariant network may be evaluated, is proposed. Furthermore, a new method of computing sensitivity indices is described and is shown to be highly efficient from a computational point of view. The index has been used to investigate the sensitivity performance of a wide range of passive and active filter structures. It has also been used to generate a so-called "optimum tolerance set" for the elements of such filters and the effect of employing these optimum tolerance sets has been investigated.

The index of performance and the concept of the optimum tolerance set is extended to the case of RC active filters. A "two-level" optimization procedure is proposed, whereby an optimum nominal element value set may be combined with the corresponding optimum tolerance set to obtain a marked improvement in the sensitivity performance of the network. Finally, the synthesis of a highly selective RC-active filter is considered, and it is shown how an optimal structure and tolerance set can be obtained for such a network.

ACKNOWLEDGEMENTS

The author particularly wishes to thank Dr. S. S. Haykim for his helpful advice, criticism and encouragement, and for the many useful suggestions received during the course of this work. The author is also grateful to Dr. J. Shewchun and Dr. N. K. Sinha, the other two members of his Ph.D. Supervisory Committee, and to Dr. J. W. Bandler, who have helped considerably by way of valuable and stimulating discussions. He is also indebted to Mr. V.A.K. Temple, who introduced him to the use of the digital computer and whose timely help facilitated the early computational effort.

Finally, he is indebted to McMaster University for a Faculty Fellowship, and to Standard Cables and Telephones Ltd. for an honorarium received during the course of this work.

ABSTRACT

The realization of inductorless filters by means of RC-gyrator structures has been investigated. A procedure has been proposed whereby a conventional LC-ladder filter may be transformed into an inductorless filter which uses capacitors and grounded three-terminal gyrators. The predistortion technique has been used to compensate for the effect of the parasitics associated with a practical gyrator circuit. The procedure has been used to construct low-pass and asymmetric band-pass filters and close agreement with theory is reported. The sensitivity of the response of these networks with respect to variations in supply voltages has been measured and the results indicate that the filters are remarkably insensitive to such variations.

In order to investigate the effect of simultaneous variations in several or all component parameters of such networks, a new multiparameter sensitivity index of performance has been proposed for use with linear, time-invariant networks. An algorithm has been devised for computing this index. The algorithm derives partial derivatives of network functions with respect to component network parameters exactly and efficiently. It also avoids the need for repeated analyses of adjoint or auxiliary networks and may be used to evaluate n^{th}-order partial derivatives and corresponding sensitivity functions. The index of performance has been

used to evaluate the effects of varying the order of complexity, passband ripple, dissipation and source/load resistance ratio upon the overall sensitivity performance of low-pass LC-ladder filters.

A procedure has been developed which determines for a given filter, an "optimum tolerance set" which ensures that the various element changes contribute equally to the total change in the filter performance. The effect of using such optimum tolerance sets has been investigated, and it is shown that such use leads to a considerable improvement in the sensitivity performance of a network.

The procedure has also been used to obtain optimum tolerance sets for the variations in pole-zero locations of various low-pass filters. This approach is particularly suitable for the synthesis of active networks where higher-order filters may be realized by a cascade of second-order sections isolated by buffer amplifiers. In the synthesis of such second-order sections, optimal search techniques have been used in conjunction with the index of performance to obtain optimum nominal element value sets for a particular configuration. This "two-level" optimization technique is then shown to be highly effective in the optimal design of a highly-selective RC-active filter.

TABLE OF CONTENTS

		Page
CHAPTER I:	INTRODUCTION	1
CHAPTER II:	RC-GYRATOR FILTERS	5
2.1	Introduction	5
2.2	The Gyrator and its Practical Implementation	10
	2.2.1 The Y-model Gyrator	10
	2.2.2 The Z-model Gyrator	15
2.3	RC-Gyrator Ladder Filters	24
	2.3.1 Low-pass Filter	28
	2.3.2 Bandpass Filter	35
	2.3.3 Sensitivity Considerations	39
2.4	Conclusion	44
CHAPTER III:	THE MULTIPARAMETER SENSITIVITY PROBLEM	46
3.1	Introduction	46
3.2	Multiparameter Sensitivity Functions	48
3.3	Properties of Sensitivity Functions	51
3.4	Continuously Equivalent Network Approach to Optimal Synthesis	55
3.5	Methods for Computing Sensitivity Functions	57
	3.5.1 The Feedback Theory Approach	57
	3.5.2 The Bilinear Theorem Approach	59
	3.5.3 Approaches Based on the use of a Related Network	63

Page

	3.5.4 Connection Between the Feedback Theory and Director-Rohrer Approaches	82
	3.5.5 Other Procedures	88
3.6	Conclusion	89
CHAPTER IV:	THE MULTIPARAMETER SENSITIVITY INDEX OF PERFORMANCE	91
4.1	Introduction	91
4.2	A New Multiparameter Sensitivity Index of Performance	92
4.3	Choice of Weighting Function $\psi(\omega)$	99
4.4	Optimum Tolerance Sets	104
4.5	Conclusion	105
CHAPTER V:	COMPUTATIONAL PROCEDURES	106
5.1	Introduction	106
5.2	The Computational Algorithm	107
5.3	A Coding Technique for Reduced Storage	113
5.4	Efficiency of Computation, a Quantitative Comparison	114
5.5	Computer Programming	118
5.6	Conclusion	122
CHAPTER VI;	A MULTIPARAMETER SENSITIVITY STUDY OF LC LADDER NETWORKS	123
6.1	Introduction	123
6.2	Standard LC Ladder Filters	125
6.3	Factors Affecting the Index of Performance	125

Page

6.4 Optimum Tolerance Sets ---------- 127

6.5 Comparison of Sensitivity Performance of Networks with Optimum and Uniform Tolerance Sets ------ 134

6.6 Conclusion ---------- 146

CHAPTER VII: A MULTIPARAMETER SENSITIVITY STUDY OF RC-ACTIVE NETWORKS ---------- 147

7.1 Introduction ---------- 147

7.2 Pole-zero Index, P_{pz} ---------- 149

7.3 Computational Results ---------- 150

7.4 Sensitivity Analysis of Typical RC-active Second-order Sections ---------- 156

7.5 A New RC-active Second-order Section --------- 156

7.6 Sensitivity Analysis and Optimal Synthesis of the Network ---------- 164

7.6.1 Analysis of the Network ---------- 164

7.6.2 Synthesis of the Network ---------- 165

7.7 The Optimal Search Routine ---------- 172

7.8 Sensitivity Performance of Optimized Networks - 175

7.8.1 Optimization of Second-order Butterworth Section ---------- 175

7.8.2 Statistical Analysis of Errors of Optimized and Non-optimized Versions of the Filter ---------- 179

7.8.3 Other Optimized Networks ---------- 181

7.9 A "Two-level" Optimization Procedure --------- 183

7.10 Design of a Highly-selective RC-active Filter - 183

Page

CHAPTER VIII: CONCLUSIONS ---------- 197

APPENDIX "A" SENSITIVITY ANALYSIS BASED ON THE POLE-SENSITIVITY FUNCTION ---------- 199

APPENDIX "B" DESIGN OF TENTH-ORDER RC-ACTIVE FILTER ------- 203

REFERENCES ---------- 207

FIGURE CAPTIONS

Figure		Page
2.1	(a) Ideal NIC terminated with load impedance Z_L --	8
	(b) Ideal gyrator, terminated with load impedance Z_L ----------	8
2.2	"Y-model" representation of gyrator ----------	12
2.3	Gyrator realization: (a) Forward transmission ---	13
	(b) Reverse transmission ---	13
2.4	Three-transistor gyrator ----------	14
2.5	Improved version of gyrator ----------	16
2.6	Gyrator containing field-effect transistors -------	17
2.7	"Z-model" representation of gyrator ----------	19
2.8	Equivalent circuit of capacitively-terminated lossy gyrator ----------	21
2.9	Circuit diagram for Z-model gyrator ----------	23
2.10	Z-model gyrator response characteristic ----------	25
2.11	Low-pass filter; gyrator-capacitor equivalent circuit	27
2.12	High-pass filter; gyrator-capacitor equivalent circuit	29
2.13	Asymmetric bandpass filter; gyrator-capacitor equivalent circuit ----------	30
2.14	RC-gyrator equivalent circuit for low-pass LC-ladder filter ----------	32
2.15	RC-gyrator low-pass filter; circuit diagram -------	34

Figure		Page

2.16	RC-gyrator low-pass filter response ----------	36
2.17	Asymmetric bandpass filter ----------	38
2.18	Asymmetric bandpass filter; circuit diagram -------	40
2.19	Asymmetric bandpass filter response ----------	41
2.20	Asymmetric bandpass filter; sensitivity to supply voltage variation ----------	43
3.1	Bilinear theorem approach; Parker's procedure -----	60
3.2	Network for Example 3.1 ----------	62
3.3	Leeds' procedure, the jth typical branch ----------	64
3.4	Leeds' auxiliary network for Example 3.2 ----------	70
3.5	Director and Rohrer's adjoint network for Example 3.3	79
3.6	Original and adjoint networks for Example 3.4 -----	81
3.7	Original network, N, with a voltage-controlled current-source singled out for special consideration	83
3.8	The adjoint network, $\hat{N}$ ----------	84
4.1	Nominal and perturbed response characteristics of hypothetical networks ----------	95
4.2	Integrand $\hat{E}$ for second-order, Butterworth, passive filters ----------	101
4.3	Integrand $\hat{E}$ for second-order RC-active filters ----	102
4.4	Integrand for index of the $\sum_i \lvert S^T_{x_i} \rvert^2$ type ----------	103
5.1	Network used in optimization procedure ----------	115
5.2	Comparison of computation efficiencies ----------	117
5.3	Flow-chart for network characterization operation --	119

Figure		Page
5.4	Flow-chart representation of the procedure used to compute the index P_1	120
5.5	Flow-chart representation of procedure used to obtain optimum tolerance sets	121
6.1	Doubly terminated network	124
6.2	Variation of index P_1 with order of filter	126
6.3	Variation of index P_1 with magnitude of passband ripple	128
6.4	Effect of dissipation on index P_1	129
6.5	Effect of varying source/load resistance ratio on index P_1 for odd-ordered filters	130
6.6	Effect of varying source/load resistance ratio for even-order filters	131
6.7	Optimum tolerance set for a fifth-order Butterworth filter with $R_{SL} = 1$	132
6.8	Optimum tolerance set for a ninth-order Butterworth filter with $R_{SL} = 1$	133
6.9	Optimum tolerance set for a seventh-order Chebyshev filter, 1/4 dB ripple, with $R_{SL} = 1/3$	135
7.1	Cascade synthesis	148
7.2	Variation of index P_{pz} with order of filter for Butterworth filters	151
7.3	Variation of index P_{pz} with magnitude of passband ripple	152
7.4	Optimum migration areas for a tenth-order Butterworth filter	153
7.5	RC-NIC second-order low-pass filter	157
7.6	RC-gyrator second-order low-pass filter	158

Figure		Page

7.7	RC-active second-order low-pass filter employing one operational amplifier ----------	159
7.8	RC-active second-order low-pass filter employing one operational amplifier ----------	160
7.9	RC-active second-order low-pass filter employing three operational amplifiers ----------	161
7.10	Sensitivity performance of various RC-active filters	162
7.11	RC-active filter employing a fixed-gain amplifier --	163
7.12	Variation of the index P_1 with ζ for the network of Figure 7.11 ----------	168
7.13	Constrained search, two-parameter problem ---------	170
7.14	Flow-chart representation of the optimal search routine ----------	174
7.15	Effect of optimization; second-order Butterworth RC-active filter ----------	176
7.16	Sensitivity performance of optimized and non-optimized versions of RC-active filter with second-order Butterworth response ----------	177
7.17	Standard deviation of errors in network response --	180
7.18	Sensitivity performance of RC-active filter with ζ = 0.9 (20% tolerance on all elements) ----------	184
7.19	Sensitivity performance of RC-active filter with ζ = 0.6 (20% tolerance on all parameters) --------	185
7.20	Sensitivity performance of RC-active filter with ζ = 0.3 (20% tolerance on all parameters) ---------	186
7.21	Results obtained when optimization routine was applied to network synthesized in Appendix "A" ----	187
7.22	Improvement obtained by use of optimal synthesis technique for different values of relative damping factor ζ ----------	188
7.23	Improvement obtained through use of "two-level" optimization procedure ----------	191

Figure		Page
7.24	Exploded view of Figure 7.22 with linear scales ----	192
7.25	Sensitivity performance of tenth-order RC-active filter ----------	196

CHAPTER I

INTRODUCTION

The sensitivity problem is one which has been receiving much attention both in control and network theory in recent years. The problem is usually expressed in terms of a sensitivity function (e.g., pole-zero sensitivity) or index of performance which defines the influence of a variation in one or more network parameters on the performance of the network. The sensitivity criterion thus chosen is used to obtain an optimum design by indicating an optimum choice of realizable network structure, or the element values for a less sensitive structure.

In network theory, the early sensitivity studies were concerned with a single variable, such as the sensitivity of some network function with respect to a particular parameter. However, with the increased use of the digital computer as a design tool, we are now able to tackle the more complex problem of evaluating the sensitivity of a network to simultaneous variations in a multitude of network parameters. Also, the advent of integrated and other micro-electronic circuitry has brought the multiparameter sensitivity problem into further prominence, since, with such networks, we can no longer call for close tolerances indiscriminately, nor can we expect a high degree of parameter constancy even from passive elements.

In this thesis, some new concepts and ideas are introduced and are used to investigate and optimize the multiparameter sensitivity performance of a wide range of LC-passive and RC-active filter structures.

(1) In Chapter II, the use of gyrators in the synthesis of inductorless filters is considered, and the sensitivity of several such RC-gyrator structures to variations in supply voltages is investigated. It is shown that these networks are particularly insensitive to such perturbations. This result was not unexpected, as the gyrators which were used were specifically designed to be practically independent of variations in the active parameters. Clearly, however, this type of sensitivity measure is of somewhat limited use in a practical situation, where, for example, we might wish to realize an RC-gyrator filter in integrated form. In such a situation, we would be concerned with the sensitivity of the network response to simultaneous variations in some or all of the network parameters It was, therefore, considered necessary to define a multiparameter sensitivity index of performance by which a more meaningful measure of the sensitivity performance of linear time-invariant networks (in general) might be obtained.

(2) In Chapter III, the sensitivity problem in network theory is surveyed in some detail, with emphasis being placed on multiparameter sensitivity. During the course of this survey, the various multiparameter sensitivity criteria which have already been proposed in the literature, and the methods by which such criteria may be computed, are critically appraised, and their inherent limitations are discussed.

(3) In Chapter IV, a new multiparameter sensitivity index of performance for use with linear, time-invariant networks is proposed, and a procedure for determining a so-called "optimum tolerance set" for a given network is described. In Chapter V, the problem of computing the index of performance is discussed, and a new computational procedure is described. The procedure is shown to be highly efficient with respect to computer time and storage requirements.

(4) The index of performance has been used to investigate the dependence of the sensitivity performance of low-pass LC-ladder filters on the order of complexity, the magnitude of the passband ripple, the amount of dissipation and the source/load resistance ratio of such networks. Optimum tolerance sets have been obtained for a number of networks, and the improvement in sensitivity performance obtained through use of these optimum tolerance sets has been investigated. In Chapter VI, the computational techniques used to undertake these investigations and the results obtained are discussed in detail.

(5) In Chapter VII, the index of performance and the concept of the optimum tolerance set is extended to the case of active filters. In the case of such filters, the second-order section is of particular importance as higher order networks may be realized by a cascade of a number of such sections. The index of performance has been used to evaluate the multiparameter sensitivity performance of several alternative second-order sections thus facilitating the choice of the particular section to be used. It has also been used, in conjunction with optimal search techniques, to obtain the optimum element value set for the chosen section, the optimum tolerance set for such optimum nominal set then being obtained.

Finally, the optimum tolerance sets for the various second-order sections thus obtained are related to each other by defining the variables of the overall network to be its pole coordinates in the complex frequency plane. The optimum tolerance set for such pole coordinates is then obtained. This set, in defining the limits of pole migration for each pole relative to the others, may then be used to obtain the absolute value of the tolerance on each element of the entire network.

CHAPTER II

RC-GYRATOR FILTERS

2.1 Introduction:

The classical network synthesis problem involves two steps: (i) the approximation problem, and, (ii) the realization problem. The approximation problem is one of deriving an approximating function which minimizes the error between itself and the desired response function over a band of frequencies, while at the same time satisfying certain realizability conditions. Having determined such a function, we may then proceed to realize the network in a suitable form. In the case of passive networks, many suitable synthesis procedures have been developed over the years. In particular, we have the very powerful techniques of Foster, Cauer, Brune, Bode and Darlington for the classical synthesis of networks containing lumped, linear, finite, passive and bilateral elements.

Due to the accelerated growth of solid-state technology since the early 1950's, the interest in filter theory has shifted significantly from the area of passive filters to that of RC-active filters, i.e., filter structures which use resistors, capacitors and active devices only. One advantage of this type of structure is that the need for inductors, which are less nearly ideal than are resistors and capacitors, and which become extremely bulky at very low frequencies, is eliminated. Furthermore, the

recent advent of thin-film and integrated circuit methods of microminiaturization has generated a real need for frequency selective networks which do not require inductors, as it has been found that the quality of an inductor deteriorates rapidly with decreasing volume.

In the case of a network structure consisting of resistors and capacitors only, the natural frequencies of the network are restricted to lie exclusively on the negative real axis of the complex frequency plane. This, therefore, means that in the case of a passive RC filter, the poles of the transfer function, which are the natural frequencies of the network, can only occur on the negative real axis. This restriction seriously limits the degree of selectivity that can be obtained from such networks. However, by including one or more active elements in the network, it is possible to shift these poles anywhere in the left half of the complex frequency plane, and thus realize the same degree of selectivity that is obtainable from an LC filter.

Significant contributions to the theory of active network synthesis have been made by Linvill, Yanagisawa, Sandberg, Kinarawala, Horowitz and Calahan, to name but a few. The most commonly used RC-active synthesis procedures are based on the partitioning of the network function of interest into one of two forms:

(i) Positive RC-negative RC partitioning in which the numerator and/or denominator of the network function are formed by the sum of positive and negative RC immittances, and in which a negative impedance converter is used to implement the subtraction process. A negative impedance converter (NIC), in its ideal form, is defined as a two-port network for which the input impedance at either port is proportional to the negative of the

impedance connected across the other port. For example, if an ideal NIC, with conversion ratio k, is terminated with an impedance Z_L as depicted in Figure 2.1(a), then the impedance looking into the input terminals of the NIC is given by

$$Z_{in} = -kZ_L \tag{2.1}$$

The conversion ratio, k, is usually assigned a nominal value of unity.

(ii) Positive RC-positive RL partitioning, in which the numerator and/or denominator are formed by the sum of positive RC and positive RL immittances. In this case, a gyrator terminated with a suitable RC network may be used to implement the RL immittance. A gyrator in its ideal form is characterized by the voltage-current relations

$$V_1 = -rI_2$$
$$V_2 = rI_1$$

where r is the gyration resistance. Thus, the impedance measured, looking into either port of a gyrator is proportional to the impedance connected across the other port. For example, if an ideal gyrator is termined with an impedance Z_L, as depicted in Figure 2.1(b), then the impedance looking into the input terminals is given by

$$Z_{in} = \frac{r^2}{Z_L} \tag{2.2}$$

Thus, an ideal gyrator, terminated with a capacitance C, is equivalent to an inductance with a value of r^2C.

In the early sensitivity studies of RC-active filters, the network sensitivity was usually defined in terms of the pole-sensitivity function, $S_x^{p_i}$, defined by

$$S_x^{p_i} = \frac{dp_i}{dx/x} \tag{2.3}$$

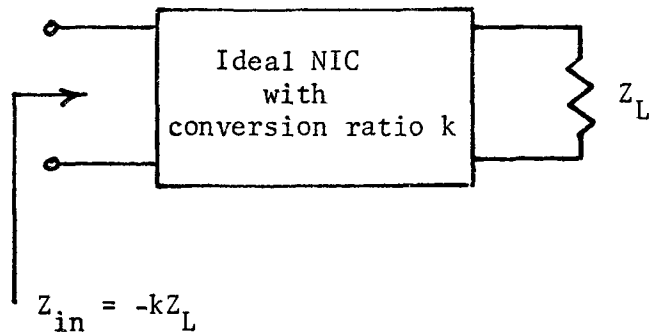

(a)

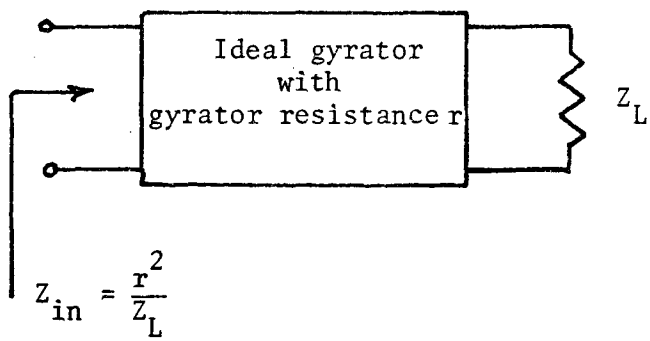

(b)

Figure 2.1: (a) Ideal NIC terminated with load impedance Z_L

(b) Ideal gyrator terminated with load impedance Z_L

where x is the variable parameter of interest. It can be shown that when the characteristic polynomial of the network contains two or more pairs of complex conjugate roots, then terms of the form $(s_i - s_j)$, $i \neq j$, will appear in the denominator of each pole sensitivity function. Hence, should the separation between the various poles become small, the pole-sensitivity of the network would become so inordinately large that a practical realization of the filter using a single RC-active section would not be feasible. Consequently, we find that when a network function has more than one pair of complex-conjugate poles, it is often realized as a cascade of second-order sections suitably isolated by means of buffer amplifiers where necessary. For this reason, the second-order section is of fundamental importance in the synthesis of RC-active filters, and the choice of structure for its implementation warrants careful consideration.

Such a choice will be based on several factors, e.g., economy of components, suitability for integration, and, of course, sensitivity considerations. The relative insensitivity of a gyrator filter is a characteristic which has been observed by several authors[1,2]. In the first place, negative feedback is employed in the realization of a gyrator, whereas in the case of a NIC, positive feedback is used. We would therefore expect the gyrator to be the less sensitive structure. Secondly, a synthesis procedure which is based on the addition of functions (as in the case of a positive RC-positive RL decomposition) is obviously less sensitive to parameter variation than is one which is based on the difference of two functions (as is the case in positive RC-negative RC decompositions). Furthermore, Calahan[1] has shown that regardless of the degree of the polynomial being decomposed, whenever an RC-RL decomposition

is possible at all, such a decomposition can be found which results in a lower pole-sensitivity than any RC-NIC decomposition.

In the case of a second-order transfer function, with zeros at infinity, an RC-RL decomposition always exists. We may therefore conclude that in the case of an active-RC filter which is to be realized as a cascade of such second-order sections, an RC-gyrator structure appears most attractive from the sensitivity point of view. As a first step in the investigation of the sensitivity of a wide range of linear time-invariant networks, both to active and passive parameter variations, a number of RC-gyrator filters were constructed and the sensitivity of their response characteristics to supply voltage variations was measured.

2.2 The Gyrator and its Practical Implementation:

2.2.1 The Y-model gyrator

The practical realization of a gyrator may begin with the decomposition of the admittance matrix, as shown by[3,4,5]

$$\mathbf{Y} = \begin{bmatrix} 0 & -g_{12} \\ g_{21} & 0 \end{bmatrix} = \begin{bmatrix} 0 & 0 \\ g_{21} & 0 \end{bmatrix} + \begin{bmatrix} 0 & -g_{12} \\ 0 & 0 \end{bmatrix} \tag{2.4}$$

that is,

$$\mathbf{Y} = \mathbf{Y}_a + \mathbf{Y}_b \tag{2.5}$$

The admittance matrices, $\mathbf{Y}_a$ and $\mathbf{Y}_b$, may then be implemented in circuit form, and connected in parallel. The resulting circuit consists of two ideal voltage-controlled current sources, one transmitting in the forward direction only, with control parameter equal to g_{21}, the second transmitting in the reverse direction only, with control parameter equal to $-g_{12}$ as

shown in Figure 2.2. A simple, but effective, implementation has been proposed by Haykim[4], in which Y_a is realized by two common emitter stages, each with its own local series feedback as shown in Figure 2.3(a). Provided that resistors R_a and R_c satisfy the conditions

$$R_a \gg \frac{h_{ie_1}}{1 + h_{fe_1}} \tag{2.6}$$

and

$$R_c \gg \frac{h_{ie_2}}{1 + h_{fe_2}} \tag{2.7}$$

where the h_{ie} and h_{fe} are the common emitter h-parameters of the pertinent transistors, then y_{21} approximates closely to R_b/R_aR_c and the other parameters are negligibly small and can justifiably be ignored. In a similar manner Y_b can be implemented by a single common-emitter stage, with local series feedback provided by R_e, as shown in Figure 2.3(b). Provided that

$$R_e \gg \frac{h_{ie_3}}{1 + h_{fe_3}} \tag{2.8}$$

then y_{12} is clearly equal to $-1/R_e$ and the remaining y-parameters are negligibly small.

The gyrator is realized by connecting these two circuits in parallel. The resulting circuit is shown in Figure 2.4, where, for convenience of biasing, we have used PNP and NPN transistors. If the gyrator is to be passive, then $y_{21} = -y_{12}$, and the necessary condition is that

$$R_e = \frac{R_aR_c}{R_b} \tag{2.9}$$

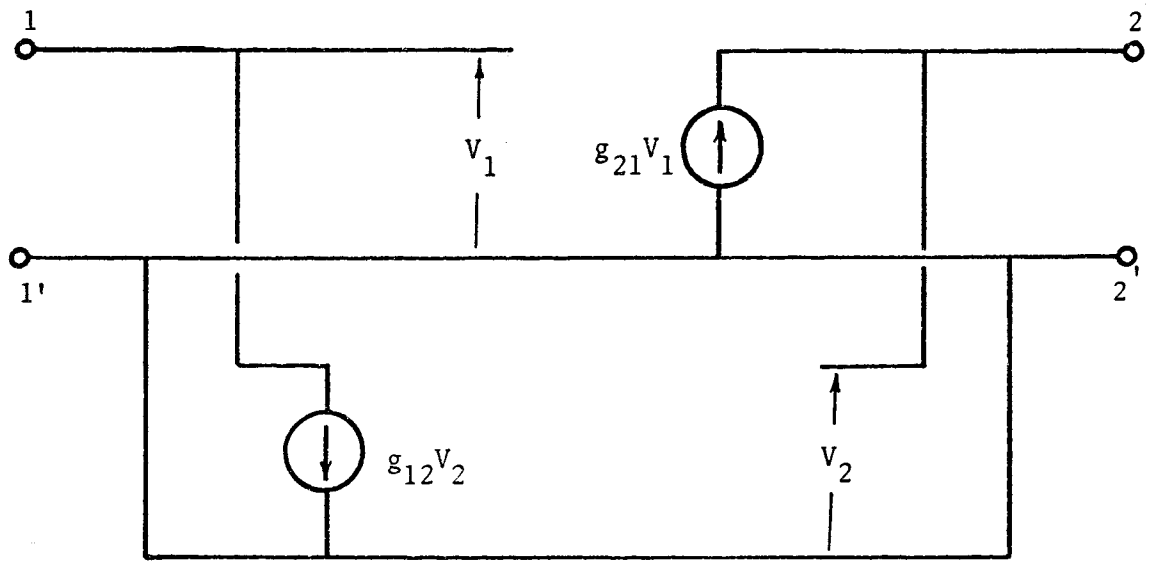

Figure 2.2: "Y-model" representation of gyrator

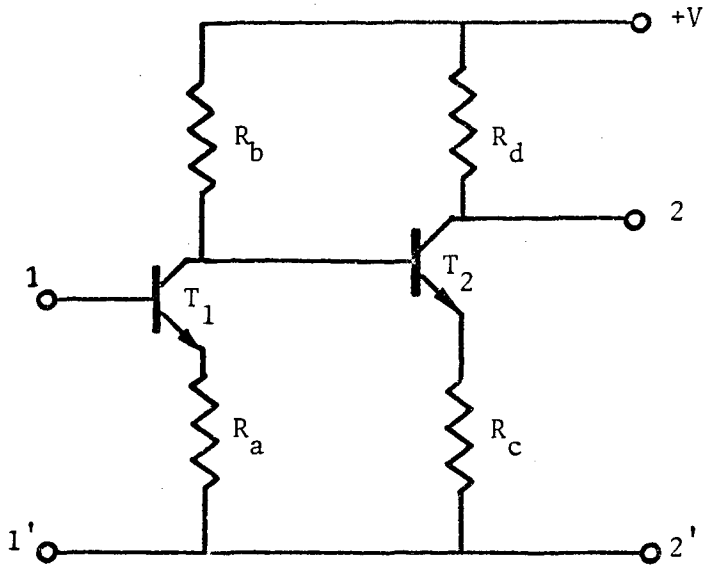

(a)

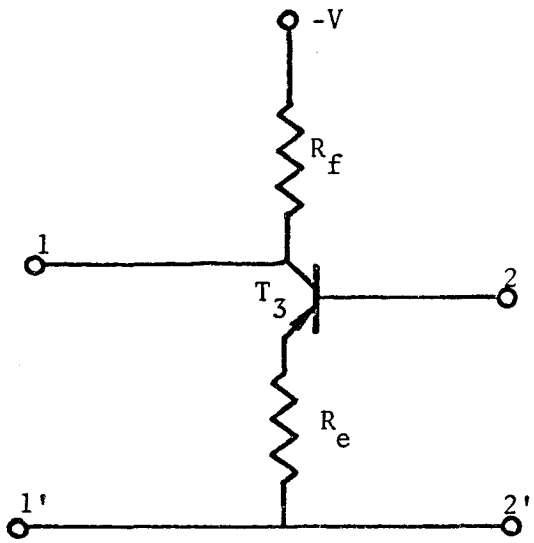

(b)

Figure 2.3: Gyrator realization: (a) forward transmission

(b) reverse transmission

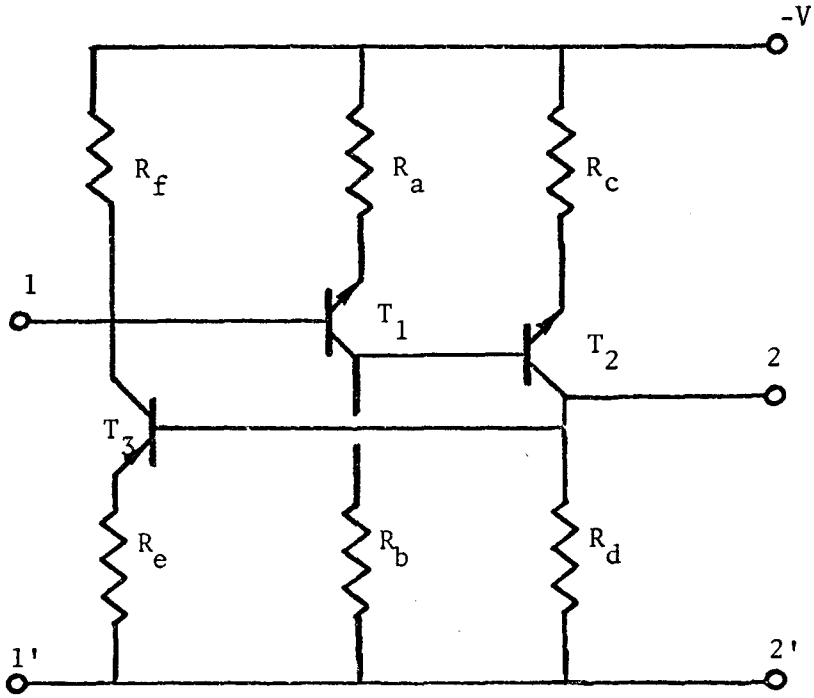

Figure 2.4: Three-transistor gyrator

The inclusion of biassing resistors R_f and R_d as shown in Figure 2.4 degrades the performance of the gyrator in as much as the y_{11} and y_{22} are no longer negligibly small. This problem may be overcome by modifying the circuit to reduce these parasitic effects and by using the predistortion technique to compensate for whatever residual parasitics remain after such modification.

In our particular case, the resistors R_f and R_d were replaced by equivalent current sources as is shown in Figure 2.5. Having performed this step, the parasitics were measured and were found to be sufficiently small so that the predistortion technique could be used without further modification. However, in the event that the measured parasitics were still too large to be accommodated by the predistortion technique, it is possible to use field-effect transistors at the input of both the forward and reverse transmission paths. In this way, advantage can be taken of their high input impedance to further reduce the unwanted parasitics. Several such networks were constructed, and Q-factors up to 700 were measured. A typical circuit diagram for such a gyrator is shown in Figure 2.6.

2.2.2 The Z-model gyrator

The various circuits proposed thus far for the gyrator are based on the Y-model representation in which the gyrator is realized by a parallel-parallel connection of two voltage-controlled current sources, with one source transmitting in the forward direction and the other in the reverse direction. In this section, an alternative Z-model realization of the gyrator is described. The gyrator, in this case, is characterized

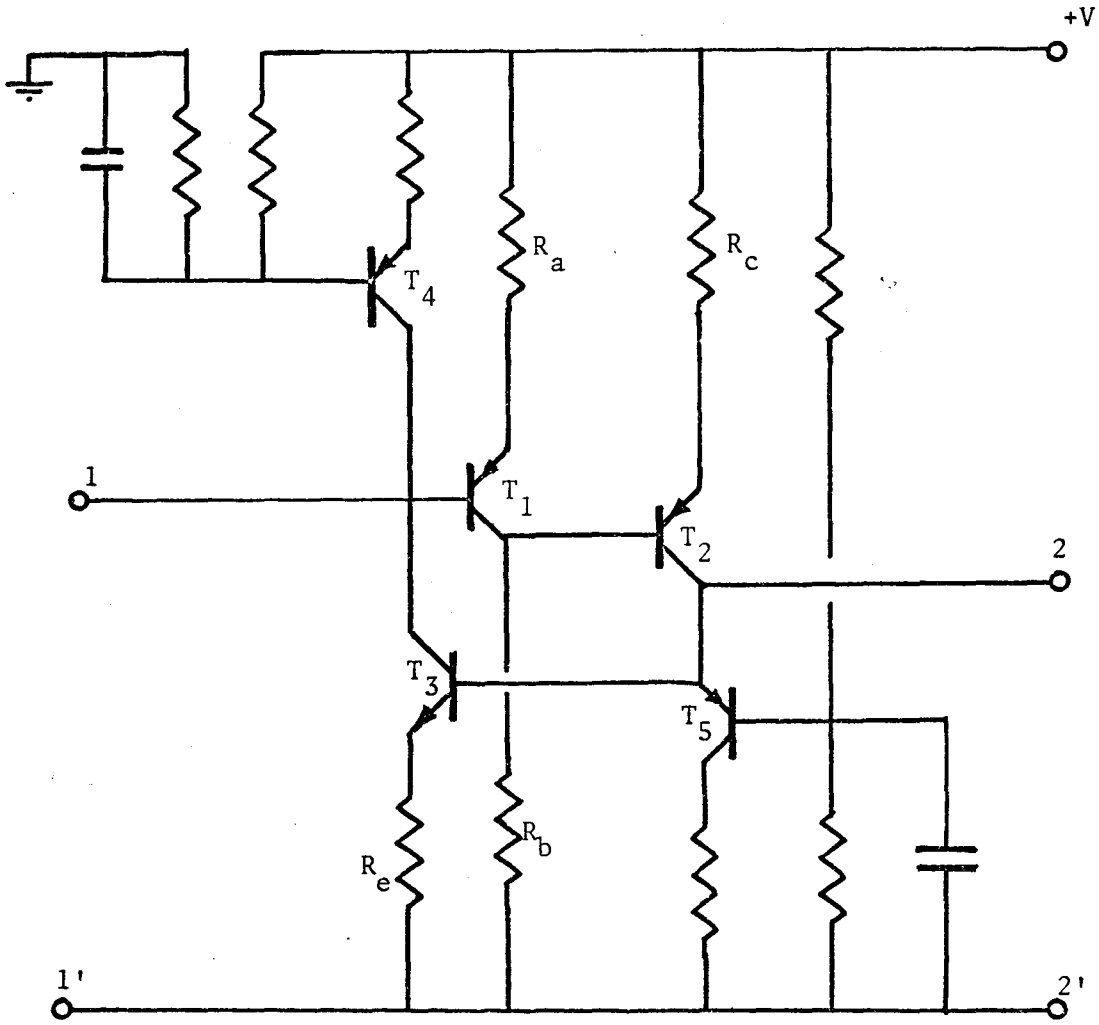

Figure 2.5: Improved version of gyrator

Figure 2.6: Gyrator containing field-effect transistors

R_1 = 25.00	R_{11} = 11.80
R_2 = 4.90	R_{12} = 2.90
R_3 = 4.70	R_{13} = 1.00
R_4 = 4.15	R_{14} = 15.00
R_5 = 4.80	R_{15} = 15.20
R_6 = 4.15	R_{16} = 14.80
R_7 = 0.39	C_1 = 10.00
R_8 = 4.20	C_2 = 10.00
R_9 = 1.00	C_3 = 10.00
R_{10} = 5.90	C_4 = 10.00

(All resistances in Kilo-ohms,
all capacitances in Micro-farads)

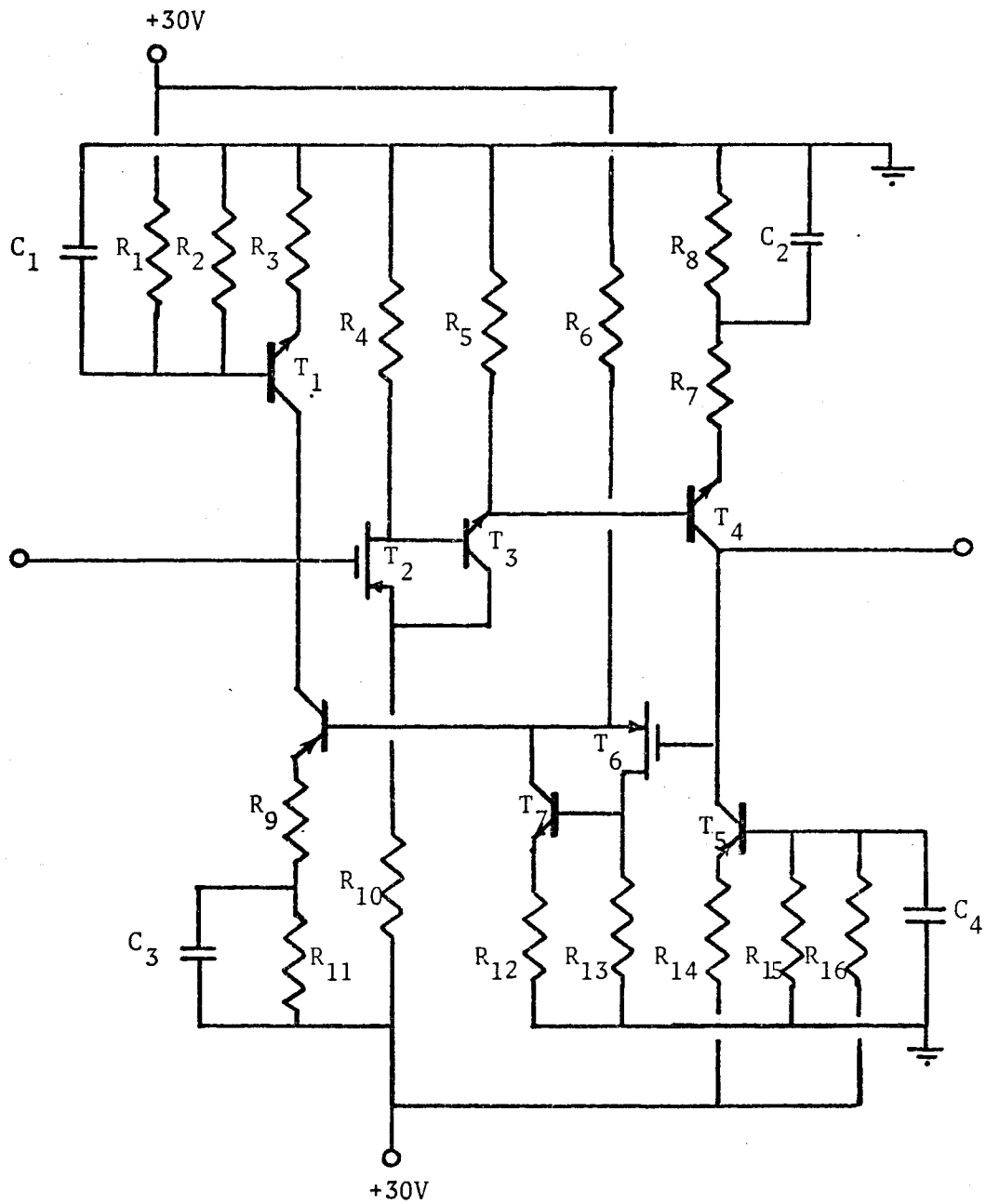

Figure 2.6: Gyrator containing field-effect transistors

by the impedance matrix Z, where

$$Z = \begin{bmatrix} 0 & -r_r \\ r_f & 0 \end{bmatrix} \tag{2.10}$$

Decomposing this matrix into the form

$$Z = \begin{bmatrix} 0 & 0 \\ r_f & 0 \end{bmatrix} + \begin{bmatrix} 0 & -r_r \\ 0 & 0 \end{bmatrix} \tag{2.11}$$

we obtain the model shown in Figure 2.7. It consists of two current-controlled voltage sources connected in series at their input and output ports. One controlled source transmits in the forward direction, and has a control parameter equal to r_f, the other transmits in the reverse direction with control parameter equal to $-r_r$.

The use of bipolar transistors, on account of their low input resistances, is ideally suited for the practical implementation of the controlled current sources in Figure 2.7. In a practical circuit, however, we find that the elements on the principal diagonal of the z-matrix in Equation 2.10 are small but, nevertheless, finite. Furthermore, the control parameters of the controlled sources may not be exactly equal in magnitude. We may, therefore, represent the z-matrix of a practical gyrator circuit based on the z-parameters model as follows

$$Z = \begin{bmatrix} r_1 & -r_r \\ r_f & r_o \end{bmatrix} \tag{2.12}$$

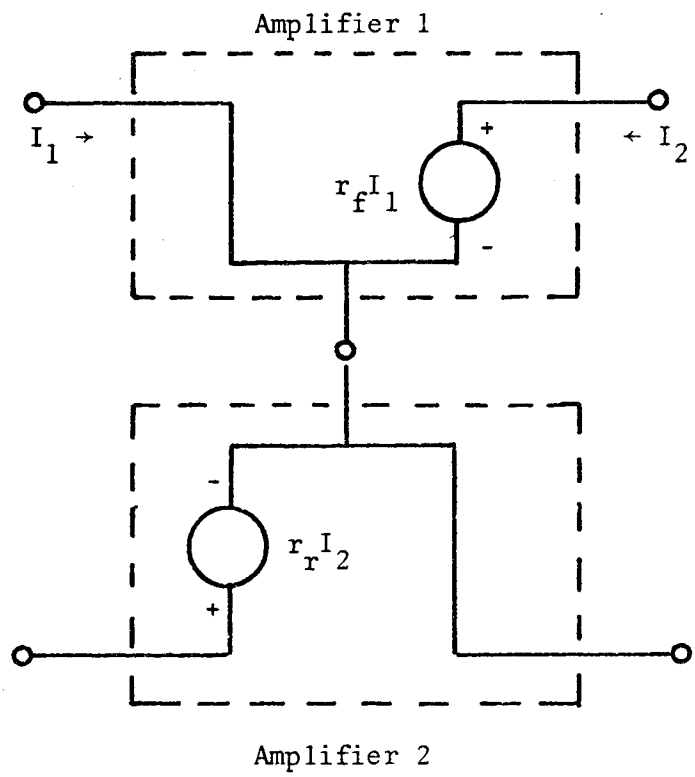

Figure 2.7: "Z-model" representation of gyrator

Such a gyrator would be active if

$$(r_f - r_r)^2 > 4\, r_i r_o \tag{2.13}$$

Suppose the non-ideal gyrator is terminated with a perfect capacitor C; the resulting input impedance is, therefore,

$$Z_{in} = r_i + \frac{r_f r_r}{r_o + 1/sC} \tag{2.14}$$

where s is the complex frequency variable. The impedance Z_{in} may be represented by the equivalent network shown in Figure 2.8. i.e. the input impedance is of the form

$$Z_{in} = r_i + \frac{r_f r_r}{r_o} \left[\frac{s + \omega_1}{s + \omega_2}\right] \tag{2.15}$$

where the corner frequencies ω_1 and ω_2 are defined by

$$\omega_1 = \frac{r_i}{C(r_i r_o + r_f r_r)}$$

$$\omega_2 = \frac{1}{C r_o} \tag{2.16}$$

Within the frequency band defined by $\omega_2 > \omega > \omega_1$, Z_{in} approximates to the impedance of an inductor with inductance

$$L = C r_f r_r \left[1 + \frac{r_i r_o}{r_f r_r}\right] \simeq C r_f r_r \tag{2.17}$$

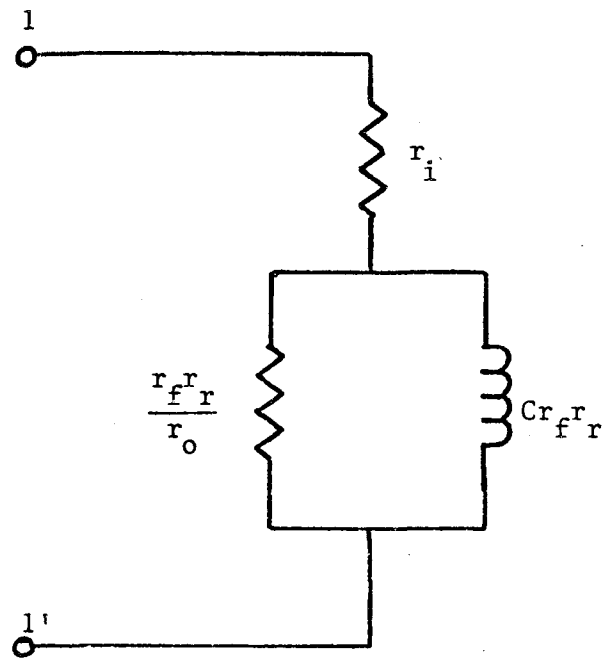

Figure 2.8: Equivalent circuit of capacitively terminated lossy gyrator

The logarithmic plot of $|Z_{in}|^2$ against frequency can be approximated asymptotically by a straight line with positive slope of 6dB/octave between the corner frequencies ω_1 and ω_2. We may use this predicted response as a measure of the performance of the gyrator.

The gyrator circuit diagram is given in Figure 2.9. Transistors T_1 and T_2 constitute amplifier 1 of Figure 2.7. Advantage has been taken of the low input and low output impedances of the common-base and common-collector modes, respectively. To reduce these impedances further, a negative feedback loop through transistor T_3 is added, the transistor providing the required phase reversal. Resistor R_2 provides a means of varying the amount of feedback and can therefore be adjusted for optimum operation of the circuit within the required frequency range. Transistors T_4, T_5 and T_6 constitute amplifier 2 of Figure 2.7. Again, advantage has been taken of the characteristics of the common-base and common-collector modes, and a negative feedback path through R_{11} and C_5 has been added to further reduce the input and output impedance levels. R_{11}, the variable feedback resistor, performs the same function as R_2. Capacitors C_7, C_8 and C_9 are used for high frequency stability. Capacitor C_3 presents a negligible impedance inside the useful frequency band, shorting the d.c. power lines for amplifiers 1 and 2 to a.c. signals, thereby completing the series-series connection of the two amplifiers as required. Transistors T_7 and T_8, simulating constant current sources, isolate the common point of the two amplifiers from the d.c. power supply lines.

The gyrator was terminated with a low-loss capacitor. The driving-point impedance at its input terminals was measured as a function of

Figure 2.9: Circuit diagram of z-model gyrator

$R_1 = 0.47$	$R_{12} = 3.30$	$C_1 = 10.0$
$R_2 = 10.00$	$R_{13} = 12.00$	$C_2 = 10.0$
$R_3 = 3.30$	$R_{14} = 82.00$	$C_3 = 10.0$
$R_4 = 82.00$	$R_{15} = 3.30$	$C_4 = 10.0$
$R_5 = 12.00$	$R_{16} = 3.30$	$C_5 = 10.0$
$R_6 = 6.81$	$R_{17} = 3.30$	$C_5 = 10.0$
$R_7 = 0.22$	$R_{18} = 40.00$	$C_6 = 10.0$
$R_8 = 5.60$	$R_{19} = 3.30$	$C_7 = 330$ pfd.
$R_9 = 5.60$	$R_{20} = 0.22$	$C_8 = 330$ pfd.
$R_{10} = 0.47$	$R_{21} = 39.00$	$C_9 = 330$ pfd.
$R_{11} = 10.00$	$R_{22} = 0.22$	
	$R_{23} = 0.22$	

(All resistances in Kilo-ohms, all capacitances in micro-farads except where stated to the contrary)

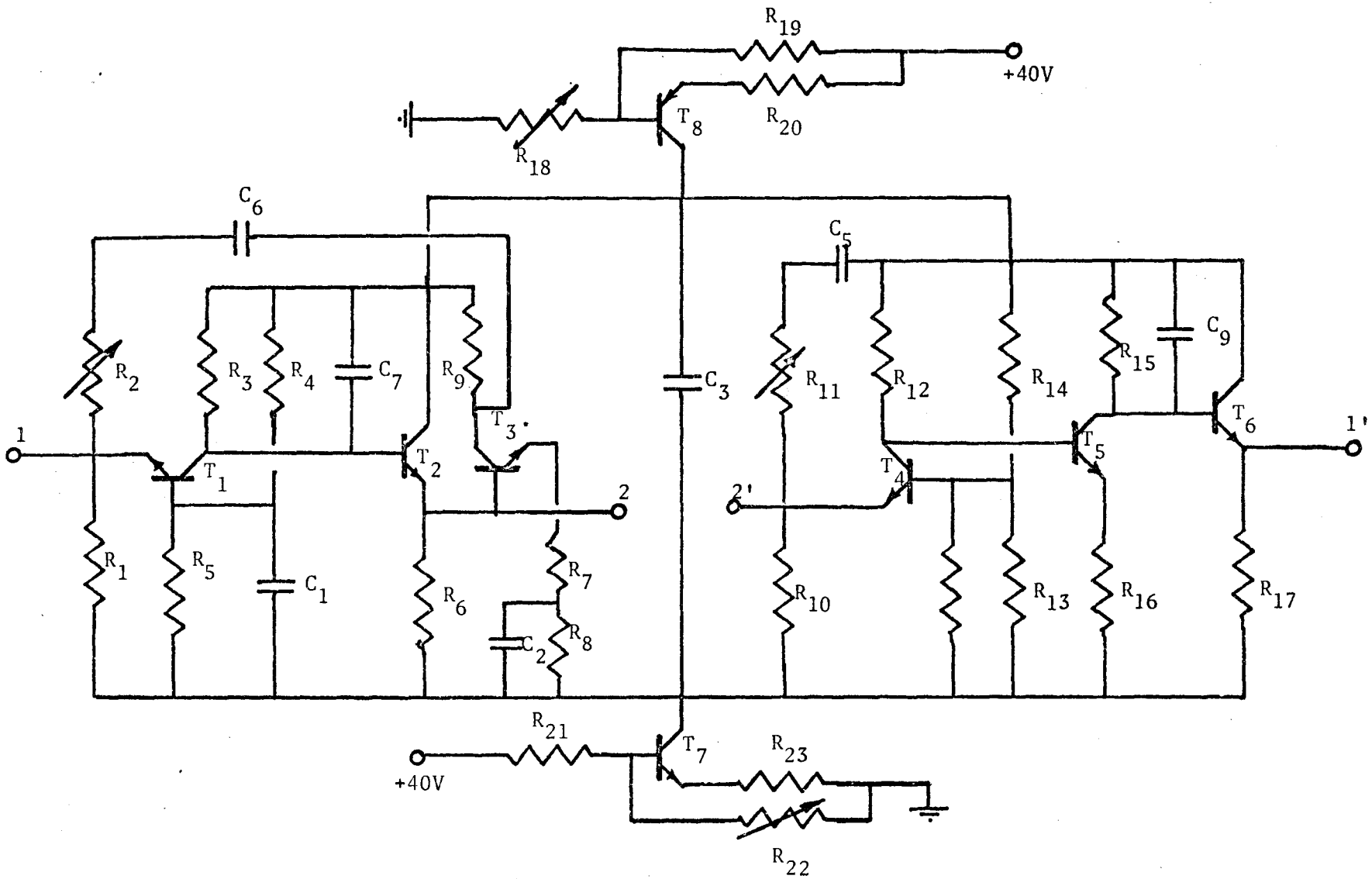

Figure 2.9: Circuit diagram of Z-model gyrator

frequency, and the results obtained are shown plotted in Figure 2.10 where close agreement with the predicted impedance response is observed. The small deviation at low frequencies may be attributed in part to the effects of decoupling and bypass capacitors in this frequency range.

An alternative criterion of performance is the Q-factor of the simulated inductance. Some representative values of the measured Q-factor for the capacitively terminated gyrator are given in Table 2.1.

f_o	2.2 KHz.	3.86 KHz.	4.3 KHz.
Q-factor	16.8	77.2	54.0

Table 2.1

2.3 RC-Gyrator Ladder Filters:

The gyrator can be used in the synthesis of inductorless filters in two basic ways:

(1) The filter may be realized by a cascade of second-order sections suitably buffered by means of isolation amplifiers. Each such section consists of a pair of two-port RC networks coupled by a gyrator.

(2) A conventional LC ladder filter is first designed to meet the prescribed specifications. Each inductor in the filter is then replaced by a gyrator terminated with an appropriate capacitor. In this way, it is possible to make use of the various classical synthesis techniques which have been developed for LC passive filters in the synthesis of an RC-active network. This procedure, however, may require the use of a

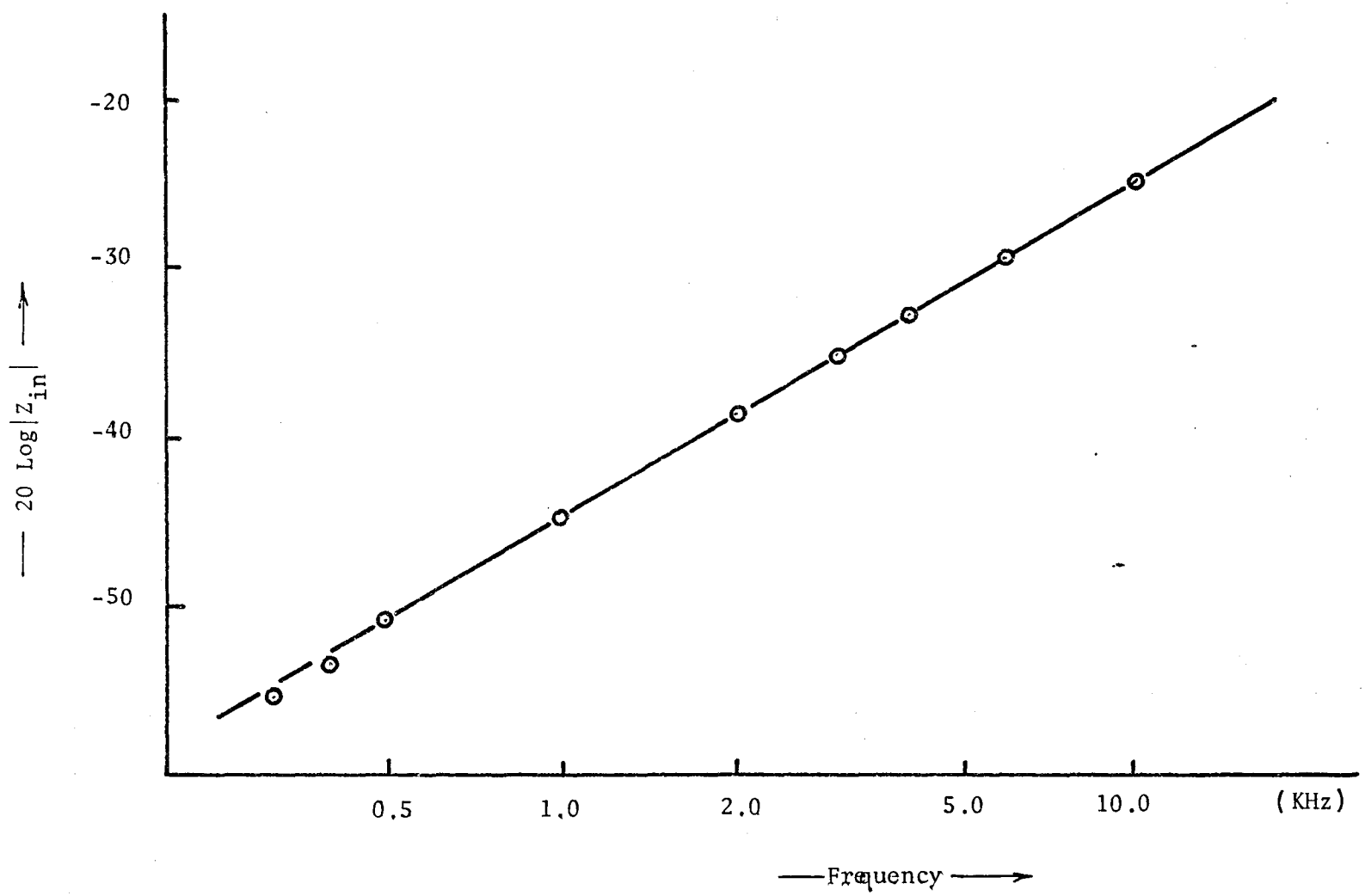

Figure 2.10: Z-model gyrator response characteristic

floating gyrator. Such a need may be eliminated, at the expense of an increase in the number of three-terminal gyrators used, by employing the following procedure.

Consider, for example, the fourth-order low-pass filter of Figure 2.11(a). Working from the source to the load, and recognizing that a shunt capacitor connected across the output port of a gyrator is equivalent to a series inductor at the input port, we can eliminate the need for series inductor L_2 by inserting a gyrator with gyration resistance r_1, as depicted in Figure 2.11(b). Effectively, the T-section made up of inductors L_2 and L_4 and the capacitor C_3 has been replaced by a π-section consisting of capacitors C_2', C_4' and inductor L_3', which are defined by

$$\begin{aligned} C_2' &= g_1^2 L_2 \\ L_3' &= r_1^2 C_3 \\ C_4' &= g_1^2 L_4 \\ R_2' &= r_1^2 / R_2 \end{aligned} \tag{2.18}$$

Next, to eliminate the inductor L_3' in Figure 2.11(b), we introduce a second gyrator of gyration resistance r_2, as in Figure 2.11(c), where

$$\begin{aligned} C_3'' &= g_2^2 L_3' = r_1^2 g_2^2 C_3 \\ L_4'' &= r_2^2 C_4' = g_1^2 r_2^2 L_4 \\ R_2'' &= r_2^2 / R_2' = g_1^2 r_2^2 R_2 \end{aligned} \tag{2.19}$$

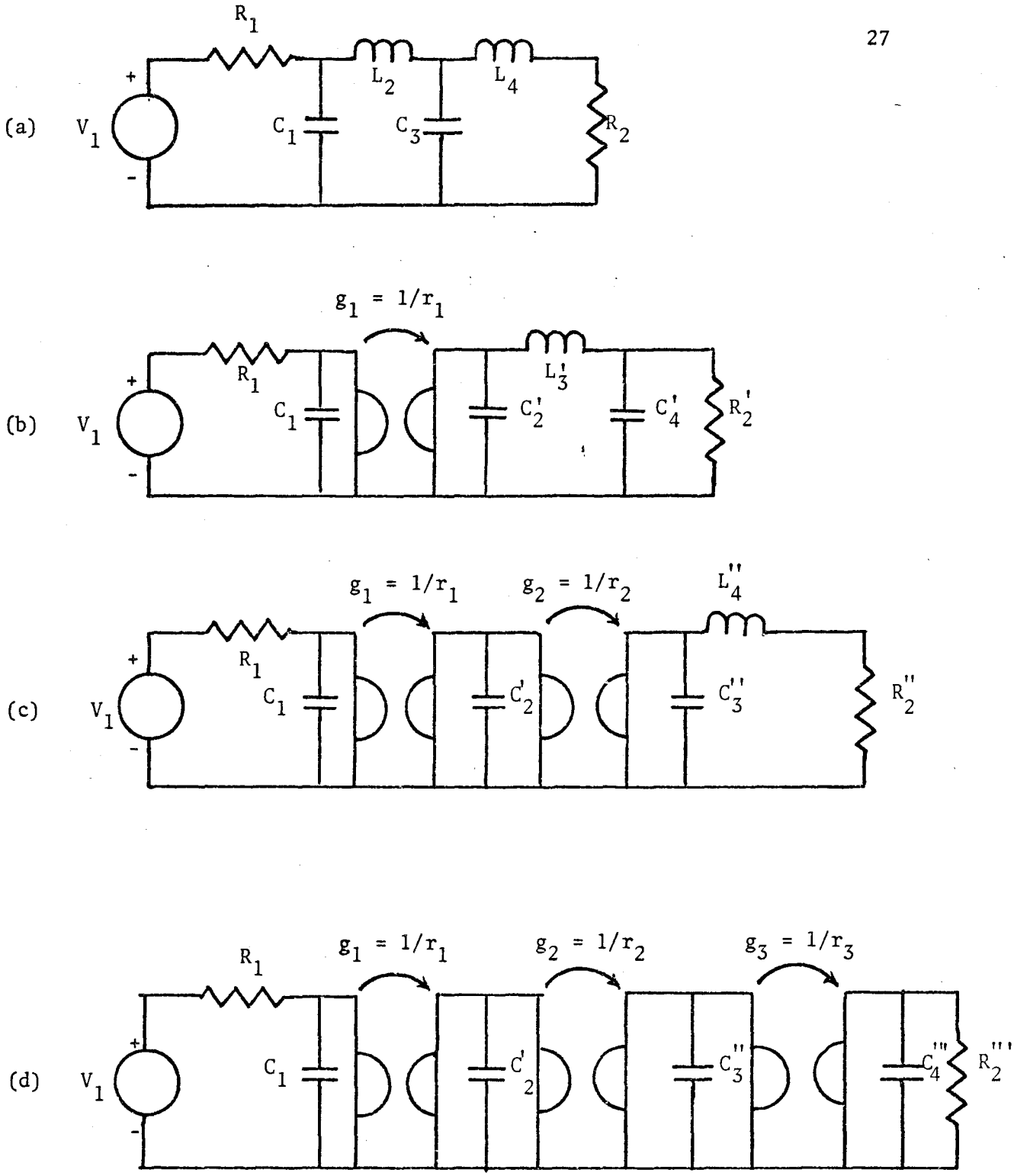

Figure 2.11: Low-pass filter; gyrator-capacitor equivalent circuit

Finally, to eliminate the inductor L_4'' in Figure 2.11(c), we introduce a third gyrator of gyration resistance r_3, as in Figure 2.11(d), where

$$C_4''' = g_3^2 L_4'' = g_1^2 r_2^2 g_3^2 L_4$$

$$R_2''' = r_3^2/R_2'' = r_1^2 g_2^2 r_3^2/R_2 \tag{2.20}$$

The resulting network is thus an inductorless low-pass filter consisting of a cascade of grounded three-terminal gyrators with shunt capacitors accounting for the cut-off at high frequencies. In general, to realize a filter of order n, the procedure requires the use of (n-1) grounded gyrators. On the other hand, the direct replacement of series inductors with capacitively terminated gyrators a minimum of n/2 floating gyrators if n is even, or (n-1)/2 floating gyrators if n is odd.

In a similar manner, we can obtain the gyrator-RC equivalents for other filter configurations. Figures 2.12 and 2.13 for example, show these equivalents for a high-pass and an asymmetric band-pass filter, respectively. In the case of the high-pass filter, the inductors appear as shunt elements, and may therefore be directly replaced with grounded gyrator-RC combinations, thereby reducing the number of gyrators needed.

2.3.1 Low-pass filter

To illustrate the synthesis procedure, we will consider the design of a fourth-order, low-pass Butterworth filter with a cut-off frequency of 500 Hz. The filter is to be driven by a current source and is to be terminated with a 1 Kilo-ohm load. To compensate for the degrading effect

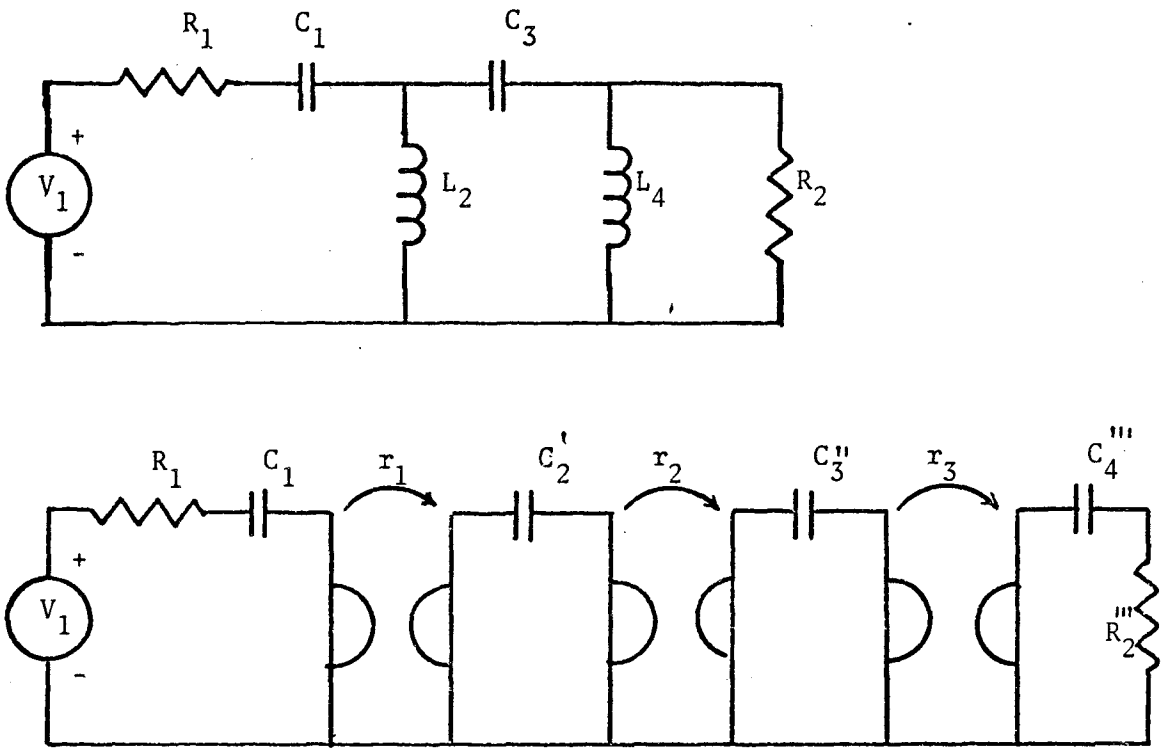

Figure 2.12: High-pass filter; gyrator-capacitor equivalent circuit

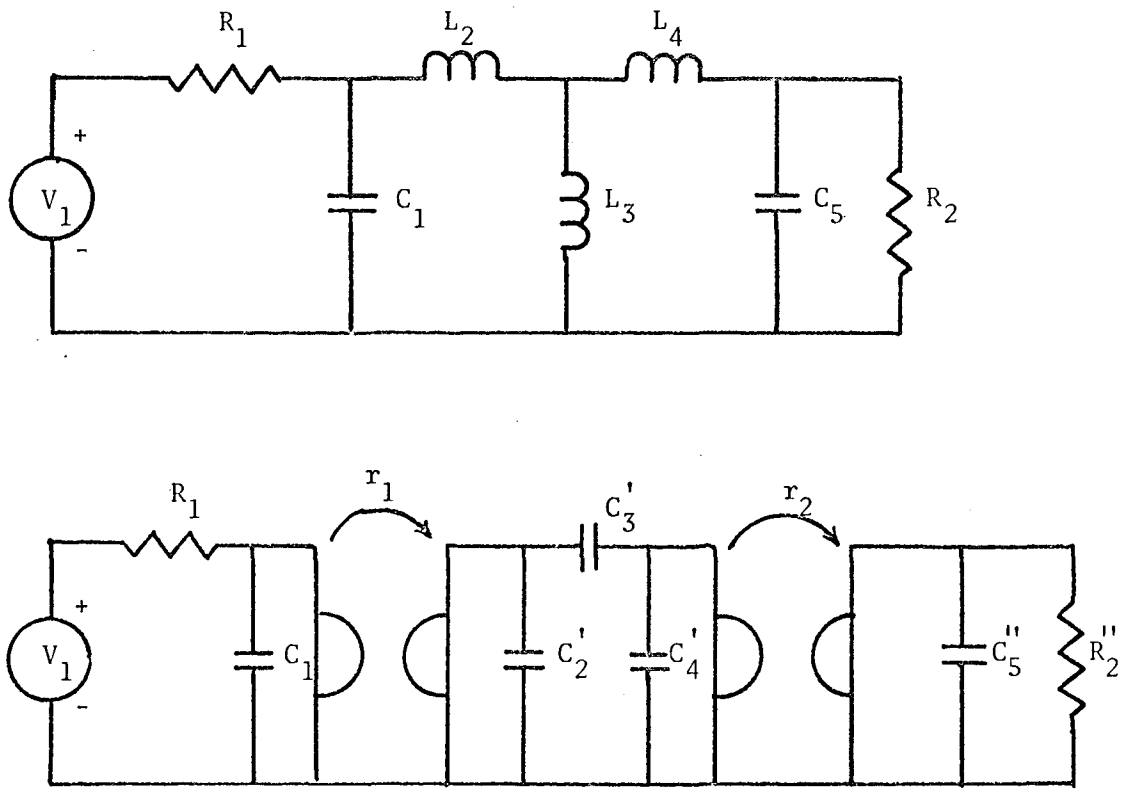

Figure 2.13: Asymmetric band-pass filter; gyrator-capacitor equivalent circuit

of the parasitic immittances of the imperfect gyrators, the predistortion technique of conventional filter theory is used.

The first step in the procedure is to obtain a suitable transfer function, which, in this case, is available from published tables[7], and determine its pole locations. The function is given by

$$Z_{21}(s) = \frac{1}{(s + .3827 \pm j.9239)(s + .9289 \pm j.3827)} \qquad \text{---------- (2.21)}$$

The poles of $Z_{21}(s)$ are now predistorted by an amount σ_o; in this case σ_o is chosen to be 0.2. In other words, a transformation of $s = p - 0.2$ is made, yielding the new impedance function

$$Z'_{21}(p) = Z_{21}(s)\Big|_{s = p - 0.2} \qquad (2.22)$$

that is

$$Z'_{21}(p) = \frac{1}{(p + .1827 \pm j.9239)(p + .7237 \pm j.3827)} \qquad (2.23)$$

or

$$Z'_{21}(p) = \frac{1}{p^4 + 1.1813p^3 + 2.087p^2 + 1.529p + .595} \qquad (2.24)$$

from which we obtain an expression for z_{22}:

$$z_{22} = \frac{p^4 + 2.087p^2 + .595}{1.813p^3 + 1.529p} \qquad (2.25)$$

Expanding z_{22} as a continued fraction expansion, we obtain the network of Figure 2.14(a).

Figure 2.14: RC-gyrator equivalent circuit for low-pass LC-ladder filter

(a) Low-pass filter:

$C_1 = 1.1130F.$ $L_2 = 1.8785H.$ $R_L = 1.000\Omega$

$C_3 = 1.4585F.$ $L_4 = 0.5514H.$

(b) Low-pass filter with uniform dissipation:

$R_1 = 4.4920\Omega$ $R_3 = 3.4280\Omega$

$R_2 = 0.3757\Omega$ $R_4 = 0.1103\Omega$

(c) RC-gyrator equivalent circuit:

$C_1''' = 0.1654$ mfd. $R_1''' = 9.600$ K-ohms

$C_2'' = 0.0987$ mfd. $R_2'' = 16.10$ K-ohms

$C_3' = 0.5370$ mfd. $R_3' = 2.960$ K-ohms

$C_4' = 0.1756$ mfd. $R_4 = 9.070$ K-ohms

$r_1 = 3.650$ K-ohm

$r_2 = 2.445$ K-ohm

$r_3 = 0.943$ K-ohm

(a)

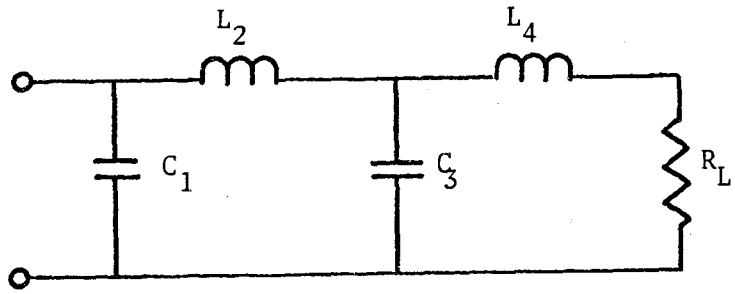
L_2
L_4
C_1
C_3
R_L

(b)

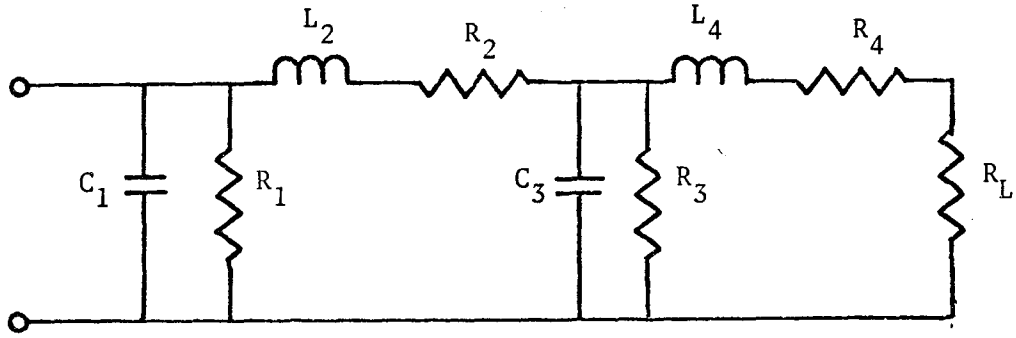
L_2
R_2
L_4
R_4
C_1
R_1
C_3
R_3
R_L

(c)

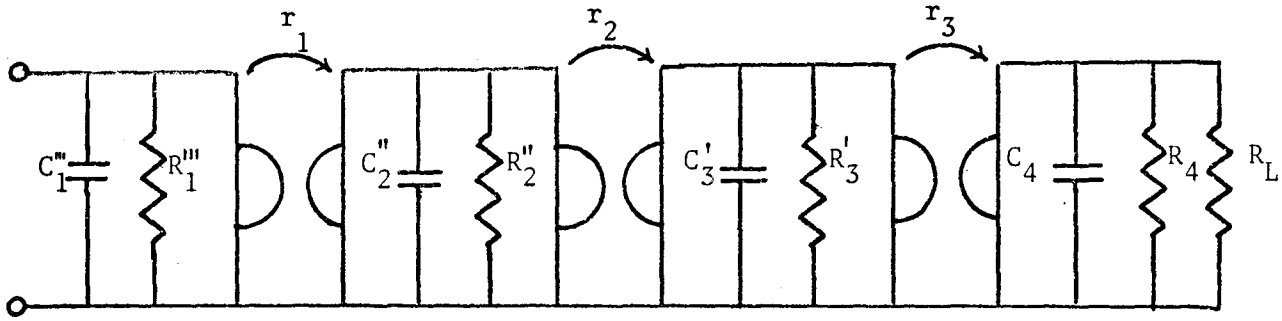
r_1
r_2
r_3
C_1'''
R_1'''
C_2''
R_2''
C_3'
R_3'
C_4
R_4
R_L

If we now arrange to have uniform dissipation across each element of this filter, the effect will be to shift the poles away from the $j\omega$-axis in a direction parallel to the real axis. By choosing the correct amount of dissipation we arrange to have the poles shift to the positions held before transformation, and in this way we are able to obtain an exact response. The circuit with dissipative elements inserted is shown in Figure 2.14(b).

It is now necessary to choose an RC-gyrator configuration which is equivalent to the circuit of Figure 2.14(b). Using the y-parameter model of the gyrator, a suitable equivalent circuit is shown in Figure 2.14(c). The resistances R_1 through R_4 represent the parasitics of the imperfect gyrators. The parameters r_1 through r_3 represent the effective gyration resistances, the subscript referring to the pertinent gyrator.

Each element of the circuit of Figure 2.14(c) can now readily be identified with a corresponding element of the circuit of Figure 2.14(b). The resulting relationships enable us to determine the allowable values of parasitics and capacitor values to be used. The constraints on the values of the parasitics are used to determine the values of biasing the resistors necessary, the problem now being reduced to one of determining suitable d-c operating points for all transistors within the framework of these constraints.

The circuit diagram for the complete filter is shown in Figure 2.15. Because of direct coupling between stages, it was unnecessary to include resistor R_d of Figure 2.4 in either gyrator 1 or 2; it was also convenient to combine resistor R_d of gyrator 3 with the load resistor. All resistors and capacitors in Figure 2.15 have been denormalized with respect to a

Figure 2.15: RC-gyrator low-pass filter; circuit diagram

R_1	= 9.74	R_{12}	= 2.29
R_2	= 10.0	R_{13}	= 25.1
R_3	= 2.56	R_{14}	= 0.93
R_4	= 17.3	R_{15}	= 7.60
R_5	= 12.0	R_{16}	= 0.90
R_6	= 4.81	C_1	= 0.1654
R_7	= 2.97	C_2	= 0.0987
R_8	= 4.70	C_3	= 0.5370
R_9	= 1.50	C_4	= 0.1756
R_{10}	= 3.60		
R_{11}	= 7.20		

(All resistances in Kilo-ohms and all capacitances in micro-farads.)

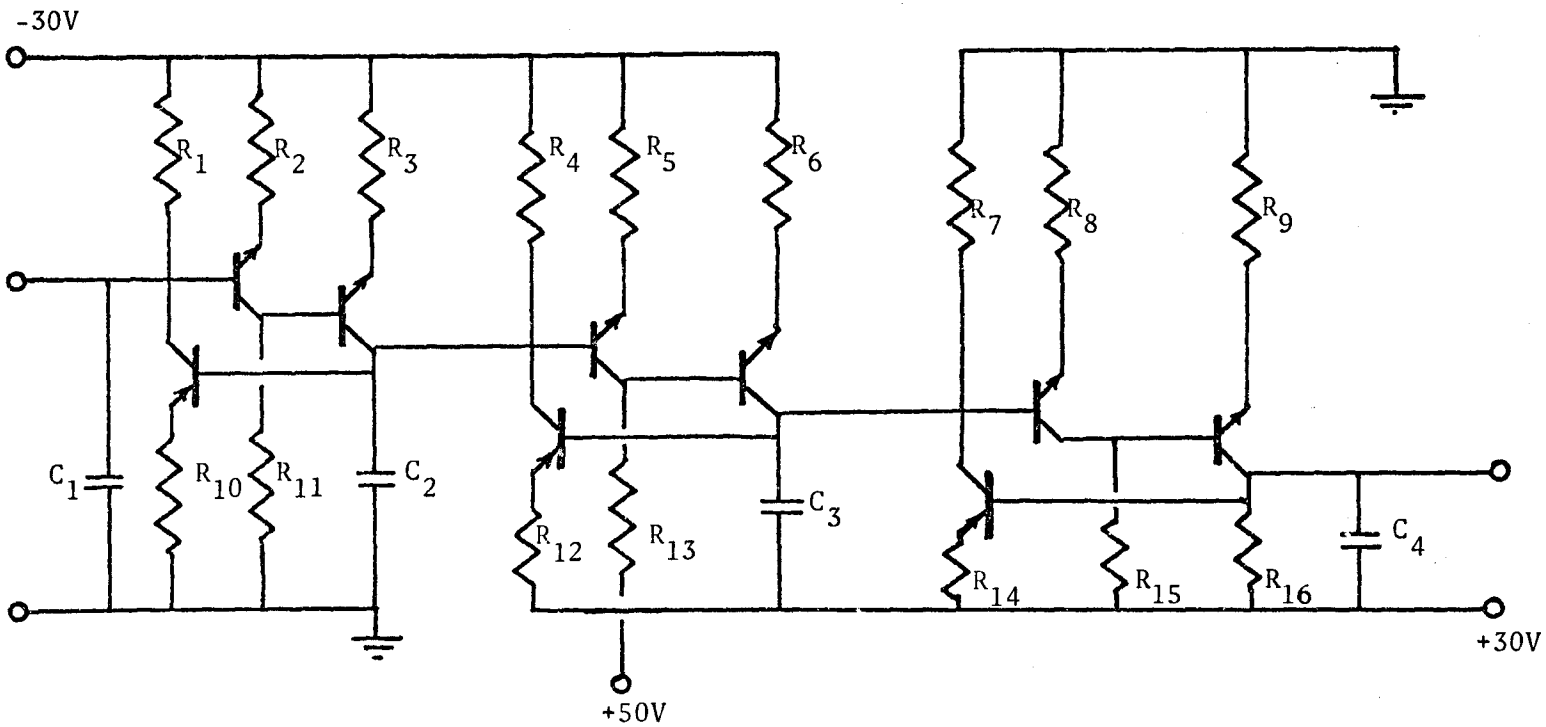
-30V
R1
R2
R3
R4
R5
R6
R7
R8
R9
C1
R10
R11
C2
R12
R13
C3
R14
R15
R16
C4
+30V
+50V

load resistance of 1 Kilo-ohm and a cut-off frequency of 500 Hz.

The measured filter response is shown plotted in Figure 2.16, where Z_{21n} denotes the transfer impedance of the filter normalized with respect to the zero frequency value. It is noted that close agreement with the predicted response is observed. The noise performance and harmonic distortion performance of the filter were investigated. The results indicate that the noise level was never less that 80 dBs below signal level in the range covered (20 Hz to 1 KHz). The output levels of the second through fifth harmonics of an input signal of 80 Hz were measured as the level of the input signal was increased from 1 millivolt to 1 volt. No significant increase in the harmonic content of the output signal was observed until the input level exceeded 0.7 volts.

2.3.2 Band-pass filter

The second configuration studied was that of an asymmetrical band-pass filter with upper cut-off frequency of 10 KHz, bandwidth of 3 KHz, 1 dB ripple in the passband, and cut-off rates of 6 dB/octave and 18 dB/octave, respectively, at low and high frequencies. The filter was driven by a current source and terminated with a 10 K-ohm load resistor. The general expression characterizing this type of response is given by

$$|Z_{21}|^2 = \frac{1}{1 + \eta^2|\xi|^2} \tag{2.26}$$

where η is a constant which determines the ripple magnitude and $|\xi|^2$ is the characteristic function defining the insertion loss of the filter. A suitable function for $|\xi|^2$ is given by[8]

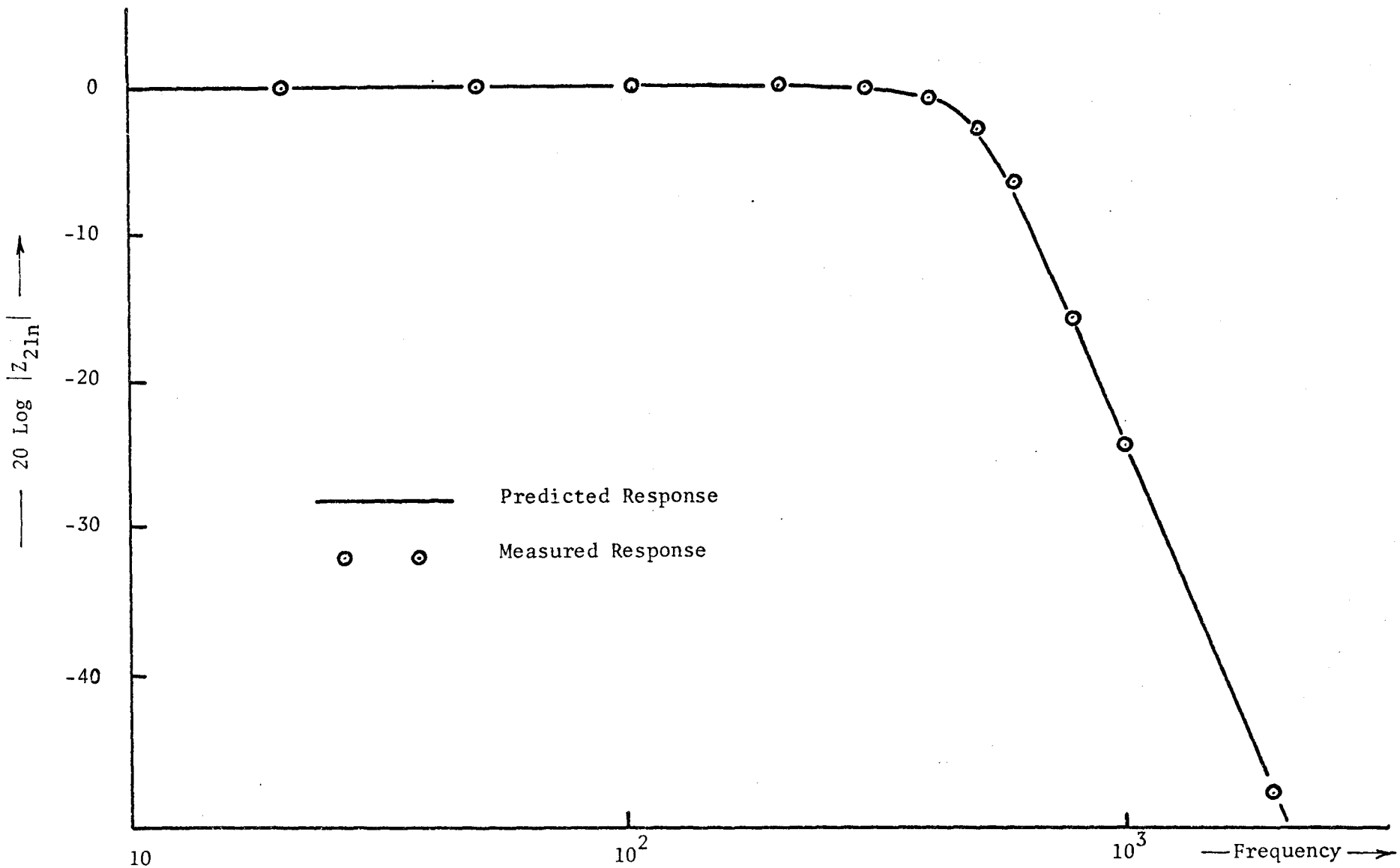

Figure 2.16: RC-gyrator low-pass filter response

$$|\xi|^2 = \frac{1}{\omega^2}\left[\omega^8 - 2.935\,\omega^6 + 3.165\,\omega^4 - 1.4844\,\omega^2 + .25578\right] \qquad (2.27)$$

from which we obtain

$$|Z_{21}|^2 = \frac{.00565\,\omega^2}{\omega^8 - 2.935\,\omega^6 + 3.165\,\omega^4 - 1.4787\,\omega^2 + .25578} \qquad (2.28)$$

putting $\omega^2 = -s^2$, and retaining those poles in the left half of the s-plane, we obtain an expression for $Z_{21}(s)$

$$Z_{21}(s) = \frac{.075188s}{(s + .081995 \pm j.715)(s + .081995 \pm j.98474)} \qquad (2.29)$$

To compensate for the parasitics of the imperfect gyrators we use the predistortion technique by applying the transformation $s = p - 0.05$ to the denominator only, with the numerator being left unchanged. We thus obtain

$$Z'_{21}(p) = \frac{.075188p}{p^4 + .12798p^3 + 1.487p^2 + .0949p + .49726} \qquad (2.30)$$

from which we determine

$$z_{22} = \frac{.12798p^3 + .0949p}{p^4 + 1.487p^2 + .49726} \qquad (2.31)$$

It now remains to choose an RC-gyrator configuration which is equivalent to this circuit. Such a circuit is shown in Figure 2.17(b), where R_1 through R_4 represent the parasitics of the two gyrators, and R_5 is an additional resistor included to obtain equal dissipation across C_3.

Figure 2.17 Asymmetric band-pass filter

(a) With uniform dissipation:

C_1 = 7.7960 F.	L_1 = 0.1316 H.	R_1 = 2.5650
C_2 = 7.8130 F.	L_2 = 0.0608 H.	R_2 = .00658
	L_3 = 0.1300 H.	R_3 = .00304
		R_4 = 0.0065
		R_5 = 2.5600
		R_6 = 1.0000

(b) RC-gyrator equivalent circuit:

C_1'' = 0.01265 mfd.	R_1'' = 24.76 K-ohms.	r_1 = 1.074 K-ohms.
C_2' = 0.01784 mfd.	R_2' = 18.18 K-ohms.	r_2 = 1.094 K-ohms.
C_3' = 0.00814 mfd.	R_3' = 18.40 K-ohms.	
C_4' = 0.01724 mfd.	R_4' = 25.59 K-ohms.	
C_5 = 0.01243 mfd.	R_5 = 39.33 K-ohms.	

(a)

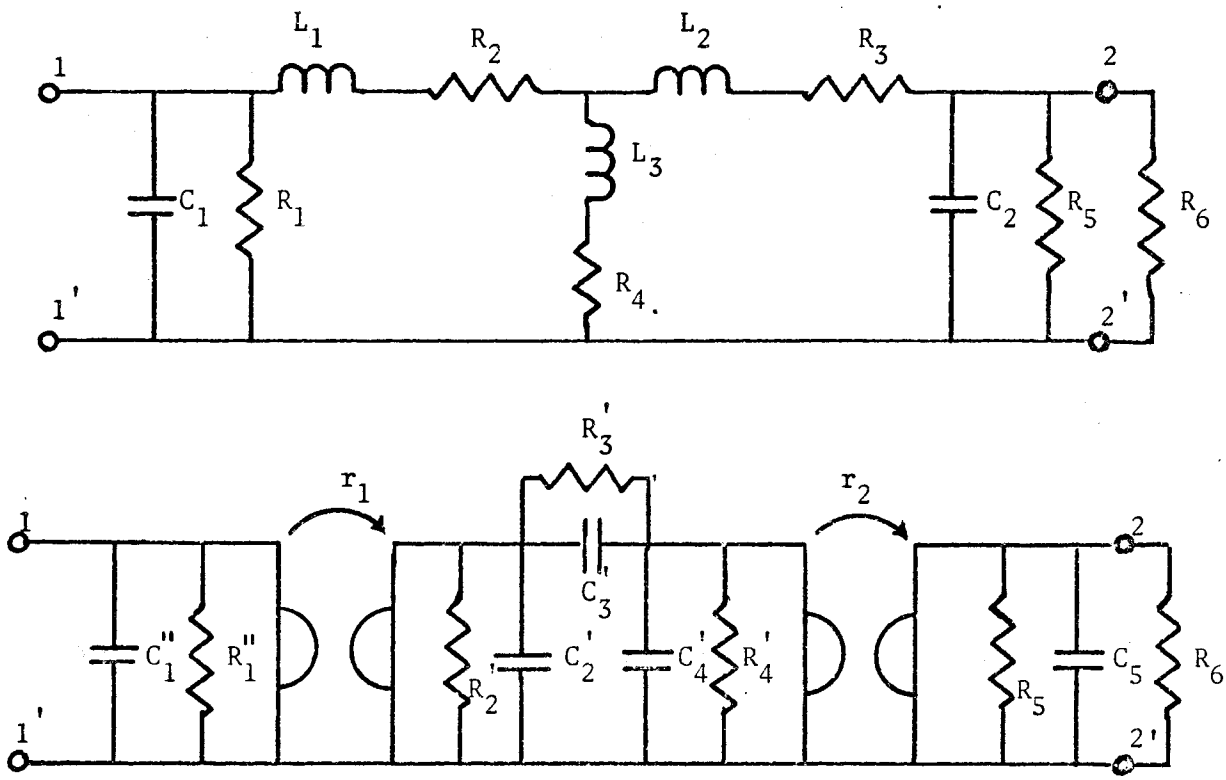
1
1'
2
2'
L_1
R_2
L_2
R_3
L_3
C_1
R_1
R_4
C_2
R_5
R_6
R_3'
r_1
r_2
C_3'
C_1''
R_1''
R_2'
C_2'
C_4'
R_4'
R_5
C_5
R_6

The equivalence of this network to that of Figure 2.17(a) is apparent on looking in through terminals 22'. In this way we can identify each element of the network with a corresponding element of the network of Figure 2.17(a). The resulting relationships are used to determine the necessary parasistic and capacitor values. The measured parasitics may then be adjusted to satisfy these constraints.

The complete circuit diagram is shown in Figure 2.18, in which all components have been denormalized with respect to an upper cut-off frequency of 10 KHz and a load resistance of 10K-ohms. In the network of Figure 2.18, transistors T_1, T_5, T_6, and T_{10} have been introduced as current generators, replacing biasing resistors R_f and R_d of Figure 2.4. Resistors R_{18}, R_{19}, R_{20} and R_{21} are used to adjust the parasitics at the input ports of both gyrators to the required values. R_{11} adjusts the parasitic at the output port of gyrator 1 to the required value, and R_{27} accounts for the combined effect of the load resistance paralleled by the pertinent parasitic at the output port of gyrator 2. The parallel combination of C_3 and R_5 of the circuit of Figure 2.17(b) has been replaced by its series equivalent to prevent any change in the d-c operating point of either gyrator.

The measured filter response is shown plotted in Figure 2.19 where close agreement with the predicted response is again observed.

2.3.3 Sensitivity considerations

The sensitivity of the network response to variations in supply voltage was investigated for both the low-pass and the band-pass filters. In the case of the low-pass filter, some typical results are given in

Figure 2.18: Asymmetric band-pass filters; circuit diagram

R_1	=	19.20	R_{13}	=	19.2	R_{25}	=	3.90
R_2	=	0.820	R_{14}	=	0.82	R_{26}	=	5.90
R_3	=	1.000	R_{15}	=	1.00	R_{27}	=	6.80
R_4	=	5.100	R_{16}	=	5.10	C_1	=	0.01265
R_5	=	3.700	R_{17}	=	3.66	C_2	=	0.01784
R_6	=	1.000	R_{18}	=	33.0	C_3	=	0.00814
R_7	=	18.80	R_{19}	=	27.0	C_4	=	0.01724
R_8	=	1.200	R_{20}	=	68.0	C_5	=	0.01243
R_9	=	5.900	R_{21}	=	120.0	C_6	=	10.0
R_{10}	=	5.900	R_{22}	=	1.00	C_7	=	10.0
R_{11}	=	27.00	R_{23}	=	18.8	C_8	=	10.0
R_{12}	=	0.100	R_{24}	=	2.20	C_9	=	10.0

(All resistances in Kilo-ohms; all capacitances in microfarads)

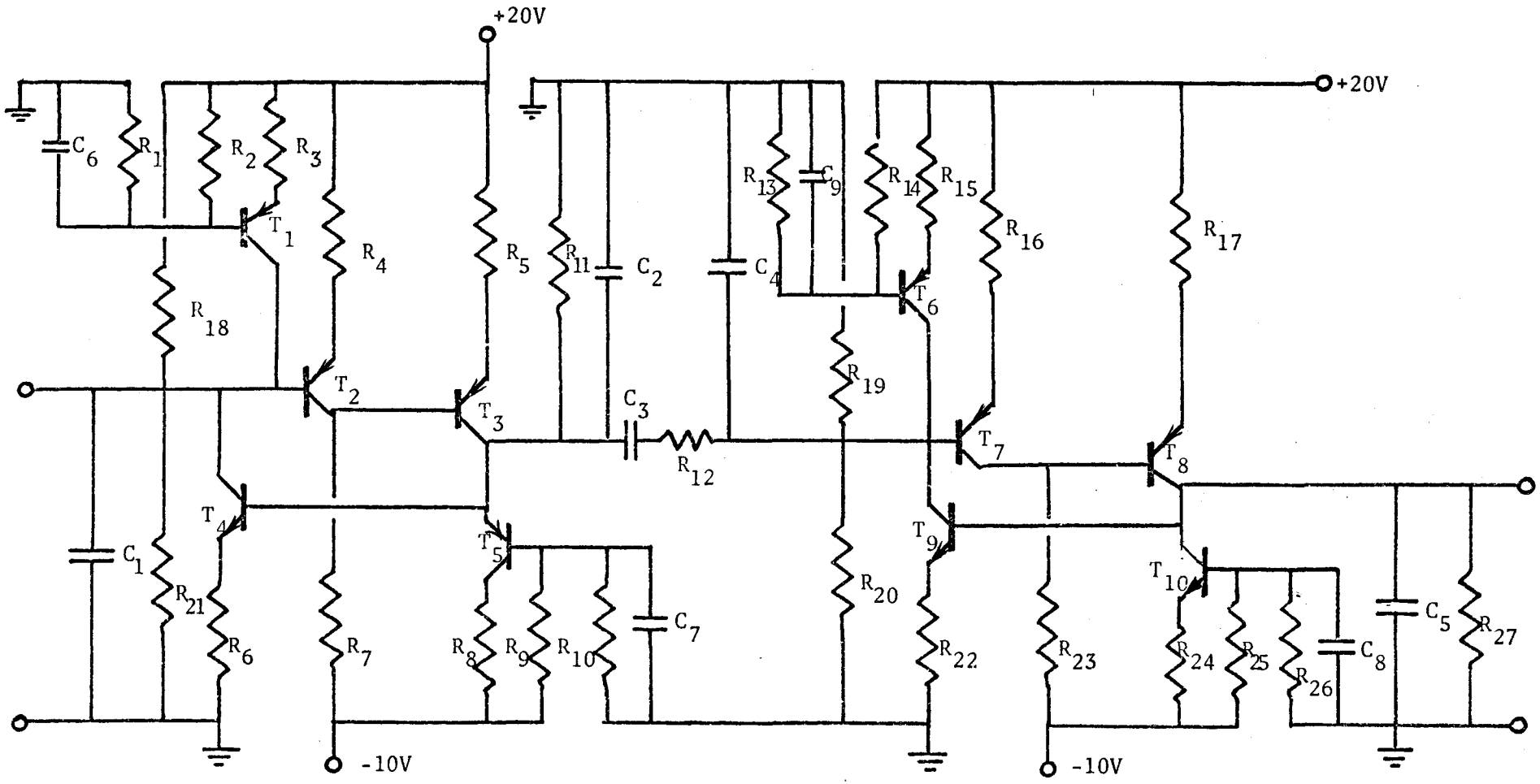
+20V
+20V
C6
R1
R2
R3
T1
R4
R5
R11
C2
C4
R13
C9
R14
R15
R16
R17
T6
R18
T2
T3
C3
R12
R19
T7
T8
T4
T5
T9
T10
C1
R21
R6
R7
R8
R9
R10
C7
R20
R22
R23
R24
R25
R26
C8
C5
R27
-10V
-10V

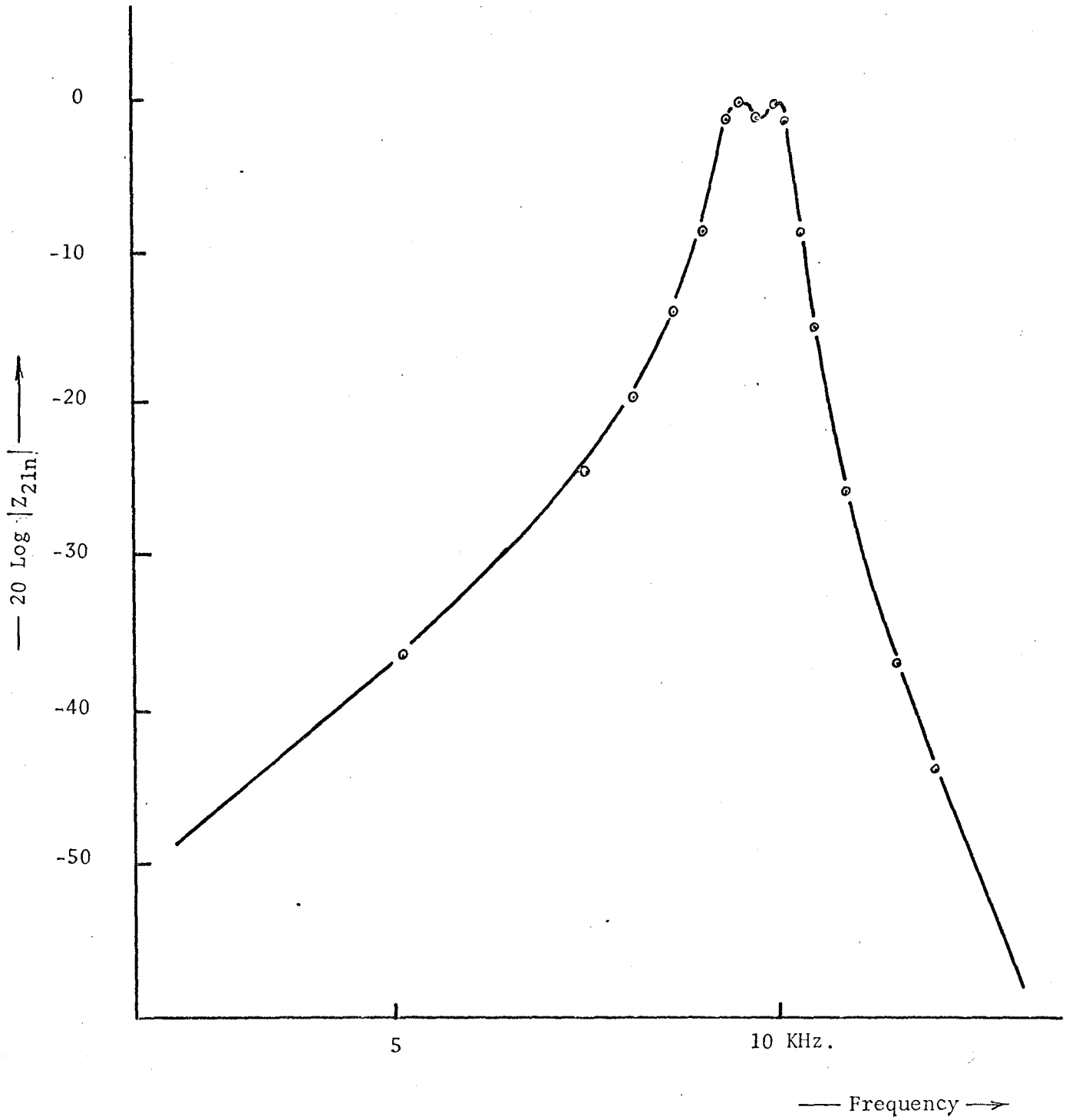

Figure 2.19: Asymmetric band-pass filter response

——— Predicted response

—o— Measured response

Table 2.2. We note that the overall response remains essentially the same although bias supplies were reduced to as little as 15% of their nominal value.

Frequency (Hz)	Nominal Output (mV)	Output with d-c supplies at 50% of nominal	Output with d-c supplies at 15% of nominal
100	1.000	1.000	1.000
200	1.000	1.000	1.000
300	0.975	0.975	0.968
400	0.915	0.917	0.888
500	0.707	0.698	0.663
600	0.415	0.400	0.363
700	0.024	0.023	0.021
1000	0.006	0.006	0.005

Table 2.2: Effect of supply voltage variation; low-pass filter

In the case of the band-pass filter both supplies were varied by as much as ±50% and the most extreme changes in the filter response are shown in Figure 2.20. We note, again, that the response is remarkably insensitive to supply variations.

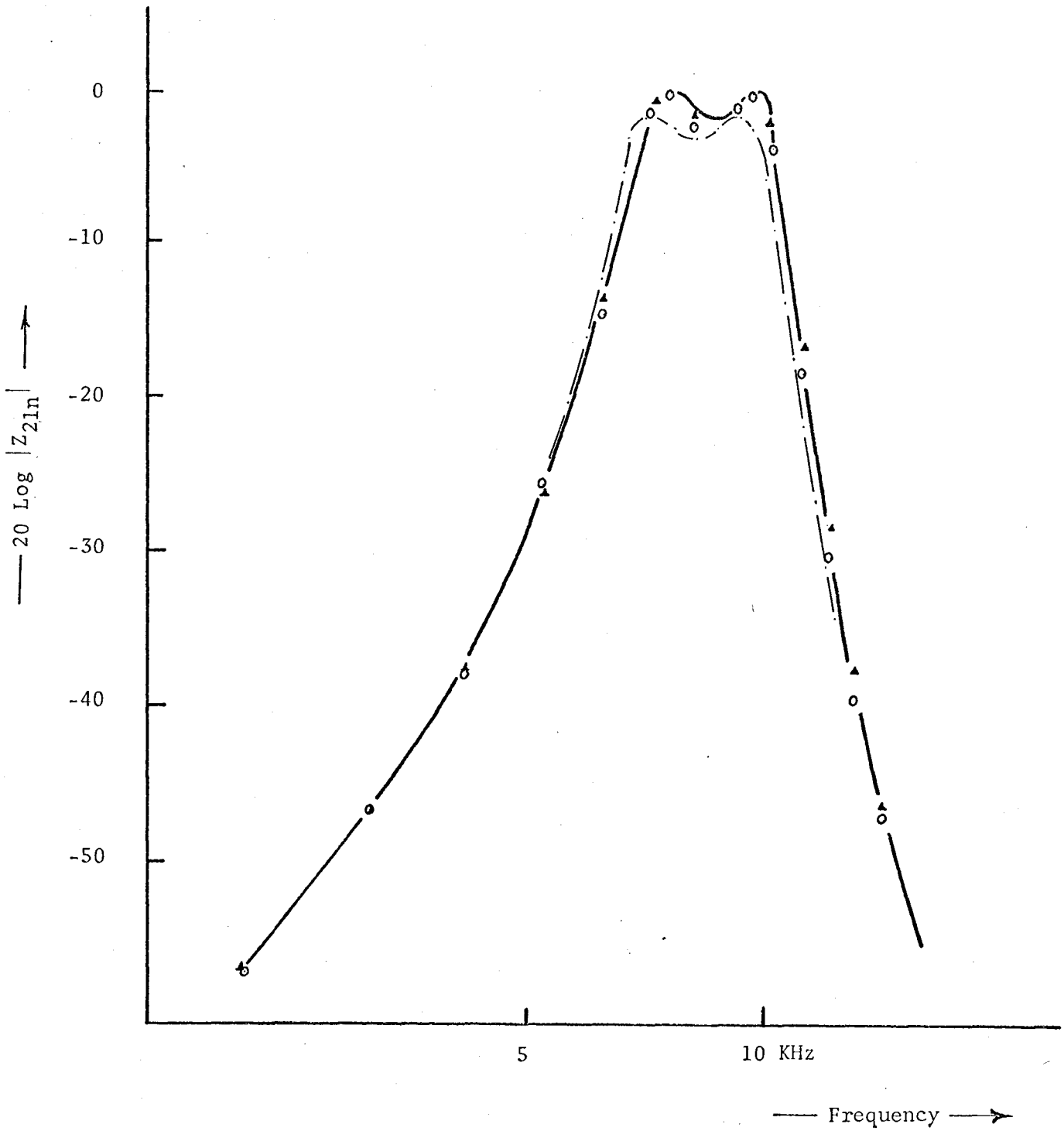

Figure 2.20: Asymmetric band-pass filter; sensitivity to supply voltage variation:

- ——— Normal response with supplies at +20 and -10v
- —▲— Response with supplies at +30 and -10v
- —o— Response with supplies at +30 and -7.5v
- —·—·— Response with supplies at +20 and -15v

2.4 Conclusion:

A procedure for developing RC-gyrator networks equivalent to LC ladder filters has been described. The procedure has been used to construct uniformly dissipative low-pass and band-pass filters, with measured responses showing very close agreement with theory. In synthesising the predistorted dissipation-compensated RC-gyrator filter, it is convenient to use the Y-model for characterizing the imperfect gyrator if shunt capacitors are connected directly across the input and output ports of the gyrator. On the other hand, if capacitors are connected in series with the input and output ports, then it is more convenient to use the Z-model characterization.

The sensitivity of the filter response to changes in the level of the dc-supply voltages was measured, and the experimental results obtained indicate that substantially large changes in supply voltages affect the measured loss characteristic only slightly. However, it is clear that such a sensitivity measure is of limited practical value, in that it is only adequate for the case of a lumped-element realization of the filter, in which the passive elements are not considered as variable parameters. However, in many practical situations (integrated circuits, for example), all of the network elements are subject to change. In such cases, there is a need for a quantitative measure of the multiparameter sensitivity performance of the network. It was, therefore, decided that an investigation of this problem should be undertaken. In the following chapter, a survey of the literature as it pertains to the multiparameter sensitivity problem in network theory is presented. In particular, a critical appraisal is made of several multiparameter sensitivity functions,

and problems involved in their computation are considered. Several procedures for their evaluation are described, with attention focussed on the auxiliary network approach of Leeds and Ugron, and the adjoint network approach of Director and Rohrer.

CHAPTER III

THE MULTIPARAMETER SENSITIVITY PROBLEM

3.1 Introduction:

In the early studies of the sensitivity problem in network theory the problem was defined in terms of the sensitivity, $S_x^T(s)$, of some network function with respect to a single parameter, x. A formal definition of the sensitivity function was first proposed by Bode[9] in 1945. Mason[10] used the reciprocal of Bode's definition and this has turned out to be the accepted definition of the classical sensitivity function as shown by

$$S_x^T(s) = \frac{d[\ln T(s)]}{d[\ln x]} \tag{3.1}$$

or equivalently,

$$S_x^T(s) = \frac{dT/T}{dx/x} \tag{3.2}$$

According to Equation 3.2, we may interpret the sensitivity function as the ratio of the fractional change in the network function, T(s), to the fractional change in the parameter x which caused the initial change in T(s), provided that all changes considered are differentially small. For the case of large parameter changes, we may use Horowitz's definition[11] as follows:

$$S_x^T(s) = \frac{\Delta T/T_f}{\Delta x/x_f} \tag{3.3}$$

where ΔT is the change in T due to the change Δx in x, and T_f and x_f are the final values of the network function and of the parameter under consideration, respectively. When the leakage transmission through the network is zero (that is, T(s) is zero when x is zero), Horowitz has shown that the classical definition of Equation 3.2 and that of Equation 3.3 have the same value, although they are defined differently.

Returning to Equation 3.2, suppose we define the network function T(s) in terms of its poles and zeros as follows:

$$T(s) = H\frac{\Pi(s + z_i)}{\Pi(s + p_i)} \tag{3.4}$$

where H is a scale factor, and the z_i and p_i are the zeros and poles of T(s), respectively. Then using Equation 3.4 in 3.2 we obtain:

$$S_x^T(s) = S_x^H + \sum_i \frac{S_x^{p_i}}{s + p_i} - \sum_i \frac{S_x^{z_i}}{s + z_i} \tag{3.5}$$

where

$$S_x^H = \frac{dH/H}{dx/x} \tag{3.6}$$

and $S_x^{p_i}$ and $S_x^{z_i}$ are the pole and zero sensitivities, respectively, defined by

$$S_x^{p_i} = \frac{dp_i}{dx/x} \tag{3.7}$$

and

$$S_x^{z_i} = \frac{dz_i}{dx/x} \tag{3.8}$$

Equation 3.5 shows that the poles and zeros of the network function, T(s), make up the poles of the sensitivity function with residues equal to $S_x^{p_i}$ and $-S_x^{z_i}$.

Up to this point we have only considered the sensitivity of a network function with respect to variations in a single parameter. However, in a practical situation (e.g., in the design of an integrated circuit), we have to accommodate simultaneous variations in several parameters of the network. In an early contribution to the study of multiparameter sensitivity, a complete generalization of the concept and various theorems on return difference from the single-loop case to the multiple loop case was made by Sandberg[12]. During the early 1960's, several multiparameter sensitivity functions were proposed. In the following sections, we will consider these various functions, examine their properties, the methods which have been proposed for their evaluation, and we will discuss their inherent limitations.

3.2 Multiparameter Sensitivity Functions:

To a first order of approximation, the fractional change in $T(s,x_i)$ for small variations in x_i is given by

$$\frac{\Delta T}{T} = \sum_i \frac{\partial(\ln T)}{\partial(\ln x_i)} \, d(\ln x_i) \tag{3.9}$$

where x_i $(i = 1, 2, \ldots, n)$ = the variable parameters of the network. If we let the set of fractional parameter increments, $d(\ln x_i)$, be considered as a vector, dY, i.e.,

$$dY = \{d(\ln x_i), d(\ln x_2), \ldots d(\ln x_n)\} \tag{3.10}$$

and we put $y_i = \ln x_i$, then Equation 3.9 becomes

$$\frac{\Delta T}{T} = \nabla\{\ln T(y_1, y_2, \ldots, y_n)\}.d\Upsilon \tag{3.11}$$

Thus, the fractional change in the network function $T(s,x_i)$ depends on the gradient vector $\nabla(\ln T)$. Accordingly, Goldstein and Kuo[13] have suggested that the multiparameter sensitivity, $S^T_{x_i}$, be defined as

$$S^T_{x_i} = \nabla(\ln T) \tag{3.12}$$

i.e.

$$S^T_{x_i} = \left\{\frac{\partial \ln T}{\partial \ln x_1}, \frac{\partial \ln T}{\partial \ln x_2}, \ldots \frac{\partial \ln T}{\partial \ln x_n}\right\} \tag{3.13}$$

The magnitude of the sensitivity function, which gives the maximum rate of change of ln T with respect to $\ln x_i$, is given by

$$\left|S^T_{x_i}\right|^2 = S^T_{x_i} \cdot S^{T*}_{x_i} \tag{3.14}$$

where the asterisk denotes the complex conjugate.

Clearly, Equation 3.12 is a logical extension of the classical sensitivity function for the single parameter case. The fact that it is comprised of n single parameter sensitivity functions, as is evident in Equation 3.13, poses the question as to whether relationships exist between the various component sensitivity functions, $\frac{\partial \ln T}{\partial \ln x_i}$. The function $S^T_{x_i}$ has been defined on the basis of the fact that the n parameters of $T(s, x_i)$ can vary simultaneously and independently, and thus may be considered as n linearly independent vectors. However, it is possible

that some of these parameters may be linearly dependent with respect to $T(s, x_i)$ in the sense that the variation of $T(s, x_i)$ due to a change in one of the parameters might also be effected by a change in one or more of the other parameters for all values of s. This possibility has been considered by Lee[14], who has introduced the concept of a "sensitivity group". Such a group is defined as the largest sub-group of component parameters, the members of which are linearly dependent with respect to $T(s, x_i)$. In other words, if a parameter x_i varies by an arbitrary amount Δx_i, and this variation results in a change in $T(s, x_i)$ which we will denote by $\Delta T\Big|_{\Delta x_i}$, and if there exists a parameter x_j such that

$$\Delta T\Big|_{\Delta x_i} = \Delta T\Big|_{\Delta x_j} \tag{3.15}$$

where

$$\Delta x_j = k^{ji}\, \Delta x_i \tag{3.16}$$

for all values of s, and if further, k^{ji} is a non-zero constant which is independent of s, then we find that any variation of $T(s, x_i)$ due to Δx_i can equivalently be obtained from Δx_j, and therefore x_i, x_j are linearly dependent with respect to T. A sensitivity group is thus defined as the largest sub-group of such parameters, all the members of which are linearly dependent in $T(s, x_i)$

The multiparameter sensitivity function, $S^T_{x_i}$, may now be defined in terms of these sensitivity groups as follows: If we let the scalar sum of the single-parameter sensitivities of all the elements of the jth sensitivity group be denoted by S_j, i.e.,

$$S_j = \sum_{i=1}^{n_j} \frac{\partial(\ln T)}{\partial(\ln x_{ij})} \tag{3.17}$$

where n_j defines the number of elements in this sensitivity group, and x_{ij} is the ith element of the jth sensitivity group, then the multiparameter sensitivity function may be expressed as

$$S^T_{x_i} = \sum_{j=1}^{m} S_j \cdot \mathbf{s}_j \tag{3.18}$$

where the $\mathbf{s}_j$ are unit vectors, and m denotes the number of sensitivity groups.

3.3 Properties of Sensitivity Functions:

It is informative to consider further the effects of grouping the single-parameter sensitivity functions according to element type. In this respect, an important contribution was made by Blostein[15] in which he shows that multiparameter sensitivity theory can be used effectively to contribute quantitative insight into the sensitivity behaviour of networks. Let the network which is described by the transfer function, $T(s, x_i)$, have ℓ inductors, r resistors, and c capacitors, i.e.,

$$n = \ell + r + c \tag{3.19}$$

Also, let the individual components be denoted by ℓ_i, r_i and c_i, and let their reciprocals be denoted by γ_i, g_i, and e_i, respectively. From the amplitude scaling property of networks, it follows that

$$T(ar_i, a\ell_i, ae_i, s) = aT(r_i, \ell_i, e_i, s) \tag{3.20}$$

where a is an arbitrary scaling factor. Differentiating Equation 3.20 with respect to a, and letting a equal unity we obtain

$$\sum_{i=1}^{\ell} S^T_{\ell_i} + \sum_{i=1}^{r} S^T_{r_i} + \sum_{i=1}^{c} S^T_{e_i} = 1 \tag{3.21}$$

Now

$$S^T_{x_i} = -S^T_{1/x_i} \tag{3.22}$$

therefore

$$S^T_R + S^T_L - S^T_C = 1 \tag{3.23}$$

where

$$S^T_R = \sum_{i=1}^{r} S^T_{r_i} \quad \text{etc.}$$

It follows that if $T(s, x_i)$ were an admittance or dimensionless transfer function, then the right-hand side of Equation 3.23 would be -1 or zero, respectively.

A further relationship can be established by employing the concept of frequency scaling, according to which

$$T(r_i, a\ell_i, ac_i, s) = T(r_i, \ell_i, c_i, as) \tag{3.24}$$

where T may be any network function. Using the same procedure as before, we obtain

$$S^T_L + S^T_C = \frac{d(\ln T)}{d(\ln s)} = S^T_s \tag{3.25}$$

That is, the sum of the sensitivities with respect to all capacitors and inductors is equal to the sensitivity with respect to the complex frequency variable, s. Furthermore, by letting $s = j\omega$, we obtain

$$\mathfrak{Re}\ S_L^T(j\omega) + \mathfrak{Re}\ S_C^T(j\omega) = \frac{d\,\alpha(\omega)}{d\ \ln(\omega)} \tag{3.26}$$

and

$$\mathfrak{Im}\ S_L^T(j\omega) + \mathfrak{Im}\ S_C^T(j\omega) = \omega\tau_d \tag{3.27}$$

where

$$\alpha(\omega) = \ln|T(j\omega)| = \text{attenuation function}$$

$$\beta(\omega) = \arg T(j\omega) = \text{phase function}$$

and

$$\tau_d = \frac{d\beta(\omega)}{d\omega} = \text{group delay function}$$

Equation 3.26 may be interpreted physically as follows: In any network, if all inductances and capacitances undergo equal normalized perturbations, the resulting change in the magnitude characteristic is independent of the realization technique used to obtain the network and depends only on the slope of the prescribed attenuation curve.

These multiparameter sensitivity properties were later used by Blostein[16] to investigate the effects of incidental dissipation and stray terminations on the transmission characteristics of resistively terminated LC two-port networks. Bounds on such errors were obtained, and these were shown to be invariant for all equivalent two-port realizations of a given transfer function.

The property of sensitivity invariance has generated much interest in the literature. Leeds and Ugron[17] considered the network-function

sensitivity of a class of continuously equivalent networks. Their investigation led to a conjecture that the sum of the elemental sensitivity functions (over all components of each continuously equivalent LC-network) is invariant with respect to the various equivalent LC-networks. The proof of this conjecture is, of course, implicit in Equation 3.25, and formal proofs have since been given by several authors[18,19]. The following specific conclusions have been reached:

(i) The sum of the sensitivities with respect to all elements in a general RLC network is invariant under continuously equivalent transformations[15,19,20].

(ii) The sum of the sensitivities with respect to all elements of one kind is a constant for all equivalent networks (though it is a function of frequency)[21].

(iii) The sum of the sensitivities of an RC network function is invariant for all networks described by the same network function[18].

(iv) The sum of the sensitivities of an LC network is given by the frequency sensitivity of the network function[15,18].

(v) The sum of the sensitivities of an LR network is invariant over all network functions[18].

(vi) The individual sensitivity for capacitances and inductances is invariant if there are no capacitance loops and inductance cut-sets in the network[19].

The concept of summed sensitivity has also been extended to the case of RC-active networks containing all possible types of controlled sources.[22,23]

The summed sensitivity function may also be expressed in terms of the pole- and zero-sensitivities of the network. Kumpel[24] has

considered this possibility, and has shown that in the case of two-element-kind networks, the sum of the pole- and zero-sensitivities is again invariant. It is also pointed out that in the case where a network function is being approximated by use of its dominant poles and zeros only, the sum of the sensitivities for these singularities can be less than that for the poles and zeros which have been neglected. This, naturally, could lead to incorrect conclusions in an optimization procedure, for example.

It is also of interest to note that in the case of a single-loop feedback system, Huang has shown that the sum of the sensitivities of a closed-loop pole with respect to variations in the open-loop poles and zeros of the system is equal to unity.

3.4 Continuously Equivalent Network Approach to Optimal Synthesis:

It is, indeed, in the area of optimal synthesis (optimal in the sense that the multiparameter sensitivity performance of the network has been minimized) that the concept of sensitivity invariance is of great importance. The synthesis of optimal networks has been considered by several authors. Schoeffler[26] uses the theory of continuously equivalent networks to generate a sequence of networks whose transfer functions are identical, but whose elements differ from one network to another by an incremental amount. A multiparameter sensitivity performance criterion, $\emptyset$, is defined as

$$\emptyset = \frac{1}{2} \sum_i \left| S^T_{x_i} \right|^2 \tag{3.28}$$

The index $\emptyset$ is used to find the optimum network from the sequence which has been generated.

The generation of such a sequence consists of first defining what network characteristics are to remain constant. This fixes certain entries in a transformation matrix, but leaves others free of constraint. The free entries are chosen arbitrarily. The matrix is used to obtain differential equations in a dummy variable X. The differential equations for the sensitivity of the transfer function to changes in the network parameters are then derived. The differential equations in both cases are linear homogeneous, with the elements of the transformation matrix as the independent variables. Consequently, they are a function of X. Thus, one may choose a value of X which minimizes the performance criterion $\emptyset$. If a new set of arbitrary entries in the transformation matrix is selected, a new sequence of continuously equivalent networks and a new minimum value of performance index will result. Thus, the problem is to determine the value of X and the arbitrary entries in the transformation matrix which will minimize the index over the allowable choices.

Leeds and Ugron[17], in the course of their minimization procedure based on Schoeffler's approach, found that the optimum network selected from a series of continuously equivalent networks tends to have the value of the summed sensitivities distributed uniformly with respect to the network elements. This, of course, is to be expected, in view of the invariance property of the summed sensitivities and the nature of the index used. In other words, the absolute minimum of the sum of the magnitude squared criterion will result when all the parts of the sum are equal.

The requirements for a network to be potentially optimally insensitive according to Schoeffler's criterion were investigated by Holt and Fidler[27]. They show that in the case of an LC network, such as that considered by Leeds and Ugron, the coefficients of the numerator and denominator polynomials of the pertinent transfer function must be such that each element appears in all coefficients of the complex frequency variable, s, unless a coefficient corresponds to either (but not both) the highest or the lowest power of s in the network function.

The theoretical limitations of the continuously-equivalent network approach were considered by Schmidt and Kasper[21], who conclude that networks with substantially lower sensitivity can be obtained only if the number of nodes, i.e., the number of network elements, is allowed to increase sufficiently.

3.5 Methods of Computing Sensitivity Functions.

In performing a sensitivity analysis, or during the course of an optimal synthesis procedure, it is often necessary to calculate either the sensitivity of a large number of network functions with respect to a single parameter, or alternatively, the sensitivity of a single network function with respect to a large number of parameters. Such calculations are invariably tedious and time consuming, and considerable effort has been expanded in devising efficient methods and algorithms for their evaluation. There are several ways of approaching this problem:

3.5.1 The Feedback Theory approach

According to Bode's theory of feedback, based on the concept of return difference, we may express the sensitivity of a network function,

T(s), with respect to a specified parameter, x_k, as follows[9,10,28,29]

$$S^T_{x_k} = \frac{1}{F_{x_k}(s)} - \frac{1}{F'_{x_k}(s)} \tag{3.29}$$

where F_{x_k} and F'_{x_k} are the return difference and null return difference, both with respect to x_k. When x_k is the control parameter of a controlled source embedded in the network, we have

$$F_{x_k}(s) = 1 + x_k t(s) \tag{3.30}$$

where t(s) is defined as the negative of the controlling signal that is developed when the externally applied excitation is reduced to zero and the controlled source in question is replaced with an independent source of unit strength. The null return difference, F'_{x_k}, is defined in a similar way, except that in this case, the externally applied excitation is adjusted to reduce the signal developed across the load to zero.

Assuming that the network function, T(s), relates the ℓth nodal voltage (or loop current) to the independent source at the first node (or in the first loop), we may express F_{x_k} and F'_{x_k} as follows:

$$F_{x_k}(s) = \frac{\Delta}{\Delta^o} \tag{3.31}$$

where Δ^o is obtained from the circuit determinant, Δ, by setting x_k equal to zero, and

$$F'_{x_k}(s) = \frac{\Delta_{1\ell}}{\Delta^o_{1\ell}} \tag{3.32}$$

where $\Delta^{o}_{1\ell}$ is obtained from the cofactor $\Delta_{1\ell}$ by setting x_k equal to zero. Hence we may express the sensitivity function $S^{T}_{x_k}$ as

$$S^{T}_{x_k} = \frac{\Delta^{o}}{\Delta} - \frac{\Delta^{o}_{1\ell}}{\Delta_{1\ell}} \tag{3.33}$$

3.5.2 The Bilinear Theorem approach

(a) Parker's Procedure: This procedure is based upon the use of the bilinear theorem, according to which the dependence of the network function, $T(s, x_k)$, on a change, Δx_k, in a particular bilateral element, x_k, can be expressed as follows[30]:

$$T(s, \Delta x_k) = \frac{W(s)\ T(s,0) + x_k\ T(s,\infty)}{W(s) + \Delta x_k} \tag{3.34}$$

where $T(s,0)$ and $T(s,\infty)$ are the limiting values of the network function for Δx_k equal to zero and infinity, respectively, and $W(s)$ is the Thevenin immittance which is measured looking back into the network from the terminals of the adjustable parameter Δx_k, as depicted in Figure 3.1 in which x_{ko} denotes the nominal value of the parameter x_k.

We note that $T(s,0)$ represents the nominal value of the network function. Subtracting $T(s,0)$ from the $T(s,\Delta x_k)$ of Equation 3.34 and allowing Δx_k to approach zero, we obtain in the limit

$$\frac{dT}{dx_k} = \frac{T(s,\infty) - T(s,0)}{x_{ko} + W'(s)} \tag{3.35}$$

where

$$W'(s) = W(s) - x_{ko} \tag{3.36}$$

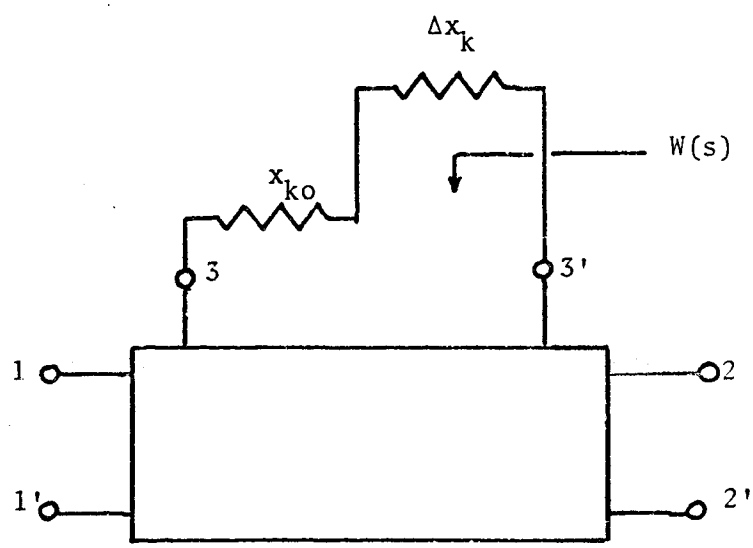

Figure 3.1: Bilinear theorem approach, Parker's Procedure

that is, $W'(s)$ is the Thevenin immittance measured looking into the network at the terminal pair 3-3' of Figure 3.1. The sensitivity function with respect to the parameter x_k is therefore given by

$$S^T_{x_k}(s) = \frac{x_{ko}}{W(s)} \left[\frac{T(s,\infty)}{T(s,0)} - 1\right] \tag{3.37}$$

Thus, we can evaluate the sensitivity function of the network without actually performing a differentiation.

Example 3.1

Consider the network shown in Figure 3.2. To determine the differential sensitivity $\frac{dT}{dL}$, say, we find by inspection, that

$$T(s,0) = \frac{1/LC}{s^2 + s\left\{\frac{R_1}{L} + \frac{1}{CR_2}\right\} + \frac{1}{LC}\left\{1 + \frac{R_1}{R_2}\right\}}$$

$$T(s,\infty) = 0 \tag{3.38}$$

$$W(s) = sL + R_1 + \frac{R_2}{1 + sCR_2}$$

Therefore, substituting in Equation 3.37, we obtain

$$S^T_L(s) = -\frac{L}{R_2}\, s(1 + SCR_2)\, T(s,0) \tag{3.39}$$

(b) Sorensen's Procedure: The use of the bilinear theorem has been extended by Sorensen[31] to include the effect of changes in unilateral elements (e.g., controlled sources). It is shown that

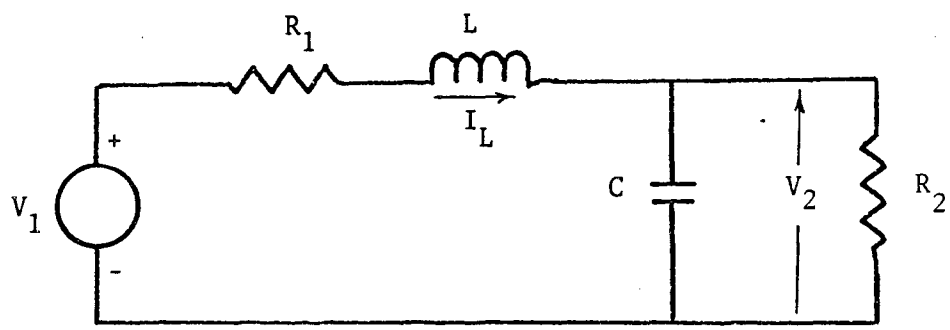

Figure 3.2: Network for Example 3.1

$$\frac{dT}{dx_k} = \frac{T(s,\infty) - T(s,0)}{x_{ko} + \frac{1}{t(s)}} \tag{3.40}$$

where x_k is the control parameter of a controlled source embedded in the network. The x_{ko}, $T(s,0)$ and $T(s,\infty)$ are as previously defined, and $t(s)$ is as defined under the feedback theory approach. It is noteworthy that when the parameter x_k is a bilateral element, we find that $1/t(s)$ takes on a role identical to that of the $W'(s)$ of Equation 3.35.

3.5.3 Approaches based on the use of a related network

In a multiparameter sensitivity analysis, each of the procedures thus far described requires at least as many network analyses as there are variable parameters. Obviously, therefore, these approaches become highly inefficient when considering networks with a large number of variable parameters. It is in this kind of situation that the use of a related network as proposed by Leeds and later extended by Director and Rohrer becomes so highly effective.

(a) Leeds' Auxiliary Network Procedure: The network considered by Leeds[32] is one in which each branch may contain a linear time-invariant resistor, capacitor or inductor. Each branch may also contain an independent current and/or voltage source as well as a dependent current source. The configuration of a typical branch, the jth, say, is shown in Figure 3.3, for which the branch relations are given by

$$\begin{aligned} V_{ej} &= V_{bj} + V_{sj} \\ I_{ej} &= I_{sj} + I_{bj} - I_{cj} \end{aligned} \tag{3.41}$$

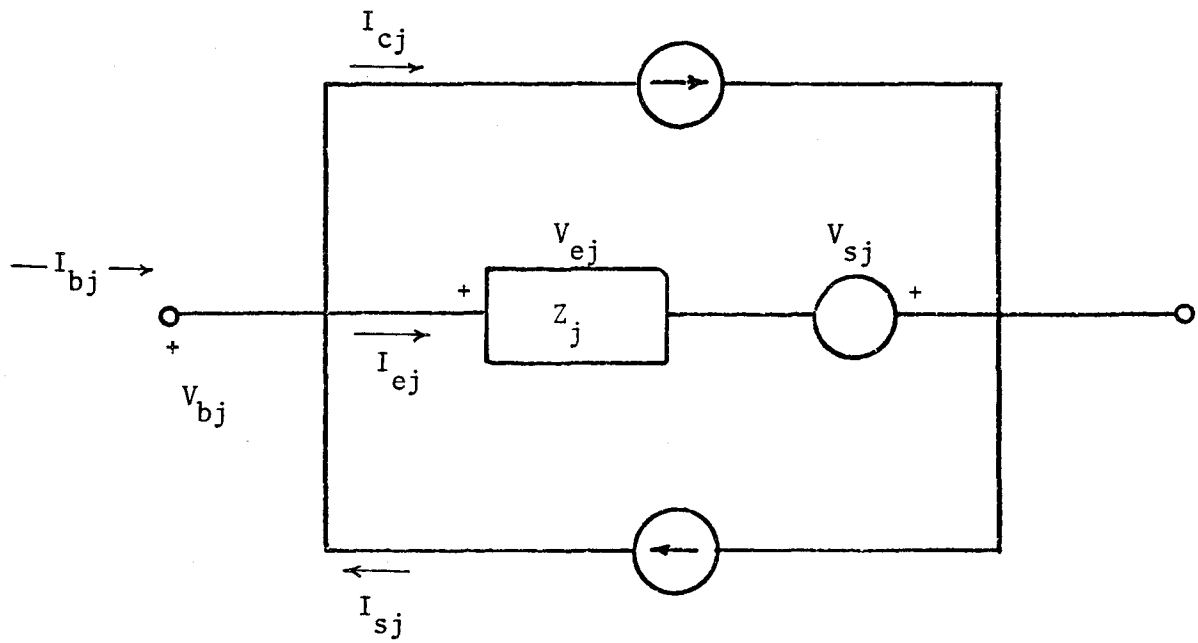

Figure 3.3: Leeds' Procedure; the jth typical branch

and the element equations will be one of the following

$$V_{ej} = R_j I_{ej}$$

$$V_{ej} = sL_j I_{ej} \tag{3.42}$$

$$I_{ej} = sC_j V_{ej}$$

In addition, for the controlled current source we have

$$I_{cj} = \beta_{mj} I_{em} \tag{3.43}$$

Differentiating Equation 3.41 with respect to x_k, the element in the kth branch, we obtain

$$\begin{aligned} V'_{ej} &= V'_{bj} \\ I'_{ej} &= I'_{bj} - I'_{cj} \end{aligned} \tag{3.44}$$

where the prime denotes partial differentiation with respect to x_k, and where derivatives with respect to the independent sources have been set equal to zero. The I'_{cj} will have the form

$$\begin{aligned} I'_{cj} &= \beta_{mj} I'_{em} && \beta_{mj} \neq x_k \\ I'_{ck} &= x_k I'_{em} + I_{em} && \beta_{mk} = x_k \end{aligned} \tag{3.45}$$

Differentiating Equation 3.42 we obtain

$$\begin{aligned} V'_{ej} &= R_j I'_{ej} && x_k \neq R_j \\ V'_{ej} &= sL_j I'_{ej} && x_k \neq L_j \\ I'_{ej} &= sC_j V'_{ej} && x_k \neq C_j \end{aligned} \tag{3.46}$$

and

$$
\begin{aligned}
V'_{ek} &= R_k I'_{ek} + I_{ek} & x_k &= R_k \\
V'_{ek} &= sL_k I'_{ek} + sI_{ek} & x_k &= L_k \\
I'_{ek} &= sC_k V'_{ek} + sV_{ek} & x_k &= C_k
\end{aligned}
\tag{3.47}
$$

The network may be described in matrix form as

$$
\begin{aligned}
\mathbf{B}\,\mathbf{V}_b &= 0 \\
\mathbf{A}\,\mathbf{I}_b &= 0
\end{aligned}
\tag{3.48}
$$

where $\mathbf{B}$ and $\mathbf{A}$ are the fundamental loop and reduced-incidence matrices for the network, and $\mathbf{V}_b$ and $\mathbf{I}_b$ are branch voltage and branch current vectors, respectively. Differentiating Equations 3.48 with respect to x_k, we obtain the sensitivity equations

$$
\begin{aligned}
\mathbf{B}\,\mathbf{V}'_b &= 0 \\
\mathbf{A}\,\mathbf{I}'_b &= 0
\end{aligned}
\tag{3.49}
$$

Substituting Equations 3.44 in 3.49, we obtain

$$
\begin{aligned}
\mathbf{B}\,\mathbf{V}'_e &= 0 \\
\mathbf{A}\,\mathbf{I}'_e + \mathbf{A}\,\mathbf{I}'_c &= 0
\end{aligned}
\tag{3.50}
$$

Substituting Equations 3.47 and 3.48 into 3.50, we see that the equations for the sensitivity calculation differ from those describing the original network in three ways:

(1) All independent sources of the original network have been set equal to zero.

(2) The kth branch now includes a new driving source which may be represented in one of the following ways, depending on the element type ($x_k \neq \beta_{mk}$):

(a) Resistor: A voltage source of value I_{ek} placed in series with the element R_k.

(b) Inductor: A voltage source of value sI_{ek} placed in series with the element L_k.

(c) Capacitor: A current source of value sV_{ek} placed in parallel with the element C_k.

(3) If the $\beta_{mk} = x_k$, a current source of value I_{em} is placed in parallel with the existing controlled current source.

Thus, the procedure for calculating the sensitivity of the various network voltages and currents to variations in a single parameter, x_k, reduces to the following:

(1) Construct an auxiliary network which is a duplicate of the original network, with all independent sources set equal to zero.

(2) Drive this auxiliary network by means of a dependent current source placed across the kth branch. The source is proportional to the current flowing in the kth branch of the original network if $x_k \neq \beta_{mk}$. The constant of proportionality is $-\frac{1}{x_k}$ for resistors and inductors, and $\frac{1}{x_k}$ for capacitors. For the case where $\beta_{mk} = x_k$, the current source is I_{em}.

(3) The voltages and currents in the auxiliary network are the voltage and current sensitivities of the original network with respect to a variation of the parameter x_k, respectively.

For the case of reciprocal networks, Leeds and Ugron[17] have shown that the sensitivity of a network function with respect to all variable parameters of the network may be determined by a single analysis of the auxiliary network. The procedure for this evaluation is as follows:

(1) Place a current source of value unity with zero phase in the auxiliary network in parallel with the network element, x_k, with respect to which the sensitivity of the network function is required.

(2) The voltage across any other element in the auxiliary network, V_j, multiplied by the current through the corresponding element in the original network and divided by the element value itself will give the voltage sensitivity, $\frac{dV_j}{dx_k}$. (For capacitors, the sign is reversed.)

(3) The sensitivity of a single network function of all elements can be obtained by repeating (2) for all elements of the network.

Example 3.2

To illustrate this procedure, consider again the network of Figure 3.2. The sensitivity function, S_L^T, is given by

$$S_L^T \triangleq \frac{dT/T}{dL/L} = \frac{L}{T}\,\frac{1}{V_1}\,\frac{dV_2}{dL} = \frac{L}{T}\,\frac{1}{V_1}\,\frac{\hat{V}_2 I_L}{L} \tag{3.51}$$

where I_L is the current through the inductor L in the original network:

$$I_L = \frac{V_1}{R_1 + sL + \dfrac{R_2}{1 + sCR_2}} \tag{3.52}$$

where $\hat{V}_2$ is the voltage across R_2 in the auxiliary network (see Figure 3.4):

$$\hat{V}_2 = \frac{R_2 \hat{V}_T}{R_2 + R_1(1 + sCR_2)} \tag{3.53}$$

with

$$\hat{V}_T = \frac{sL\left\{R_1 + \dfrac{R_2}{1 + sCR_2}\right\}}{R_1 + sL + \dfrac{R_2}{1 + sCR_2}} \tag{3.54}$$

From Equations 3.51 to 3.54, we thus obtain

$$S_L^T = -\frac{L}{R_2}\, s(1 + sCR_2)\, T(s) \tag{3.55}$$

(b) <u>Director and Rohrer's Adjoint Network Approach</u>: The approach by Leeds and Ugron has been extended to the case of non-reciprocal networks by Director and Rohrer[33,34] through the use of a so-called "adjoint" network. This approach allows the sensitivity of any network function with respect to all of the variable parameters to be ascertained by only two network analyses per frequency point over the frequency range of interest.

The adjoint network, $\hat{N}$, is derived from the originally specified network, N, through use of Tellegen's theorem. The requirement that both N and $\hat{N}$ have the same topology, but not necessarily the same element types in corresponding branches, is first imposed so that Tellegen's theorem may be applied as follows

$$\begin{aligned} \sum_i V_i \hat{I}_i &\equiv 0 \\ \sum_i \hat{V}_i I_i &\equiv 0 \end{aligned} \tag{3.56}$$

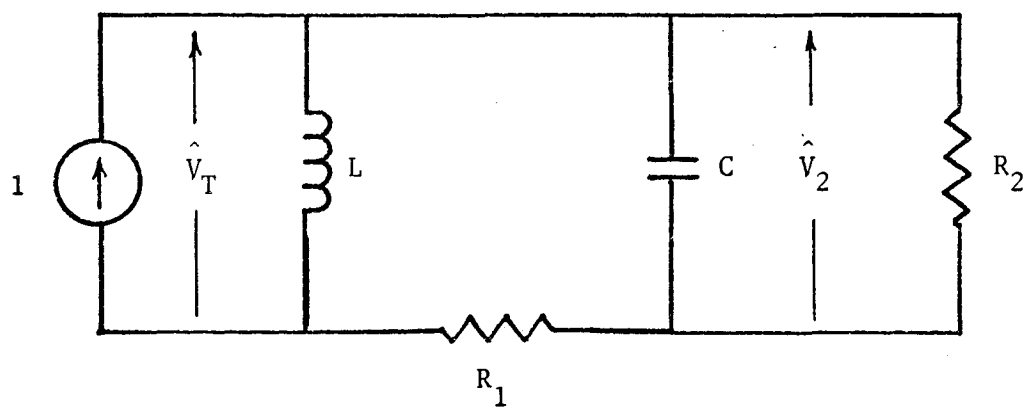

Figure 3.4: Leed's auxiliary network for Example 3.2

where the $\hat{I}_i$ and $\hat{V}_i$ refer to the adjoint network, and where the summation is taken over all branches of the networks N and $\hat{N}$. If the element values of the network N are now perturbed, thus causing a variation in the branch voltages and currents (which we will denote by ΔV_i and ΔI_i, respectively), we may write

$$\sum_i \{\Delta V_i \hat{I}_i - \Delta I_i \hat{V}_i\} \equiv 0 \tag{3.57}$$

For sensitivity calculations, we are usually interested in the sensitivity of a network response with respect to variations in the network elements, not with respect to variations in branch voltages and/or currents. Accordingly, we relate the ΔV_i and ΔI_i to the changes in element values; that is, if

$$\begin{aligned} V_i &= F_i(x_i) \\ I_i &= G_i(x_i) \end{aligned} \tag{3.58}$$

then

$$\begin{aligned} \Delta V_i &= \frac{\partial F_i}{\partial x_i} \Delta x_i \\ \Delta I_i &= \frac{\partial G_i}{\partial x_i} \Delta x_i \end{aligned} \tag{3.59}$$

Hence,

$$\sum_i \left\{ \frac{\partial F_i}{\partial x_i} \hat{I}_i - \frac{\partial G_i}{\partial x_i} \hat{V}_i \right\} \Delta x_i = 0 \tag{3.60}$$

that is

$$\frac{\partial F_i}{\partial x_i} \hat{I}_i = \frac{\partial G_i}{\partial x_i} \hat{V}_i \tag{3.61}$$

We can now interpret Equation 3.60 as the branch relationship for the ith branch of the adjoint network. In this way all of the elements of the adjoint network may be determined.

Thus, we find that the adjoint network, $\hat{N}$, is topologically equivalent to the originally specified network, N, and is defined as follows (see Tables 3.1 and 3.2):

(i) All resistance, capacitance and inductance branches and transformers in N are associated with resistance, capacitance and inductance branches and transformers in $\hat{N}$, respectively.

(ii) All gyrators in N with gyration resistance r become gyrators in $\hat{N}$ with gyration resistance -r.

(iii) All voltage-controlled voltage sources in N become current-controlled current sources in $\hat{N}$ with controlling and controlled branches reversing roles, and with voltage amplification factor, μ, becoming current amplification factor $-\mu$.

(iv) All current-controlled current sources in N become voltage-controlled voltage sources in $\hat{N}$ with controlling and controlled branches reversing roles, and with current amplification factor, β_c, becoming voltage amplification factor, $-\beta_c$.

(v) All voltage-controlled current sources and current-controlled voltage sources have their controlling and controlled branches in N reversed in $\hat{N}$.

(vi) All the independent sources in N, except the sources relevant to the network function under consideration, are associated with zero valued sources in $\hat{N}$. The relevant sources have the following inputs in N and $\hat{N}$:

(a) For the computation of the sensitivities of a driving-point impedance (admittance) at port k, insert a unit current

Element Type	Branch Relation in N	Network N 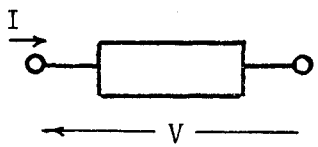	Adjoint network $\hat{N}$ 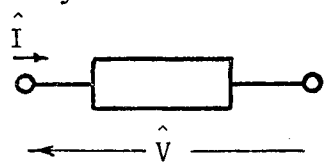	Branch Relation in $\hat{N}$	$\frac{dT}{dx_i}$
Resistance	$V = RI$			$\hat{V} = R\hat{I}$	$\frac{dT}{dR} = -I\hat{I}$
Inductance	$V = sLI$	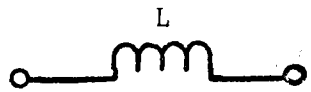	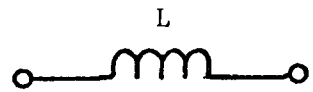	$\hat{V} = sL\hat{I}$	$\frac{dT}{dL} = -sI\hat{I}$
Capacitance	$I = sCV$	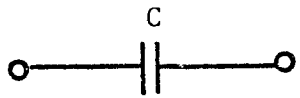	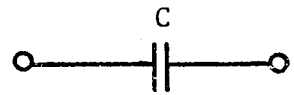	$\hat{I} = sC\hat{V}$	$\frac{dT}{dC} = sV\hat{V}$

Table 3.1

Element Type	Branch Relation in N	Network N	Adjoint Network N	Branch Relation in $\hat{N}$	$\frac{dT}{dx_i}$
Transformer	$V_2 = nV_1$ $I_1 = -nI_2$	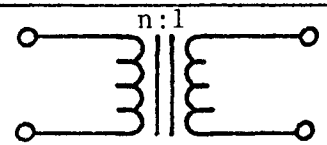	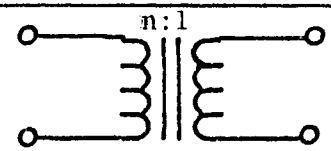	$\hat{V}_2 = n\hat{V}_1$ $\hat{I}_1 = -n\hat{I}_2$	$\frac{dT}{dn} = -(V_1\hat{I}_2+I_2\hat{V}_1)$
Gyrator	$V_1 = rI_2$ $V_2 = -rI_1$	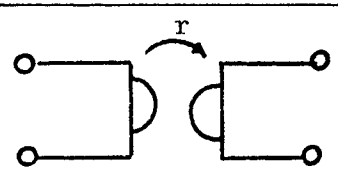	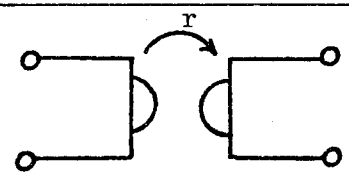	$\hat{V}_1 = -r\hat{I}_2$ $\hat{V}_2 = r\hat{I}_1$	$\frac{dT}{dr} = -(I_2\hat{I}_1-I_1\hat{I}_2)$
Voltage-controlled voltage source	$V_2 = \mu V_1$ $I_1 = 0$	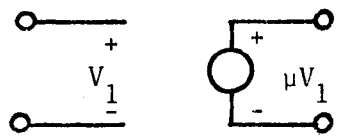	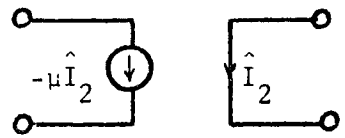	$\hat{I}_1 = -\mu\hat{I}_2$ $V_2 = 0$	$\frac{dT}{d\mu} = -V_1\hat{I}_2$
Current-controlled current source	$I_2 = \beta_c I_1$ $V_1 = 0$	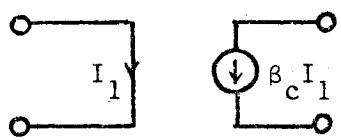	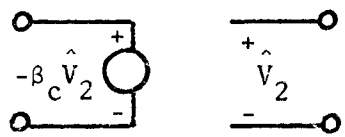	$\hat{V}_1 = -\beta_c\hat{V}_2$ $\hat{I}_2 = 0$	$\frac{dT}{d\beta_c} = I_1\hat{V}_2$
Voltage-controlled current source	$I_2 = g_m V_1$ $I_1 = 0$	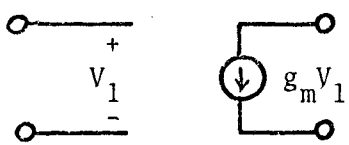	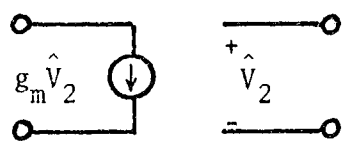	$\hat{I}_1 = g_m\hat{V}_2$ $\hat{I}_2 = 0$	$\frac{dT}{dg_m} = V_1\hat{V}_2$
Current-controlled voltage source	$V_2 = r_m I_1$ $V_1 = 0$	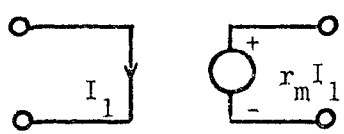	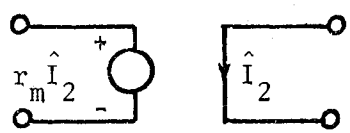	$\hat{V}_1 = r_m\hat{I}_2$ $\hat{V}_2 = 0$	$\frac{dT}{dr_m} = -I_1\hat{I}_2$

Table 3.2

(voltage) source for both N and $\hat{N}$.

(b) For the computation of the sensitivities of a transfer impedance (admittance) between ports j and k, insert a unit current (voltage) source at port j and insert a zero valued current (voltage) source at port k in the original network, and vice versa in the adjoint network $\hat{N}$.

(c) For the computation of the sensitivities of a current (voltage) transfer ratio between ports j and k, insert a unit current (voltage) source at port j, and a zero valued voltage (current) source across port k for the original network. A zero valued current (voltage) source is inserted at port j and a unit voltage (current) source is inserted at port k in the adjoint network.

The differential sensitivities, dT/dx_i, are defined in terms of the voltage or current responses in the pertinent branches of the original and the adjoint networks, as listed in Tables (1) and (2).

The significance of the Director-Rohrer approach is that the sensitivity of any network function with respect to all of the network variables can be obtained by appropriate application of unity and zero-valued sources to the original and the adjoint networks. In other words, by two runs of a network analysis program, all the various dT/dx_i can be evaluated simultaneously. The methods has recently been extended to the case where second-derivative sensitivities are required[35,36].

It is noteworthy that the computational effort that is required for the analysis of the original network and its mutually reciprocal adjoint network may be reduced considerably by taking advantage of the

fact that the nodal admittance matrix of the adjoint network is merely the transpose of the nodal admittance matrix of the original network, and by then applying LU factorization[36].

To illustrate this point, we first note that the branch relations for the original network N can be written as

$$\mathbf{I}_b = \mathbf{y}\mathbf{V}_b \tag{3.62}$$

where $\mathbf{y}$ is the branch admittance matrix, $\mathbf{I}_b$ is the branch current vector, and $\mathbf{V}_b$ is the branch voltage vector. The nodal admittance matrix, $\mathbf{Y}$, is defined as

$$\mathbf{Y} = \mathbf{A}\mathbf{y}\mathbf{A}^t \tag{3.63}$$

where $\mathbf{A}$ is the reduced nodal incidence matrix and $\mathbf{A}^t$ is its transpose. The adjoint network $\hat{N}$ has the same topology as the original network and, therefore, has the same nodal incidence matrix $\mathbf{A}$. The branch relations of the adjoint network are

$$\hat{\mathbf{I}}_b = \hat{\mathbf{y}}\hat{\mathbf{V}}_b \tag{3.64}$$

where $\hat{\mathbf{I}}_b$, $\hat{\mathbf{y}}$ and $\hat{\mathbf{V}}_b$ are as defined previously, except that they now refer to the adjoint network, $\hat{N}$. The nodal admittance matrix of $\hat{N}$ is

$$\hat{\mathbf{Y}} = \mathbf{A}\hat{\mathbf{y}}\mathbf{A}^t \tag{3.65}$$

and since

$$\hat{\mathbf{y}} = \mathbf{y}^t \tag{3.66}$$

therefore

$$\hat{\mathbf{Y}} = \mathbf{Y}^t \tag{3.67}$$

i.e., the nodal admittance matrix for N is simply the transpose of that for $\hat{N}$.

In order to calculate the first-order sensitivities of the network, it is necessary to calculate all the node voltages of the original and adjoint networks. This requires the solution of the following equations

$$\begin{aligned} \mathbf{V} &= \mathbf{Y}^{-1}\mathbf{I} \\ \hat{\mathbf{V}} &= [\mathbf{Y}^t]^{-1}\hat{\mathbf{I}} \end{aligned} \tag{3.68}$$

One possible approach is to calculate $\mathbf{Y}^{-1}$ once, noting that $[\mathbf{Y}^t]^{-1} = [\mathbf{Y}^{-1}]^t$. The inverse matrix, $\mathbf{Y}^{-1}$, may be computed by means of Gaussian elimination[37] which involves p^3 operations (one operation is defined as either one multiplication and addition or one division) where p is the order of the nodal admittance matrix, $\mathbf{Y}$. An additional p^2 operations are required to compute $\mathbf{Y}^{-1}\mathbf{I}$, so that at least $p^3 + 2p^2$ operations are necessary to calculate the required nodal voltages by the matrix inversion method.

On the other hand, a significant reduction in operations necessary can be obtained by means of LU factorization. The admittance matrix, $\mathbf{Y}$, can be decomposed into a product of a lower triangular matrix, $\mathbf{L}$, and an upper triangular matrix, $\mathbf{U}$, i.e.,

$$\mathbf{Y} = \mathbf{LU}$$

where $\mathbf{U}$ has each diagonal term equal to unity. This decomposition may be accomplished by $1/3p\ (p^2 - 1)$ operations by means of standard Guassian elimination[38]. The nodal equations for N may now be written as

$$\mathbf{LUV} = \mathbf{I} \tag{3.69}$$

The voltage vector $\mathbf{V}$ can be determined by first computing a temporary vector, $\mathbf{b}$, say, by forward substitution, that is

$$\mathbf{Lb} = \mathbf{I} \tag{3.70}$$

which requires $p(p + 1)/2$ operations. Then, we use $\mathbf{b}$ to find $\mathbf{V}$ by backward substitution,

$$\mathbf{UV} = \mathbf{b} \tag{3.71}$$

which requires $p(p - 1)/2$ operations. Thus a total of $2p^2$ operations are required to obtain all the nodal voltages in N and $\hat{N}$. This means that a total of $1/3p(p^2 - 1) + 2p^2$ operations are necessary to determine all of the first-derivative sensitivity functions using the LU factorization method. In other words, a savings of $1/3p(2p^2 + 1)$ operations is obtained by use of this method. In a similar manner, it can be shown that the same savings results when second derivative sensitivities are required.

Example 3.3

To illustrate the Director-Rohrer approach, consider again the network of Figure 3.2 and its mutually adjoint network as shown in Figure 3.5. By inspection, we have

$$I_L = \frac{1 + sCR_2}{R_2} \tag{3.72}$$

and

$$\hat{I}_L = \frac{-\hat{V}_C}{R_1 + sL} = T(s) \tag{3.73}$$

from which

$$S_L^T \triangleq \frac{L}{T} \frac{dT}{dL}$$

$$= \frac{-L}{T} sL_L \hat{I}_L \tag{3.74}$$

$$= \frac{L}{R_2} s(1 + sCR_2) T(s)$$

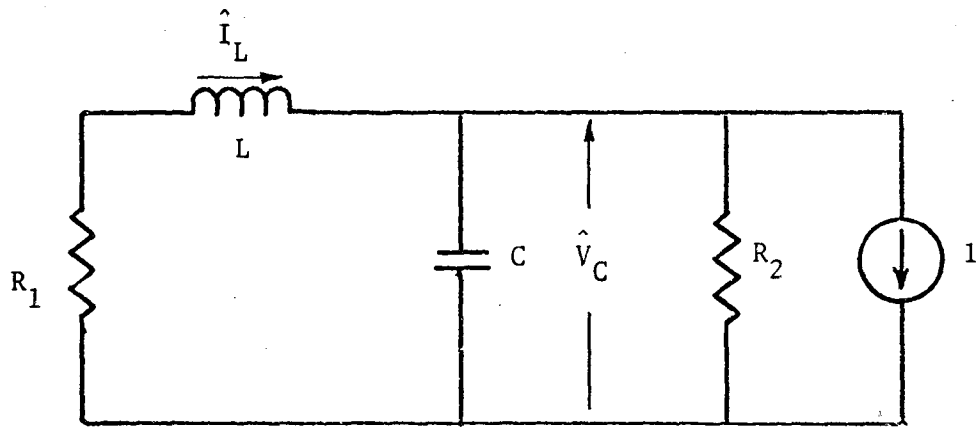

Figure 3.5: Director and Rohrer's adjoint network for Example 3.3

Example 3.4

As another example of the Director-Rohrer method, consider the network of Figure 3.6(a) which contains a voltage-controlled current source $g_m V_1$. The transfer function, T(s), is chosen as $\frac{V_2}{I_1}$. The mutually reciprocal adjoint network corresponding to this network is shown in part (b) of the diagram. Suppose it is required to determine $\frac{dT}{dg_m}$. According to the Director-Rohrer procedure, we may write

$$\frac{dT}{dg_m} = V_1 \hat{V}_2 \tag{3.75}$$

where the voltages V_1 and $\hat{V}_2$ are as defined in parts (a) and (b) of Figure 3.6, respectively. By inspection, the nodal equations for the original network are

$$\begin{bmatrix} 1 \\ 0 \end{bmatrix} = \begin{bmatrix} G_1 + sC_1 & -sC_1 \\ g_m - sC_1 & G_2 + s(C_1+C_2) \end{bmatrix} \begin{bmatrix} V_1 \\ V_2 \end{bmatrix} \tag{3.76}$$

and for the adjoint network, they are

$$\begin{bmatrix} 0 \\ 1 \end{bmatrix} = \begin{bmatrix} G_1 + sC_1 & g_m - sC_1 \\ -sC_1 & G_2 + s(C_1 + C_2) \end{bmatrix} \begin{bmatrix} \hat{V}_1 \\ \hat{V}_2 \end{bmatrix} \tag{3.77}$$

Equations 3.76 and 3.77 show, as expected, that the nodal admittance matrix of the adjoint network is the transpose of the nodal admittance matrix of the original network.

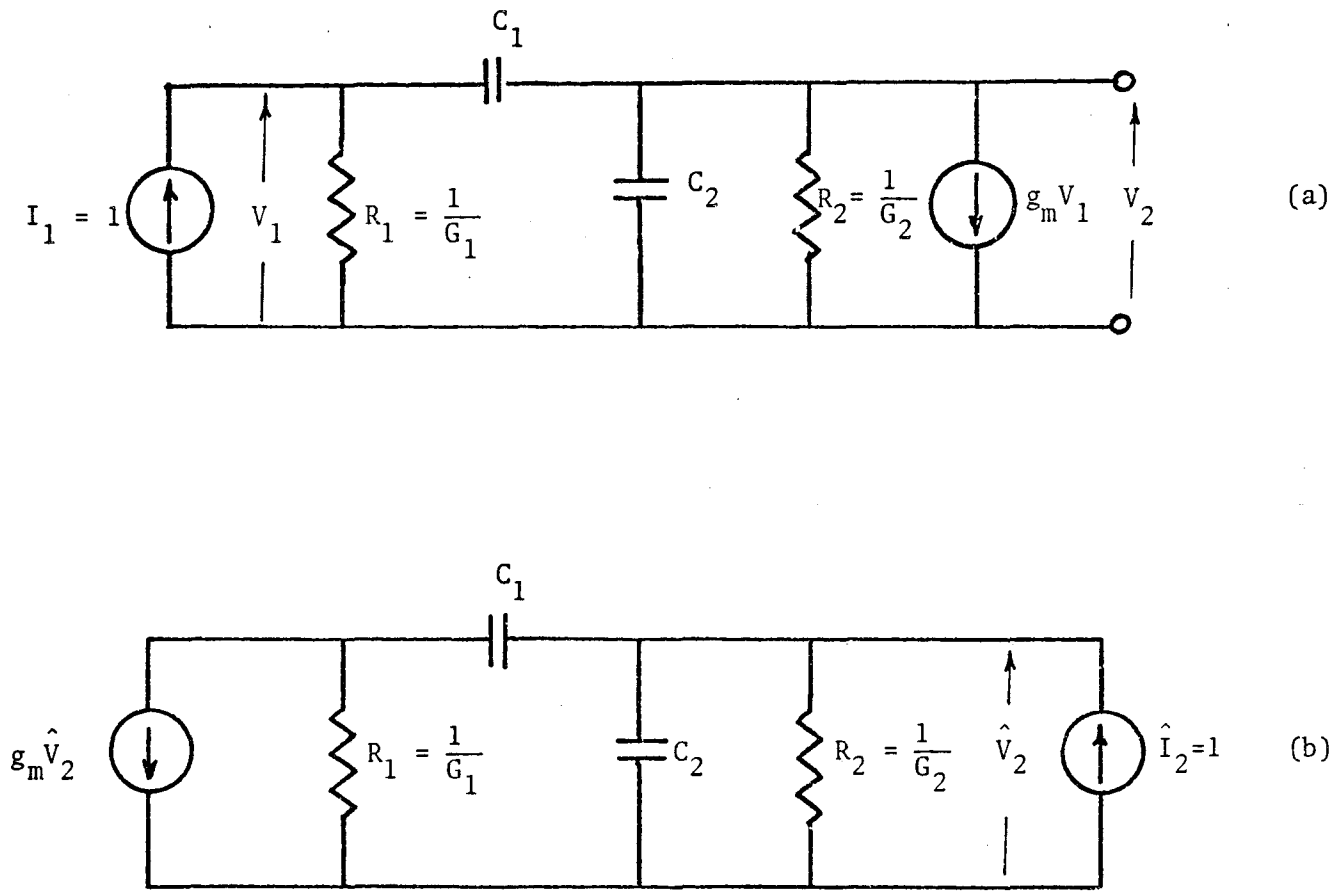

Figure 3.6: Original and adjoint networks for Example 3.4

(a) Originally specified network

(b) Its mutually reciprocal adjoint network

Using Equations 3.76 and 3.77 to evaluate V_1 and V_2, respectively, and substituting in Equation 3.75, we obtain

$$\frac{dT}{dg_m} = \frac{s^2C_1(C_1+C_2) + s(C_1G_1 + C_2G_1 + C_1G_2) + G_1G_2}{s^2C_1C_2 + s(C_1G_1 + C_2G_1 + C_1G_2 + C_1g_m) + G_1G_2} \tag{3.78}$$

3.5.4 Connection between the Feedback Theory and the Director-Rohrer Approaches

As pointed out earlier, Director and Rohrer have made use of Tellegen's theorem to derive their method of sensitivity calculation. It is also possible to use Bode's feedback theory as an alternative way of deriving their method.

Consider the network of Figure 3.7. For convenient analysis, we will assume the network consists of linear time-invariant resistors, capacitors, inductors and voltage-controlled current sources. The network is shown with a particular voltage-controlled current source singled out for special consideration. According to the Director-Rohrer method, the partial derivative of the transfer function, $T(s) = \frac{V_2}{I_1}$, with respect to the parameter, g_m, is given by

$$\frac{\partial T}{\partial g_m} = V_{ij}\,\hat{V}_{k\ell} \tag{3.79}$$

where V_{ij} is the control voltage developed between nodes i and j of the original network, and $\hat{V}_{k\ell}$ is the control voltage developed between nodes k and ℓ of the adjoint network, $\hat{N}$, shown in Figure 3.8. When the variable parameter is a bilateral element, of admittance Y, connected between nodes k and ℓ, Equation 3.79 takes on the special form

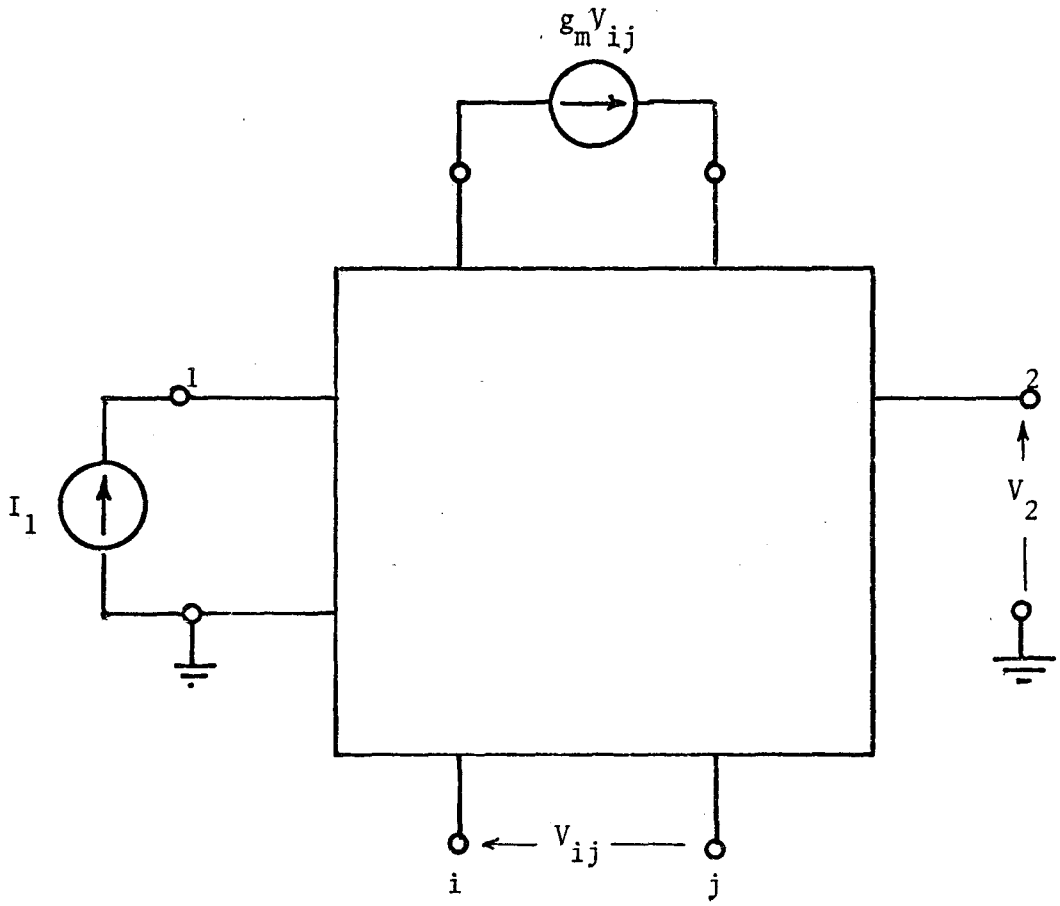

Figure 3.7: The original network N with a voltage-controlled current source singled out for special consideration

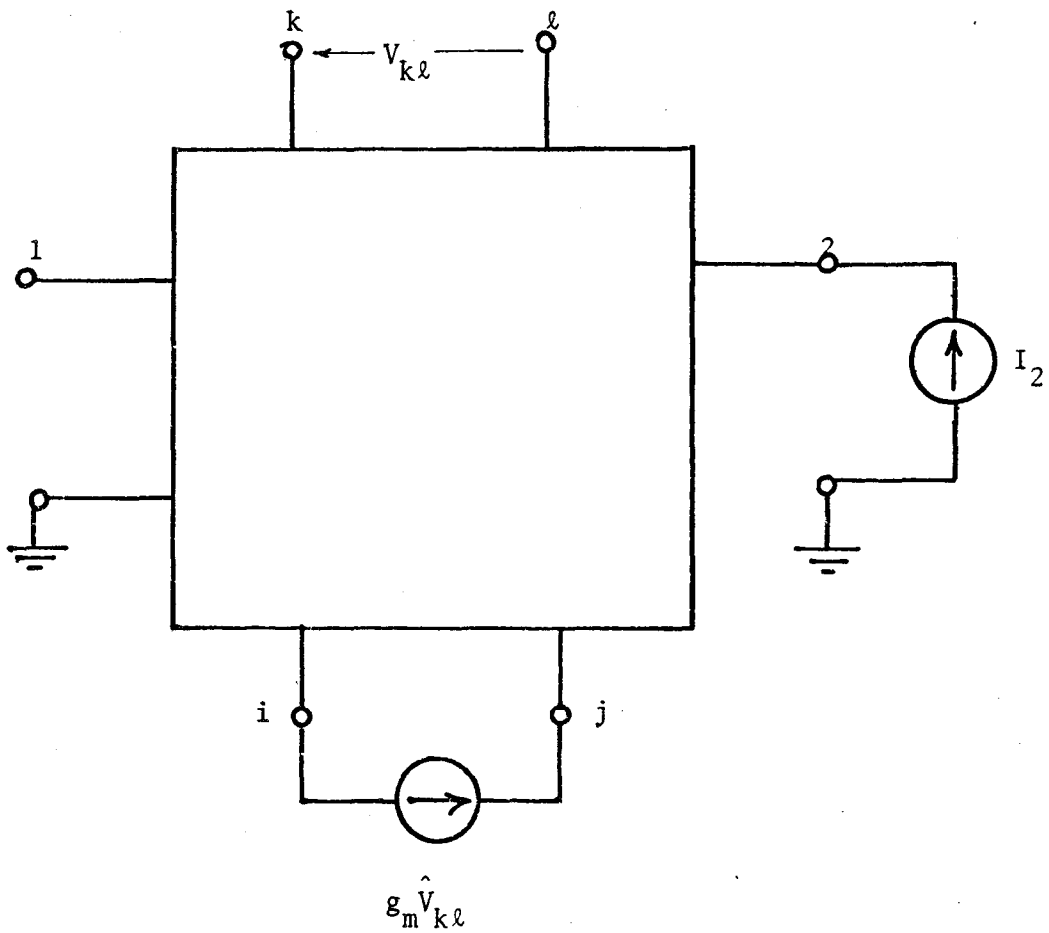

Figure 3.8: The adjoint network $\hat{N}$

$$\frac{\partial T}{\partial Y} = V_{k\ell}\hat{V}_{k\ell} \tag{3.80}$$

Using the nodal method of analysis, we may express the transfer function T(s) as follows

$$T(s) = \frac{\Delta_{12}}{\Delta} \tag{3.81}$$

where Δ is the circuit determinant of the network N, defined by

$$\Delta = \begin{vmatrix} y_{11} & y_{12} & \cdot & \cdot & y_{1i} & y_{1j} & \cdot & \cdot & y_{1n} \\ y_{21} & y_{22} & \cdot & \cdot & y_{2i} & y_{2j} & \cdot & \cdot & y_{2n} \\ \cdot & \cdot & \cdot & \cdot & \cdot & \cdot & \cdot & \cdot & \cdot \\ \cdot & \cdot & \cdot & \cdot & \cdot & \cdot & \cdot & \cdot & \cdot \\ y_{k1} & y_{k2} & \cdot & \cdot & y_{ki}+g_m & y_{kj}-g_m & \cdot & \cdot & y_{kn} \\ y_{\ell 1} & y_{\ell 2} & \cdot & \cdot & y_{\ell i}-g_m & y_{\ell j}+g_m & \cdot & \cdot & y_{\ell n} \\ \cdot & \cdot & \cdot & \cdot & \cdot & \cdot & \cdot & \cdot & \cdot \\ \cdot & \cdot & \cdot & \cdot & \cdot & \cdot & \cdot & \cdot & \cdot \\ y_{n1} & y_{n2} & \cdot & \cdot & y_{ni} & y_{nj} & \cdot & \cdot & y_{nn} \end{vmatrix} \tag{3.82}$$

and Δ_{12} is the cofactor of y_{12} in Δ. In Equation 3.82 the various y's denote the self- and mutual-admittances of the network of Figure 3.7 exclusive of the controlled source $g_m V_{ij}$. By expanding the determinant of Equation 3.82, we obtain

$$\Delta = \Delta^o + g_m\{\Delta_{ki} - \Delta_{\ell i} - \Delta_{kj} + \Delta_{\ell j}\} \tag{3.83}$$

where Δ^o is obtained from Δ by putting g_m equal to zero. Similarly, we

may express Δ_{12} as

$$\Delta_{12} = \Delta_{12}^{o} + g_m\{\Delta_{12,ki} - \Delta_{12,\ell i} - \Delta_{12,kj} + \Delta_{12,\ell j}\} \qquad \text{------ (3.84)}$$

where Δ_{12}^{o} is obtained from Δ_{12} by putting g_m equal to zero.

According to Bode's feedback theory[9], the sensitivity of T(s) with respect to g_m can be expressed as follows

$$S_{g_m}^{T} \triangleq \frac{\partial T/T}{\partial g_m/g_m} = \frac{\Delta^{o}}{\Delta} - \frac{\Delta_{12}^{o}}{\Delta_{12}} \qquad (3.85)$$

Using Equations 3.81 through 3.85 to evaluate $\frac{\partial T}{\partial g_m}$, we obtain

$$\frac{\partial T}{\partial g_m} = \frac{1}{\Delta^2} \Big\{ [\Delta\Delta_{12,ki} - \Delta_{12}\,\Delta_{ki}] - [\Delta\Delta_{12,\ell i} - \Delta_{12}\,\Delta_{\ell i}] - [\Delta\Delta_{12,kj} - \Delta_{12}\,\Delta_{kj}] + [\Delta\Delta_{12,\ell j} - \Delta_{12}\,\Delta_{\ell j}] \Big\} \qquad (3.86)$$

However, from the theory of determinants, we have the identity

$$\Delta\Delta_{ab,cd} = \Delta_{ab}\,\Delta_{cd} - \Delta_{ad}\,\Delta_{cb} \qquad (3.87)$$

Hence, we may rewrite Equation 3.86 as

$$\frac{\partial T}{\partial g_m} = \left\{\frac{\Delta_{1i}}{\Delta} - \frac{\Delta_{1j}}{\Delta}\right\} \left\{\frac{\Delta_{k2}}{\Delta} - \frac{\Delta_{\ell 2}}{\Delta}\right\} \qquad (3.88)$$

For the case of network N, we recognize that (with the independent current source $I_1 = 1$ amp) the node voltages V_i and V_j, with respect to the reference node, are given by

$$V_i = \frac{\Delta_{1i}}{\Delta} \tag{3.89}$$

$$V_j = \frac{\Delta_{1j}}{\Delta}$$

On the other hand, for the adjoint network, $\hat{N}$, we recognize that (again with the independent current source $I_2 = 1$ amp) the node voltages $\hat{V}_k$ and $\hat{V}_\ell$ are given by

$$\hat{V}_k = \frac{\hat{\Delta}_{2k}}{\hat{\Delta}}$$

$$\hat{V}_\ell = \frac{\hat{\Delta}_{2\ell}}{\hat{\Delta}} \tag{3.90}$$

where $\hat{\Delta}$ is the circuit determinant of the adjoint network $\hat{N}$. Since, by definition, the nodal admittance matrix of the adjoint network is the transpose of the original network, we have

$$\hat{\Delta} = \Delta$$

$$\hat{\Delta}_{2k} = \Delta_{k2} \tag{3.91}$$

$$\hat{\Delta}_{2\ell} = \Delta_{\ell 2}$$

Hence,

$$\hat{V}_k = \frac{\Delta_{k2}}{\Delta} \tag{3.92}$$

$$\hat{V}_\ell = \frac{\Delta_{\ell 2}}{\Delta}$$

Clearly, by combining Equations 3.88, 3.89 and 3.90, we obtain the result given in Equation 3.79. In a similar manner, we can derive Equation 3.80 for the case of a bilateral element by placing the controlled source and the control voltage across the same pair of terminals in Figures 3.7 and 3.8.

3.5.5 Other approaches

In a recent contribution[39], Neill derives an approximate linear relationship between the network function and component parameter deviations. The relationship is expressed in the form

$$T(s,x_i) = T(s,x_{io}) + \sum_{i=1}^{n} \gamma_i(s)\ \delta x_i \tag{3.93}$$

where $T(s,x_{io})$ is the exact response, x_i represents the normalized deviation of the ith parameter, and γ_i is a rational function with known coefficients. Equation 3.93 is, in effect, a first-order Taylor series expansion of the changed function $T(s,x_i)$ about its nominal value $T(s,x_{io})$. The modification necessary to incorporate second-order terms in the expansion for the case of linear and non-linear systems has been described by the same author[40,41].

Goddard and Spence[42] have also proposed a method for calculating first- and second-order sensitivities. Their results have been compared with those obtained by Neill, and the compatibility of the two sets of results is demonstrated[43].

3.6 Conclusion:

In the optimum design of a network based on sensitivity considerations, we need a sensitivity criterion, or index of performance, which gives a meaningful measure of the multiparameter sensitivity of the network. Several such indices have been proposed in the literature, and some have been used in optimal synthesis procedures. However, all of these indices appear to have the following limitations:

(1) In a sensitivity criterion of the $\left\{S^T_{x_i} . S^{T^*}_{x_i}\right\}$ type, uniform weighting is automatically assigned to each elemental sensitivity function. Now this may be justified in those cases where, for example, the parameters have uniform tolerances, or where all the parameters have equal temperature coefficients. However, in many cases these conditions do not apply, and in such cases some means of accommodating a non-uniform weighting among individual sensitivities should be incorporated into the index.

(2) No allowance has been made for the possibility of a change in one parameter compensating for the effect of a change in another.

(3) The minimization of a sensitivity criterion at a single frequency, as proposed by Schoeffler, leads to a network which is optimally insensitive at that particular frequency. In some cases, this may mean that the network is also optimally insensitive at all other frequencies[17]. However, there is evidence to suggest that this is not always the case[44], and that an index based on a range of frequencies may be more informative than one evaluated at a single frequency.

For these reasons, it is considered appropriate to define a new multiparameter sensitivity index of performance which will accommodate

non-uniform weighting among elemental sensitivities, and at the same time will not exclude the possibility of sensitivity compensation occurring. This is done in Chapter IV. In Chapter V, a new method of computing sensitivity functions is described. The method is based on an algorithm which allows the differentiation operation to be performed directly on any network function of interest. The method requires but one network analysis, regardless of the number of frequency points at which the index is to be computed, and regardless of the number of iterations in the optimal search routine.

CHAPTER IV

THE MULTIPARAMETER SENSITIVITY INDEX OF PERFORMANCE

4.1 Introduction:

The multiparameter sensitivity problem is usually expressed in terms of a sensitivity function or index of performance which defines the influence of simultaneous variations in some or all of the network parameters on the performance of the network. The sensitivity criterion thus chosen is used to obtain an optimum design by indicating an optimum choice of realizable network structure, or the element values for a less sensitive structure.

In network theory, as has been pointed out in Chapter III, the early sensitivity studies were concerned with a single variable, such as the sensitivity of some network function with respect to a particular parameter. However with the increased use of the digital computer as a design tool, we are now able to tackle the more difficult problem of evaluating the sensitivity of a network to variations in a multitude of network parameters. Also, the advent of integrated circuitry has brought the multiparameter sensitivity problem into further prominence. With such networks, no longer can we call for close tolerances nor can we expect a high degree of parameter constancy even from passive elements.

In this chapter, we shall define a new multiparameter sensitivity index of performance, and we shall describe, in some detail, a new method for the evaluation of sensitivity functions. The index has been applied

to the important cases of low-pass LC-ladder and RC-active filters. In particular, it was used to evaluate the effect of increasing the filter order, varying the magnitude of the passband ripple, varying the amount of dissipation and varying the source/load resistance ratio upon the overall sensitivity performance of LC-ladder filters. We shall also outline a procedure for determining, for a given network, an "optimum tolerance set" which ensures that the various element changes contribute equally to the total change in the network response.

4.2 A New Multiparameter Sensitivity Index of Performance:

The use of an index of performance as an aid in the optimal synthesis of control systems is a well established procedure, and while several such indices have been proposed for use in network theory, their practical use in this area to date has been limited. The choice of such an index is most important; it should be general enough to be widely applicable, yet selective enough to make the best or optimum network readily discernable. It should be both reliable and realistic, reliable in the sense that one should have confidence in the results obtained when using it, regardless of the network being analysed, and realistic in the sense that it should give a meaningful indication of the sensitivity performance of the network in question. Because the choice of index is so important, we will approach our definition in a step by step fashion, and we will try to justify each such step wherever necessary.

Consider the case of a lumped linear time-invariant network. Let the network function of interest be denoted by

$$T(s,x) = \frac{N(s,x)}{D(s,x)} \tag{4.1}$$

where $N(s,\mathbf{x})$ and $D(s,\mathbf{x})$ are polynomials in the complex frequency variable, s, with coefficients that are functions of one or more of the network variables, $\mathbf{x}$, where

$$\mathbf{x}^t = [x_1, x_2, \ldots, x_n] \tag{4.2}$$

If we are concerned only with the realization of a given characteristic without regard to its sensitivity, then an index of performance that gives a measure of the extent to which the chosen network structure and nominal element set approximates to the given network function is suitable. Such an index may be defined in terms of the absolute error between the actual and desired response functions. In other words, the problem is one of minimizing the error between a desired and a realizable characteristic, and in this case, the absolute error is a suitable criterion for determining the extent to which the desired characteristic is being approximated.

On the other hand, in sensitivity studies, we are primarily concerned with the effect of parameter changes on the shape of the response characteristic. In this case, an index of sensitivity performance is best defined in terms of the fractional, rather than the absolute, error between the nominal and perturbed network characteristic. The reason for this is two-fold. In the first place, when evaluating the sensitivity of the network element values, we might want to allocate equal weighting to the error which occurs within the passband as without. In other words, it is often just as important that unwanted frequencies should be suppressed as it is that the frequencies of interest should be transmitted with a minimum of attenuation. The second reason is closely related to the first,

and is best described by means of an example. Let us consider two hypothetical networks, N_a and N_b, both of which have the same structure, and each of which has an ideal low-pass response characteristic as is shown in Figure 4.1. Let us now apply an equal fractional change to the kth element of each network. Let the resulting changes in the network response characteristics by δT_a and δT_b, respectively, as depicted in the diagram. By inspection, the networks are equally sensitive to this perturbation. However, if we were to define their sensitivities in terms of the absolute value of the error, we would find that network N_a is ten times as sensitive as network N_b, simply because the level of transmission through N_a is ten times that through N_b. Clearly, it is the fractional error that should be considered in such a case, and accordingly, it is the fractional change in $T(s,x)$ that is considered in the following development.

Suppose we let the element x_k be changed by an incremental amount δx_k. The resulting fractional change in $T(s,x)$ is equal to $\frac{\partial T}{\partial x_k} \cdot \frac{\delta x_k}{T}$ where $\frac{\partial T}{\partial x_k}$ is a function of s, and δx_k can be a positive or negative real number. Assuming that all the network variables change simultaneously, the total fractional change in $T(s,x)$ due to all such changes, to a first-order approximation, is given by

$$\frac{\Delta T}{T} = \sum_{i=1}^{n} \frac{\partial T}{\partial x_i} \frac{\delta x_i}{T} = \sum_{i=1}^{n} S_{x_i}^{T} \frac{\delta x_i}{x_i} \tag{4.3}$$

where $S_{x_i}^{T}$, the elemental sensitivity function, is defined by

$$S_{x_i}^{T} \triangleq \frac{\partial T}{\partial x_i} \frac{x_i}{T} \tag{4.4}$$

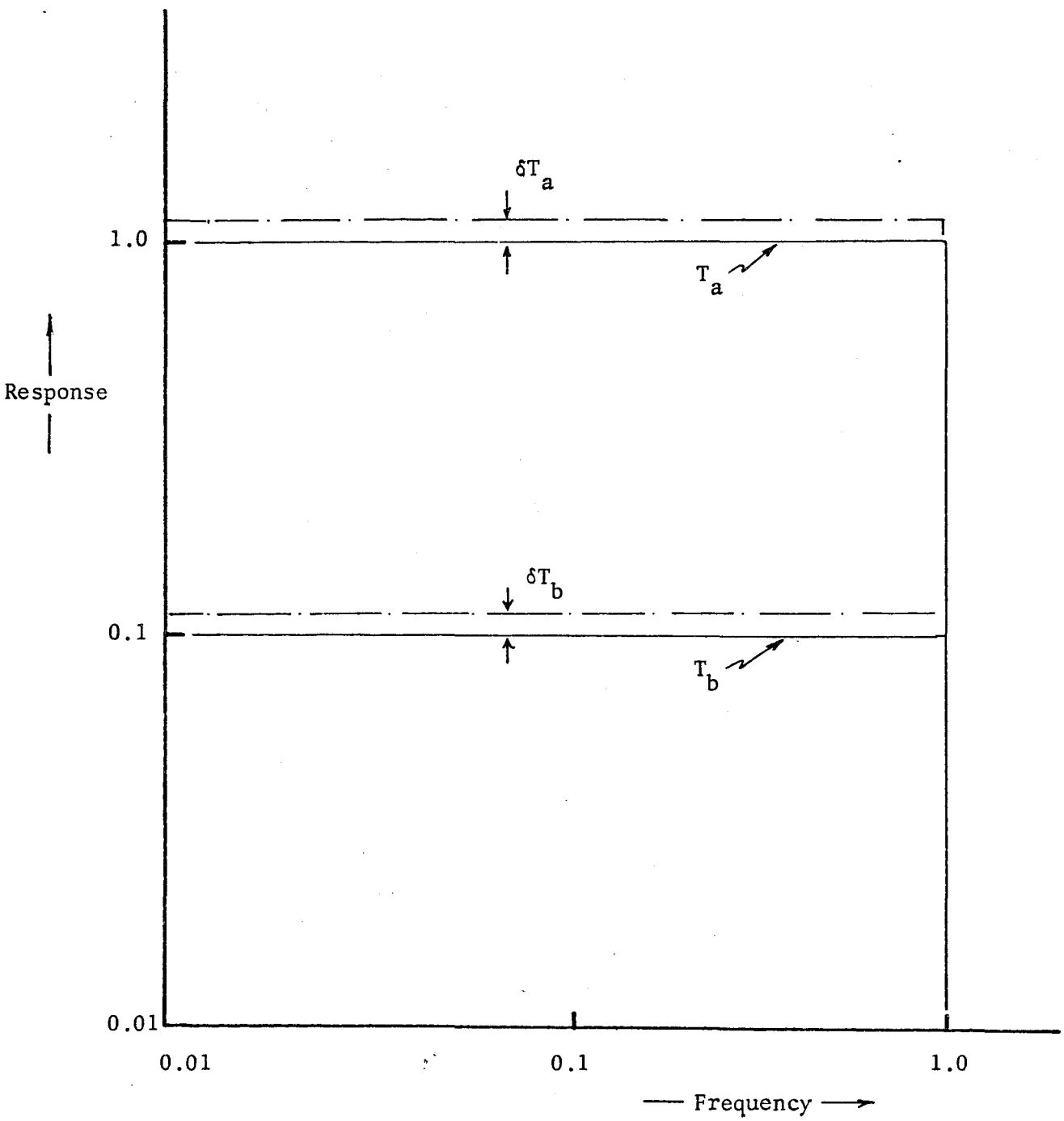

Figure 4.1: Nominal and perturbed response characteristics of hypothetical networks N_a and N_b

and n denotes the number of variables in question. Thus, $\frac{\Delta T}{T}$, which is a function of s, defines the fractional error in the network response due to simultaneous parameter variations.

We note that $\frac{\delta x_i}{x_i}$ acts as a weighting function, in that the contribution to the total error by the element x_i is determined by the product of the elemental sensitivity function, $S^T_{x_i}$, and this weighting function, $\frac{\delta x_i}{x_i}$. Accordingly, we may write

$$\frac{\Delta T}{T} = \sum_{i=1}^{n} S^T_{x_i} \chi_i \tag{4.5}$$

where $\chi_i = \frac{\delta x_i}{x_i}$ is a positive or negative real number.

There are now two meaningful approaches which may be taken for defining an index of performance and which differ only in the way that values are assigned to the weighting function χ_i:

(i) The set of n network parameters may be considered as consisting of a number of sub-sets, each of which is assigned a weighting function which has the same magnitude for all the elements of that sub-set. For example, in the case of an LCR network, for which, say, the tolerance of the inductors, capacitors and resistors is 5, 5 and 1 per cent, respectively, it would be appropriate to assign all reactive elements to one sub-set, and all the resistive elements to a second sub-set. One might then assign a magnitude of 5 to the weighting functions associated with the elements of the first sub-set, and a magnitude of unity to those associated with the elements of the second sub-set. Having thus assigned magnitudes to the various χ_i, we now allow each to assume a positive or a negative algebraic sign. In other words, $\frac{\Delta T}{T}$ can be any one of 2^n different functions,

depending on the particular combination of signs involved. If we are interested in the magnitude of the error (or the squared magnitude), we may arbitrarily assign χ_1, say, a positive (or negative) algebraic sign. Having chosen this particular frame of reference, the other possible sign combinations define 2^{n-1} different functions. We may, therefore, write

$$\left|\left\{\frac{\Delta T}{T}\right\}_j\right|^2 = \left|\left\{\sum_{i=1}^{n} S_{x_i}^T \chi_i\right\}_j\right|^2, \quad j = 1,2,\ldots,2^{n-1} \qquad \text{------- (4.6)}$$

where each value of j corresponds to one such combination of algebraic signs.

For any given frequency, the right-hand side of Equation 4.6 may have any one of 2^{n-1} different values. As such, it may be regarded as a random variable, with its value being determined by the pertinent combination of signs of the various χ_i. If we now assume that each such combination of signs is equally likely, then the probability of occurrence of any one value of $\left\{\frac{\Delta T}{T}\right\}_j$ is $1/2^{n-1}$, and the mean or expected value is given by

$$\hat{E} \triangleq E\left\{\left|\frac{\Delta T}{T}\right|^2\right\} = \frac{1}{2^{n-1}} \sum_{j=1}^{2^{n-1}} \left|\left\{\sum_{i=1}^{n} S_{x_i}^T \chi_i\right\}_j\right|^2 \qquad (4.7)$$

We note that the error function, $\hat{E}$, is a function of the real frequency variable, ω. The question now is, at what frequency or band of frequencies should this function be evaluated. Taking a general approach, we will evaluate it over the entire positive frequency range by means of an integration, but we introduce a frequency sensitive weighting function, $\psi(\omega)$, the purpose of which will be to determine what frequency

or frequencies are to be considered and what relative weighting is to be assigned to each. In other words, if we were simply to integrate $\hat{E}$ over a wide frequency range, a possibility would exist that such an integration might mask the effect of component changes at some critical frequency. We avoid this possibility by choosing a suitable $\psi(\omega)$.

We can now define a multiparameter sensitivity index of performance as

$$P_1 \triangleq \int_0^\infty \hat{E}\ \psi(\omega)\,d\omega \tag{4.8}$$

or

$$P_1 \triangleq \frac{1}{2^{n-1}} \int_0^\infty \sum_{j=1}^{2^{n-1}} \left| \left\{ \sum_{i=1}^{n} S^T_{x_i}\ \chi_i \right\}_j \right|^2 \psi(\omega)\,d\omega \tag{4.9}$$

(ii) An alternative approach to that described in (i) above is one in which both the magnitude and the algebraic sign of each χ_i is determined by some statistical process. We might, for example, allow the set of elements to vary in some random manner between a set of specified tolerances. In this way, a random choice of $\mathbf{x}$ would define a particular set of χ_i both in magnitude and in algebraic sign. The random variable, p_j, which is defined by

$$p_j \triangleq \int_0^\infty \left| \sum_{i=1}^{n} S^T_{x_i}\ \chi_i \right|^2 \psi(\omega)\,d\omega \tag{4.10}$$

could then be computed a number of times, each time using a different set of randomly generated χ_i. We therefore define an alternative index, P_2, as the mean or expected value of p_j, i.e.,

$$P_2 \triangleq E\{p_j\} = \frac{1}{Q}\int_0^{\infty} \sum_{j=1}^{Q} \left| \left\{ \sum_{i=1}^{n} S_{x_i}^T \chi_i \right\}_j \right|^2 \psi(\omega)\, d\omega \qquad (4.11)$$

where Q is the number of different sets of χ_i used.

4.3 Choice of Weighting Function $\psi(\omega)$:

The role of $\psi(\omega)$ is to bring into prominence any critical frequency or frequency range, so that the effect of component changes at such frequencies will not be masked by the integration.

Perhaps the most fundamental question to be asked is whether an integration is necessary at all. Is it possible, for example, that the evaluation of the sensitivity performance as defined by the error function $\hat{E}$, at a single frequency is sufficient? There is, in fact, some evidence to this effect: Schoeffler's criterion[26] is evaluated at a single frequency and his choice of the optimum from a number of continuously equivalent networks is based on this index. Leeds and Ugron report that an integration is unnecessary for a class of networks[17], although they fail to identify the particular class. We, however, have found that an integration is indeed necessary if the results are to be truly meaningful in a general sense.

This conclusion is based on a simple argument: The index is to be used when networks are to be compared with respect to their multiparameter sensitivity performance. If an integration is <u>not</u> required, in other words, if evaluation of $\hat{E}$ at a single frequency were sufficient, then we should find that the relative sensitivity performance of one network in comparison to that of another should be the same at all frequencies. In other words, the ratio of the $\hat{E}$ of one network to that of another network

should be the same for all frequencies. We have applied this test to a number of related networks and the results, shown plotted in Figures 4.2 and 4.3 not only demonstrate that this, in fact, is not the case, but also, by illustrating the dependence of $\hat{E}$ on frequency, they give an indication of the type of weighting function which should be used.

We have also applied the test using an index of the $\sum_i \left| S^T_{x_i} \right|^2$ type as defined by Schoeffler. The results, shown plotted in Figure 4.4 correspond to those obtained using the error function $\hat{E}$. We, therefore, conclude that an index based on an integral is more informative than one evaluated at a single frequency, as it is apparent that the relative sensitivity performance of a network is not, in general, independent of frequency.

The information contained in Figures 4.2 and 4.3 may now be used as a guide in the choice of a suitable weighting function, $\psi(\omega)$. Thus, in these figures, for example, we note that

(i) The error at very low frequencies is insignificant.

(ii) There is an increased sensitivity to component change in the vicinity of the cut-off frequency, $\omega = 1$.

(iii) Although the error is relatively large at high frequencies, it is of little practical importance because we are dealing with a low-pass network.

Three possible choices for $\psi(\omega)$ in this case are

(a) Ideal low-pass window with cut-off at $\omega = 1$,

(b) Ideal low-pass window with cut-off greater than 1,

(c) Ideal band-pass window centred at $\omega = 1$.

McMASTER UNIVERSITY LIBRARY

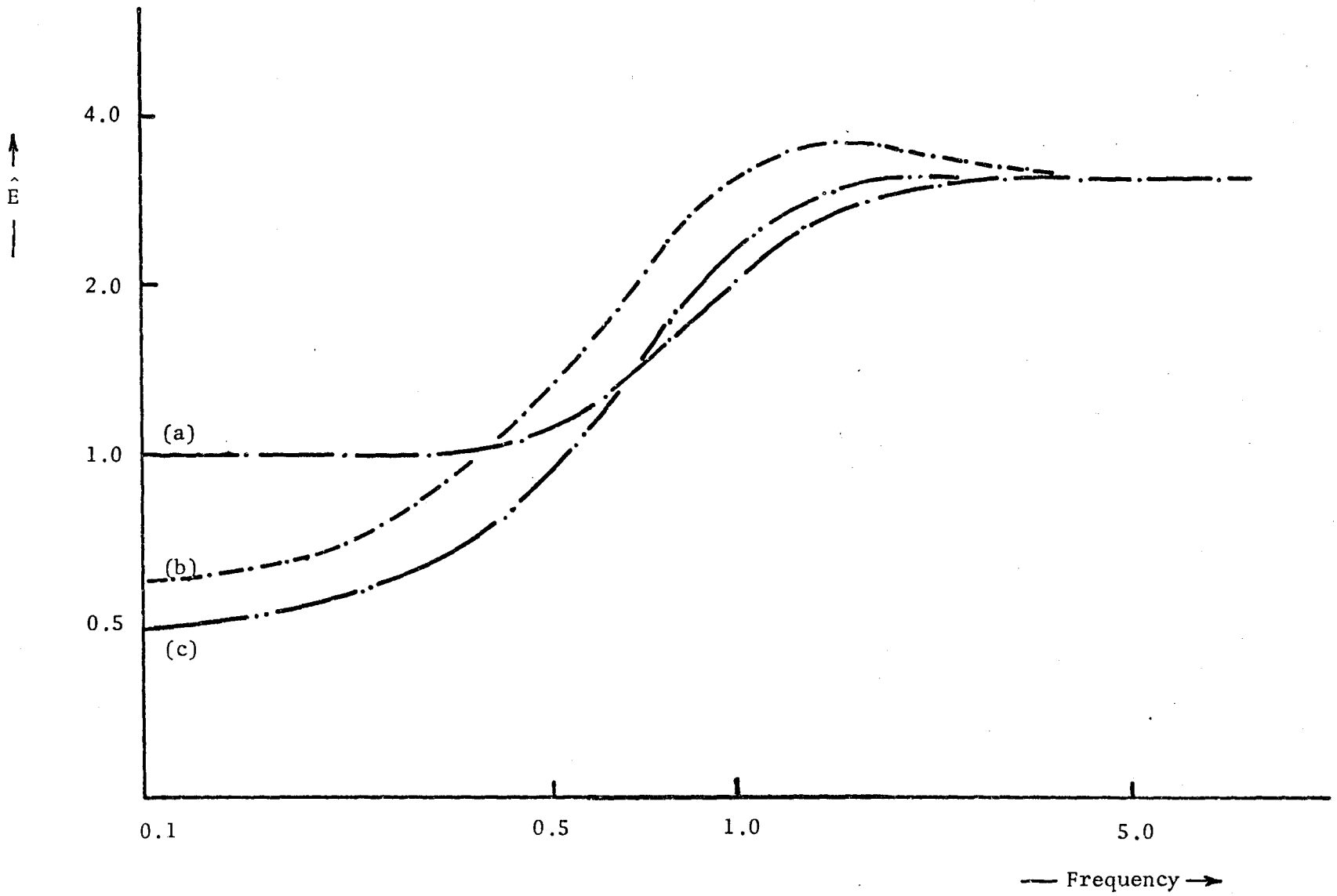

Figure 4.2: Integrand $\hat{E}$ for second-order Butterworth passive filters
(a) With source/load resistance ratio = ∞
(b) With source/load resistance ratio = 2
(c) With source/load resistance ratio = 1

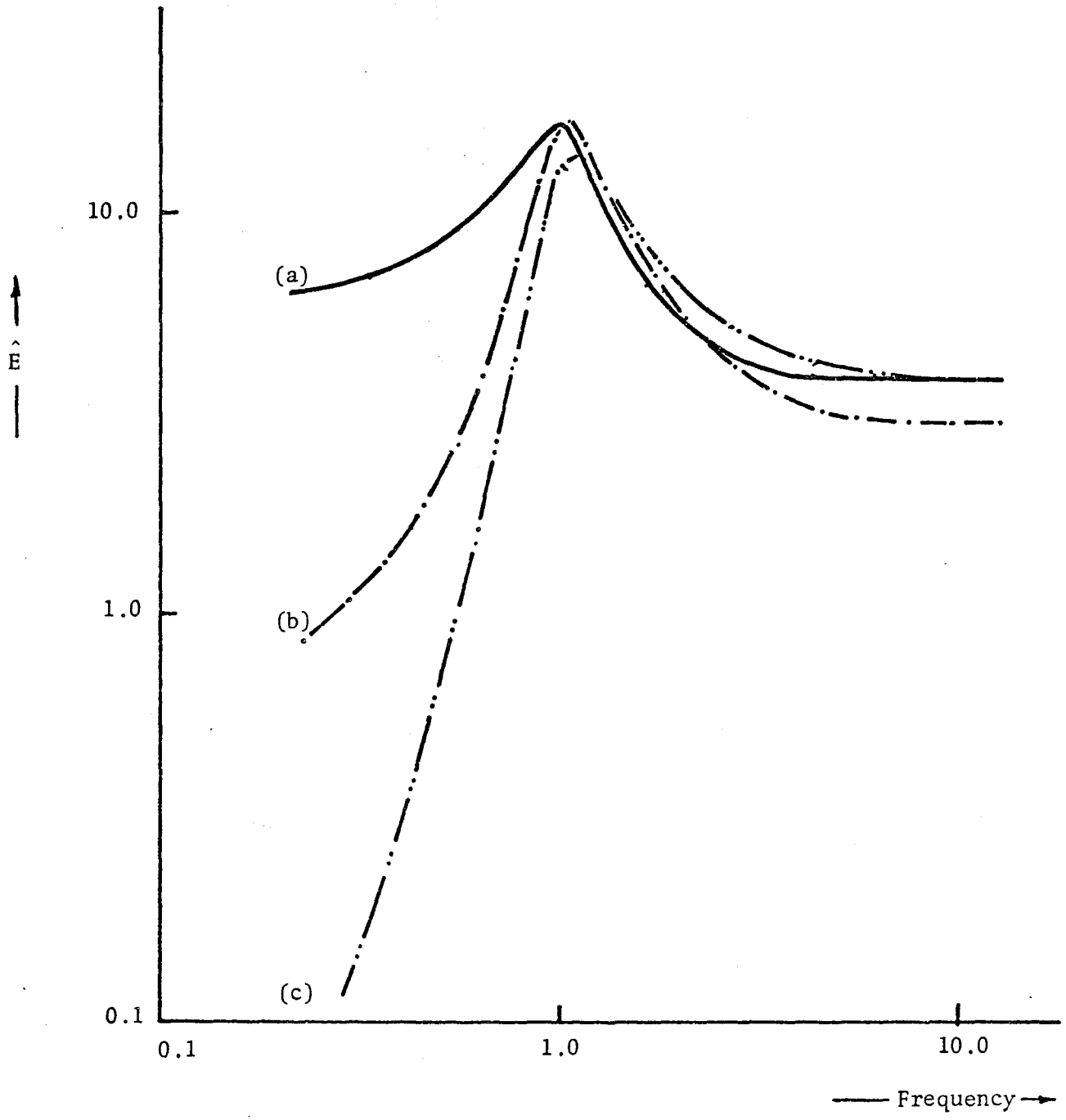

Figure 4.3: Integrand $\hat{E}$ for second-order RC-active filters

(a) For the network of Figure 7.7

(b) For the network of Figure 7.6

(c) For the network of Figure 7.11

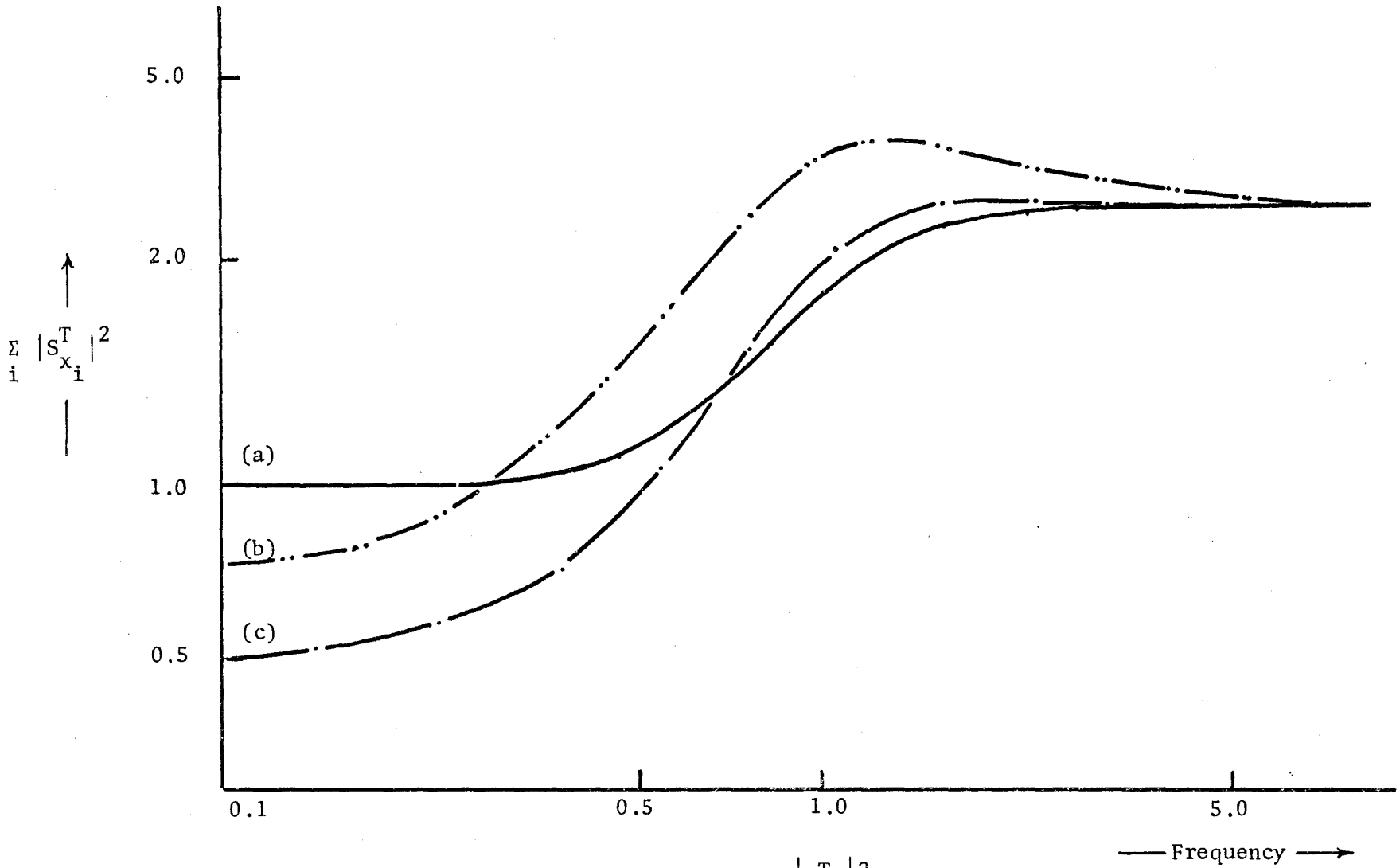

Figure 4.4: Integrand for index of the $\sum_i \left|S^T_{x_i}\right|^2$ type for the case of a second-order Butterworth LC filter

(a) With source/load resistance ratio of ∞

(b) With source/load resistance ratio = 4

(c) With source/load resistance ratio = 1

The first choice, (a), may be justified on the basis that we are dealing with a low-pass structure and as such we should primarily be concerned with frequencies within the passband. This choice, however, fails to include the relatively critical frequency range immediately outside the passband. For this reason, the second choice, (b), appears more appropriate; yet it includes, perhaps unnecessarily, the very low frequency range where the error is negligible. The third choice, that of a bandpass window centred at $\omega = 1$, is therefore perhaps the most appropriate of all three, and accordingly, has been chosen for the evaluation of the various results reported herein, except where stated to the contrary.

4.4 Optimum Tolerance Sets:

From the definition of the sensitivity index, it is apparent that some elements will contribute to its magnitude to a greater extent than will others, i.e., the overall performance of a network is more sensitive to some elements than to others. Intuitively, we feel that the tolerance of a "sensitive" element should be less than that of an "insensitive" one if the overall sensitivity performance of the network is to be optimized. We, therefore, define an "optimum tolerance set" as that set of element tolerances which allows each element to contribute equally to the overall error. In other words, if

$$\int_0^\infty \left| S^T_{x_i} \frac{\delta x_i}{x_i} \right|^2 \psi(\omega)\, d\omega = \int_0^\infty \left| S^T_{x_j} \frac{\delta x_j}{x_j} \right|^2 \psi(\omega)\, d\omega \qquad (4.12)$$

for all i, then the set of $\frac{\delta x_i}{x_i}$ for which this equation holds is defined as the optimum tolerance set for the network under consideration, and will be denoted by δx_o. In this way it is ensured that no single element

dominates the overall error.

Perhaps it should be noted that the net result, i.e., having each element of the network contribute equally to the total error, is similar to that of other optimization procedures[17]. In this case the sensitivity functions, $S^T_{x_i}$, are fixed and the tolerance set is chosen to obtain the desired effect. In other cases, the tolerances are fixed and the network configuration and/or nominal element value set is chosen such that the objective of equal contribution is attained.

These optimum tolerance sets have been obtained for a number of low-pass LC ladder filters and they have also been obtained and used in the synthesis of active-RC filters. The performance of networks using optimum tolerance sets has been evaluated and the results are given in Chapter VI.

4.5 Conclusion:

In this chapter, a new multiparameter sensitivity index of performance has been proposed for general use with linear, time-invariant networks. Two forms of the index have been defined:

(1) the index P_1, in which a deterministic perturbation is applied, and

(2) the index P_2, in which a probabalistic perturbation is applied to the nominal values of the network parameters of interest.

In addition, a procedure has been described for obtaining, for a given network, an optimum tolerance set by which each element is made to contribute equally to the total error in the network response. In the next chapter , a new method of computing these indices of performance is described in detail, and its computational efficiency is compared with other procedures.

CHAPTER V

COMPUTATIONAL PROCEDURES

5.1 Introduction:

The problem of computing sensitivity indices of performance is one of fundamental importance. These indices do not, in general, lend themselves to analytical or closed-form solution. Rather, they are most conveniently evaluated by means of a digital computer. In Chapter III, we have described several powerful methods by which such indices may be computed. These procedures have one characteristic in common, i.e., they all obtain the elemental sensitivities, $\frac{\partial T}{\partial x_i}$, without actually performing a differentiation operation. Also, they can all lead to analytical expression for the $\frac{\partial T}{\partial x_i}$. However, if the order of complexity of the network is high, then it may not be convenient to attempt to obtain the $\frac{\partial T}{\partial x_i}$ in analytical form. This difficulty may be overcome by the use of a new direct approach which is based on the use of a computer. This approach enables the network function and its partial derivatives to be obtained in analytical form.

To obtain the partial derivatives of the network function in analytical form, it is first necessary to have the network function itself in such a form, i.e., a form in which the explicit dependence of the coefficient of each power of s on the various network parameters is readily apparent. To obtain the network function in this form may require a considerable computational effort in the case of complex networks. For example, in the case of a tenth-order doubly-terminated LC-ladder filter, if the transfer function $T(s,x_i)$ were expressed as a ratio of polynomials in s, wherein the dependence of each coefficient of each power of s on the twelve network parameters is given explicitly, we would find that the denominator would contain 486 terms, each unique in its dependence on the network variables. An algorithm which allows the explicit dependence of the coefficients on the network variables to be maintained while performing standard mathematical operations, and which may be used to obtain n^{th}-order partial derivatives and corresponding sensitivity functions has been devised by Temple and Butler[45].

5.2 The Computational Algorithm:

The algorithm involves the representation in array form of information contained in elementary polynomials. Each self- and mutual-admittance of the network, analyzed on a nodal-basis, say, is represented as an array of numbers in which each term of the pertinent admittance corresponds to a row of the array. If the network has n parameters, one or more of which may be variable, then each row of the array has n + 2 elements. The first element of such a row represents the algebraic coefficient of the particular term which it represents, and is set equal

to the numerical value of that coefficient. Each one of the next n elements of the row represents one of the n network parameters. If a term contains the parameter x_k raised to power m, then the array element representing x_k is set equal to m. Finally, the last element of the row, which represents the complex frequency variable, s, is set equal to the power of s. The representation of polynomials in array form is best illustrated by means of an example.

Example 5.1(a): Array Representation

Consider, again, the network of Figure 3.6(a). Analysis on a nodal-basis yields

$$Y_{11} = G_1 + sC_1 \tag{5.1}$$

$$Y_{12} = -sC_1 \tag{5.2}$$

$$Y_{21} = g_m - sC_1 \tag{5.3}$$

$$Y_{22} = G_2 + sC_1 + sC_2 \tag{5.4}$$

$$\Delta = Y_{11}Y_{22} - Y_{12}Y_{21} \tag{5.5}$$

$$\Delta_{12} = -Y_{21} \tag{5.6}$$

Following the procedure outlined above, we may represent the admittances Y_{11}, Y_{12}, Y_{21} and Y_{22} by the arrays

$$Y_{11} = \begin{array}{c|cccccc|c} \text{Algebraic Coefficient} & G_1 & C_1 & C_2 & G_2 & g_m & s & \\ \hline 1.0 & 1 & 0 & 0 & 0 & 0 & 0 & G_1 \\ 1.0 & 0 & 1 & 0 & 0 & 0 & 1 & sC_1 \\ \hline \end{array}$$

$$Y_{12} = \begin{array}{c|ccccccc|c} \text{Algebraic Coefficient} & G_1 & C_1 & C_2 & G_2 & g_m & s & \\ \hline -1.0 & 0 & 1 & 0 & 0 & 0 & 1 & -sC_1 \end{array}$$

$$Y_{21} = \begin{array}{|ccccccc|c} 1.0 & 0 & 0 & 0 & 0 & 1 & 0 & g_m \\ -1.0 & 0 & 1 & 0 & 0 & 0 & 1 & -sC_1 \end{array}$$

$$Y_{22} = \begin{array}{|ccccccc|c} 1.0 & 0 & 0 & 0 & 1 & 0 & 0 & G_2 \\ 1.0 & 0 & 1 & 0 & 0 & 0 & 1 & sC_1 \\ 1.0 & 0 & 0 & 1 & 0 & 0 & 1 & sC_2 \end{array}$$

These arrays, representing the various network admittance functions, Y_{ij}, are easily manipulated by the computer when performing the various mathematical operations necessary to obtain the network function of interest and its partial derivatives with respect to the variable parameters. The partial derivatives may then be used to evaluate any desired sensitivity function.

To illustrate the procedure further, we now consider the problem of obtaining the transfer function $T = \frac{V_2}{I_1}$ and its partial derivative with respect to the parameter g_m. The problem entails array multiplication, addition (subtraction) and partial differentiation, examples of which now follow.

Example 5.1(b): Array Multiplication

Two rows may be multiplied together simply by adding the last n+1 elements of one row to the corresponding elements of the other, and multiplying the first elements of the rows together. Thus, for example, for $Y_{12}Y_{21}$ we have

$$\begin{bmatrix} -1.0 & 0 & 1 & 0 & 0 & 0 & 1 \end{bmatrix} \times \begin{bmatrix} 1.0 & 0 & 0 & 0 & 0 & 1 & 0 \\ -1.0 & 0 & 1 & 0 & 0 & 0 & 1 \end{bmatrix}$$

$$= \begin{bmatrix} -1.0 & 0 & 1 & 0 & 0 & 1 & 1 \\ 1.0 & 0 & 2 & 0 & 0 & 0 & 2 \end{bmatrix} = Y_{12}Y_{21}$$

i.e.,

$$Y_{12}Y_{21} = -sC_1g_m + s^2C_1^2 \tag{5.7}$$

and for $Y_{11}Y_{22}$ we have

$$\begin{bmatrix} 1.0 & 1 & 0 & 0 & 0 & 0 & 0 \\ 1.0 & 0 & 1 & 0 & 0 & 0 & 1 \end{bmatrix} \times \begin{bmatrix} 1.0 & 0 & 0 & 0 & 1 & 0 & 0 \\ 1.0 & 0 & 1 & 0 & 0 & 0 & 1 \\ 1.0 & 0 & 0 & 1 & 0 & 0 & 1 \end{bmatrix}$$

$$= \begin{bmatrix} 1.0 & 1 & 0 & 0 & 1 & 0 & 0 \\ 1.0 & 1 & 1 & 0 & 0 & 0 & 1 \\ 1.0 & 1 & 0 & 1 & 0 & 0 & 1 \\ 1.0 & 0 & 1 & 0 & 1 & 0 & 1 \\ 1.0 & 0 & 2 & 0 & 0 & 0 & 2 \\ 1.0 & 0 & 1 & 1 & 0 & 0 & 2 \end{bmatrix} = Y_{11}Y_{22}$$

i.e.

$$Y_{11}Y_{22} = G_1G_2 + s(C_1G_1 + C_2G_1 + C_1G_2) + s^2(C_1^2 + C_1C_2) \tag{5.8}$$

Example 5.1(c): Array Addition or Subtraction

To add (or subtract) two arrays, we first compare the rows of one array to those of the other, so that we may identify those like rows of the two arrays that represent terms of the same kind. If we find that the two arrays possess such rows, we add (or subtract) their respective first elements and store the sum (or difference) in a resultant array; if the sum (or difference) is zero, we may obviously omit the row in question from the resultant array. As for the remaining rows of the two arrays, we store them in the resultant array unchanged (except for an appropriate sign change of the first element of a row which is being subtracted). Thus, for example, for $Y_{11}Y_{22} - Y_{12}Y_{21} = \Delta$, we have

$$\begin{bmatrix} 1.0 & 1 & 0 & 0 & 1 & 0 & 0 \\ 1.0 & 1 & 1 & 0 & 0 & 0 & 1 \\ 1.0 & 1 & 0 & 1 & 0 & 0 & 1 \\ 1.0 & 0 & 1 & 0 & 1 & 0 & 1 \\ 1.0 & 0 & 2 & 0 & 0 & 0 & 2 \\ 1.0 & 0 & 1 & 1 & 0 & 0 & 2 \end{bmatrix} - \begin{bmatrix} -1.0 & 0 & 1 & 0 & 0 & 1 & 1 \\ 1.0 & 0 & 2 & 0 & 0 & 0 & 2 \end{bmatrix}$$

$$= \begin{array}{c} \begin{bmatrix} 1.0 & 1 & 0 & 0 & 1 & 0 & 0 \\ 1.0 & 1 & 1 & 0 & 0 & 0 & 1 \\ 1.0 & 1 & 0 & 1 & 0 & 0 & 1 \\ 1.0 & 0 & 1 & 0 & 1 & 0 & 1 \\ 1.0 & 0 & 1 & 0 & 0 & 1 & 1 \\ 1.0 & 0 & 1 & 1 & 0 & 0 & 2 \end{bmatrix} \\ \begin{array}{ccccccc} G_1 & C_1 & C_2 & G_2 & g_m & & s \end{array} \end{array} = \Delta$$

Hence, by inspection,

$$\Delta = G_1G_2 + s(G_1C_1 + G_1C_2 + G_2C_1 + C_1g_m) + s^2C_1C_2 \qquad \text{-------} \quad (5.9)$$

With $\Delta_{12} = -Y_{21} = sC_1 - g_m$, and the required transfer function being defined by

$$T = \frac{\Delta_{12}}{\Delta} \qquad (5.10)$$

We have

$$T = \frac{+sC_1 - g_m}{s^2C_1C_2 + s(G_1C_1 + G_1C_2 + G_2C_1 + g_mC_1) + G_1G_2} \qquad \text{-------} \quad (5.11)$$

Example 5.1(d): Differentiation of an Array

The derivative of an array with respect to a parameter x_k may be obtained by considering each row of the array in turn, reducing by one the $(k+1)^{th}$ element of the row, which is equal to the power m of x_k, and multiply the first element of the row by m. Rows which have their algebraic coefficients equal to zero (corresponding to terms which are independent of x_k) may then be omitted. Thus, for example, for $\frac{\partial\Delta}{\partial g_m}$, we have

$$\frac{\partial\Delta}{\partial g_m} = \boxed{1.0 \quad 0 \quad 1 \quad 0 \quad 0 \quad 0 \quad 1} = sC_1 \qquad (5.12)$$

For $\frac{\partial T}{\partial g_m}$, therefore, we have

$$\frac{\partial T}{\partial g_m} = \frac{1}{\Delta^2}\left\{\Delta\frac{\partial\Delta_{12}}{\partial g_m} - \Delta_{12}\frac{\partial\Delta}{\partial g_m}\right\} \qquad (5.13)$$

i.e.

$$\frac{\partial T}{\partial g_m} = -\frac{s^2C_1(C_1+C_2) + s(C_1G_1+C_2G_1+C_1G_2) + G_1G_2}{\{sC_1C_2 + s(C_1G_1+C_2G_1+C_1G_2+C_1g_m) + G_1G_2\}^2} \tag{5.14}$$

The procedure is not limited to first-order sensitivity functions. It may be used to obtain second- or higher-order derivatives by simply repeating the partial derivative operation on the various arrays in an appropriate manner. However, in such cases, the storage requirements increase rapidly with the order of complexity of the network. This problem can be overcome to a considerable extent by modifying the manner in which the various polynomial terms are represented in array form. One such modification will now be described.

5.3 A Coding Technique for Reduced Storage:

From Example 5.1, it is clear that most array elements in the non-coded form are integers. As such, they may be coded into a form which makes it possible to reduce the storage requirements of the algorithm considerably. One such code is one in which each pair of digits of a fourteen significant figure number represents one of the last n+1 elements of each array row. By letting even and odd numbers represent positive and negative powers, respectively, as illustrated in Table 5.1, it is possible to code seven variables, with powers ranging from -50 to +49 into a single number. Thus, for example, we would represent the admittance Y_{12} of the network of Figure 3.6(a), in coded form as

$$Y_{12} = -sC_1 = \begin{array}{c|c:c:c:c:c:c:c} -1.0 & 0\ 0 & 0\ 2 & 0\ 0 & 0\ 0 & 0\ 0 & 0\ 2 & 0\ 0 \\ \text{Algebraic coefficient} & G_1 & C_1 & C_2 & G_2 & g_m & s & \end{array} \tag{5.15}$$

If the number of network parameters exceeds six, additional fourteen-figure numbers, each able to accommodate up to seven additional parameters may be used.

Thus, it is possible to reduce the storage requirements considerably by use of a coding technique. For the given example, the storage requirement for Y_{12} is reduced by a factor of three using this particular code. The reduction becomes even more significant as the number of variables is increased; the maximum reduction being limited, of course, by the number of significant figures available from the computer.

Power	Code
-50	99
-49	97
.	.
.	.
-1	01
0	00
+1	02
.	.
.	.
+49	98

Table 5.1: Code for Reduced Storage

5.4 Efficiency of Computation, a Quantitative Comparison:

A quantitative comparison was made between the direct approach and the adjoint network approach following the numerical analysis procedure as outlined by Director and Rohrer[34]. The comparison was based on a steepest descent optimal search routine using the network of Fig. 5.1. The results

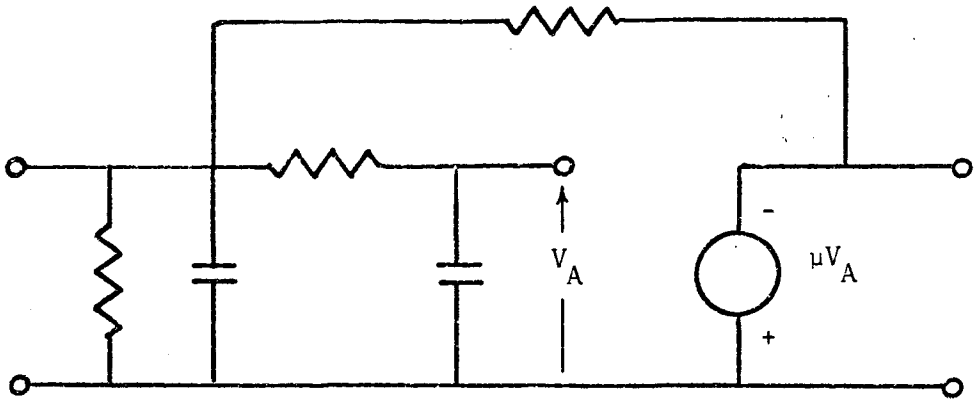

Figure 5.1: Network used in optimization procedure

obtained are shown plotted in Figure 5.2, where the number of search iterations per unit computer time is plotted as a function of the number of frequency points at which the index of performance was to be evaluated. On the basis of these results, it would appear that the direct approach is considerably more efficient when the number of frequency points at which the index is to be computed is relatively large. A desirable feature of the direct approach is that after the initial network analysis, all the partial derivatives, of whatever order, are available in analytical form. In an optimal synthesis procedure, therefore, the index of performance can be computed at each and every frequency point of interest simply by substituting the known parameter values. In other words, the need for additional network analyses at each and every frequency point for each step of the optimization procedure is eliminated. Furthermore, the derivatives of the index itself with respect to the network parameters may also be obtained in analytical form, thus providing an efficient method of obtaining the desired trajectory in parameter space.

It should be noted, however, that the algorithm used in the direct approach, in its present form, is based on Cramer's Rule for the solution of simultaneous equations. On the other hand, the Director-Rohrer procedure can readily use the Gauss elimination method of solution, which becomes highly efficient, in a comparative sense, whenever the order of the network determinant is high. We might, therefore, expect the direct approach to be relatively less advantageous in the case of complex networks.

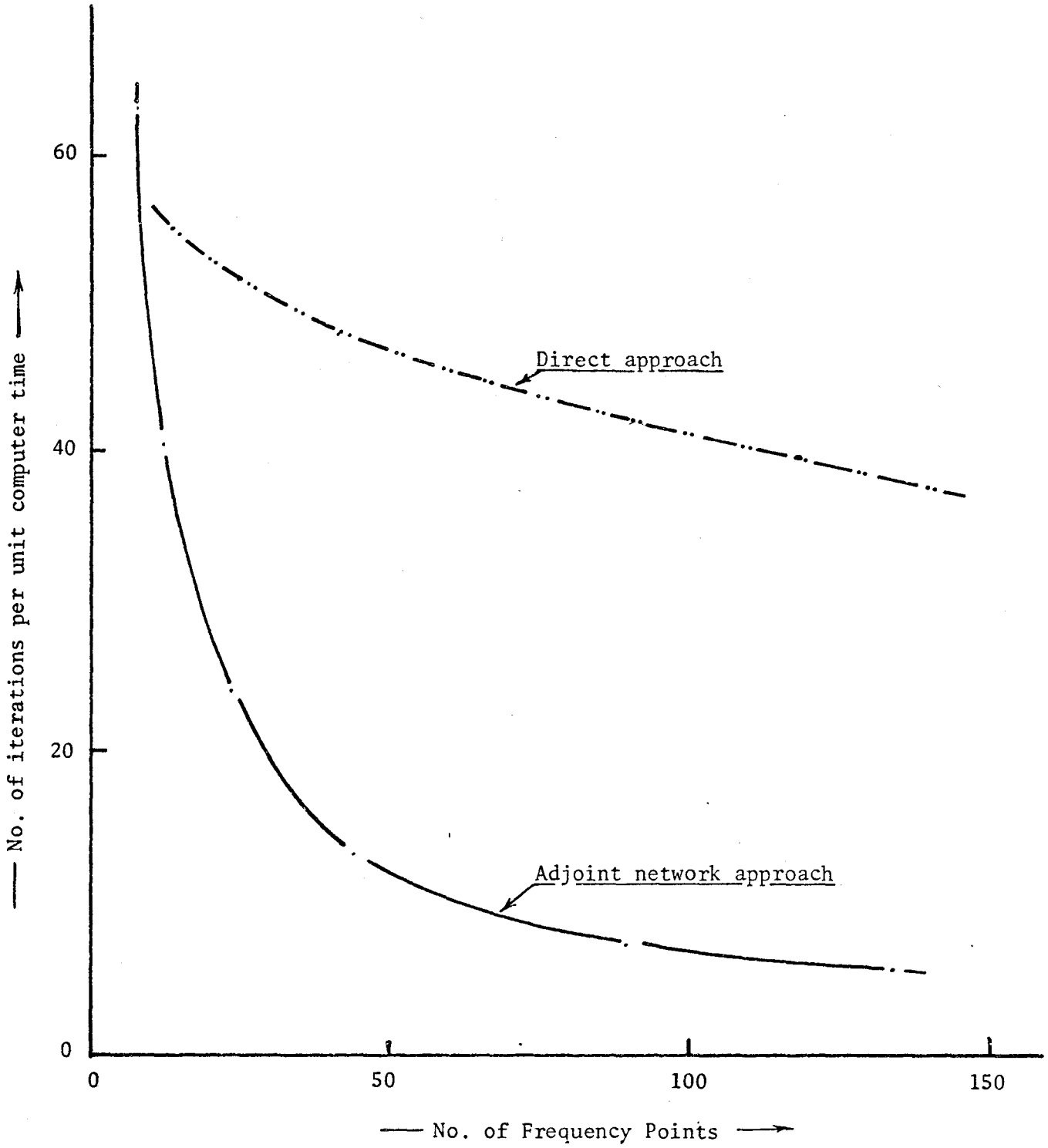

Figure 5.2: Comparison of computation efficiencies

5.5 Computer Programming:

Having described the direct approach, by which all the results reported herein were obtained, we can now briefly describe, with the aid of flow-charts, some of the salient features of the computer programs used in the computation of the index of performance and the optimum tolerance sets.

Figure 5.3 shows a flow-chart representation of what we will call the 'network characterization' operation, which is performed at the beginning of all programs. During this operation, the network function and its partial derivatives with respect to all of the variable parameters are obtained in both array and polynomial form. Figure 5.4 shows the sequence of operations performed when computing the index P_1, while Figure 5.5 shows the same for the case where the optimum tolerance sets are being obtained.

When using the index of performance for comparing the sensitivity performance of different networks, each employing a uniform tolerance set, the index P_1 was used as the basis of comparison, and a value of unity was assigned to each χ_i weighting function. On the other hand, when computing the index for a network with a non-uniform tolerance set, then a correspondingly non-uniform weighting was assigned to the various χ_i. Furthermore, whenever an optimized network (i.e., one which had an optimum tolerance set or an optimum nominal element set or a combination of the two) was compared with a non-optimized one, the index P_2 was used as the basis of comparison.

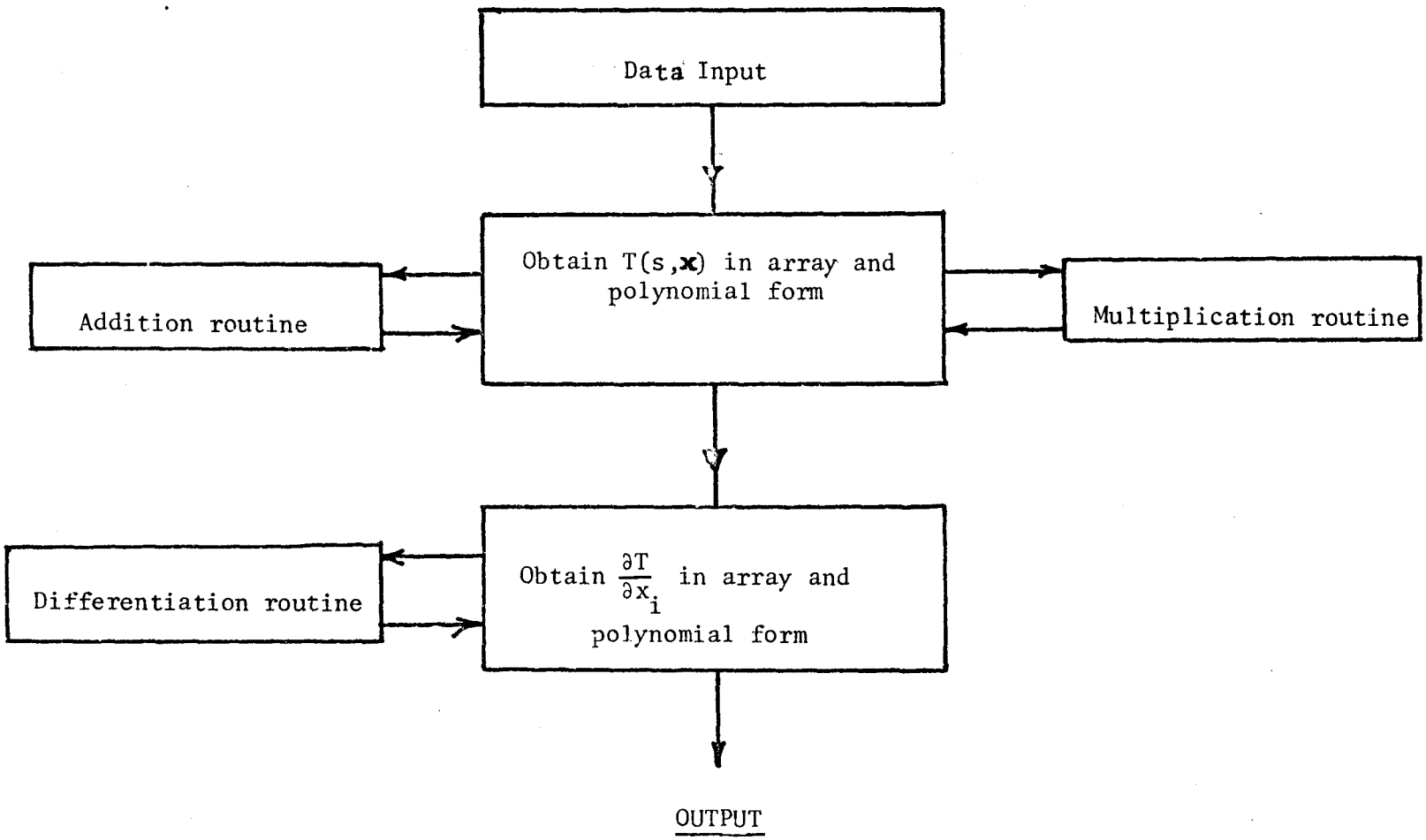

Figure 5.3: Flow-chart for network characterization operation

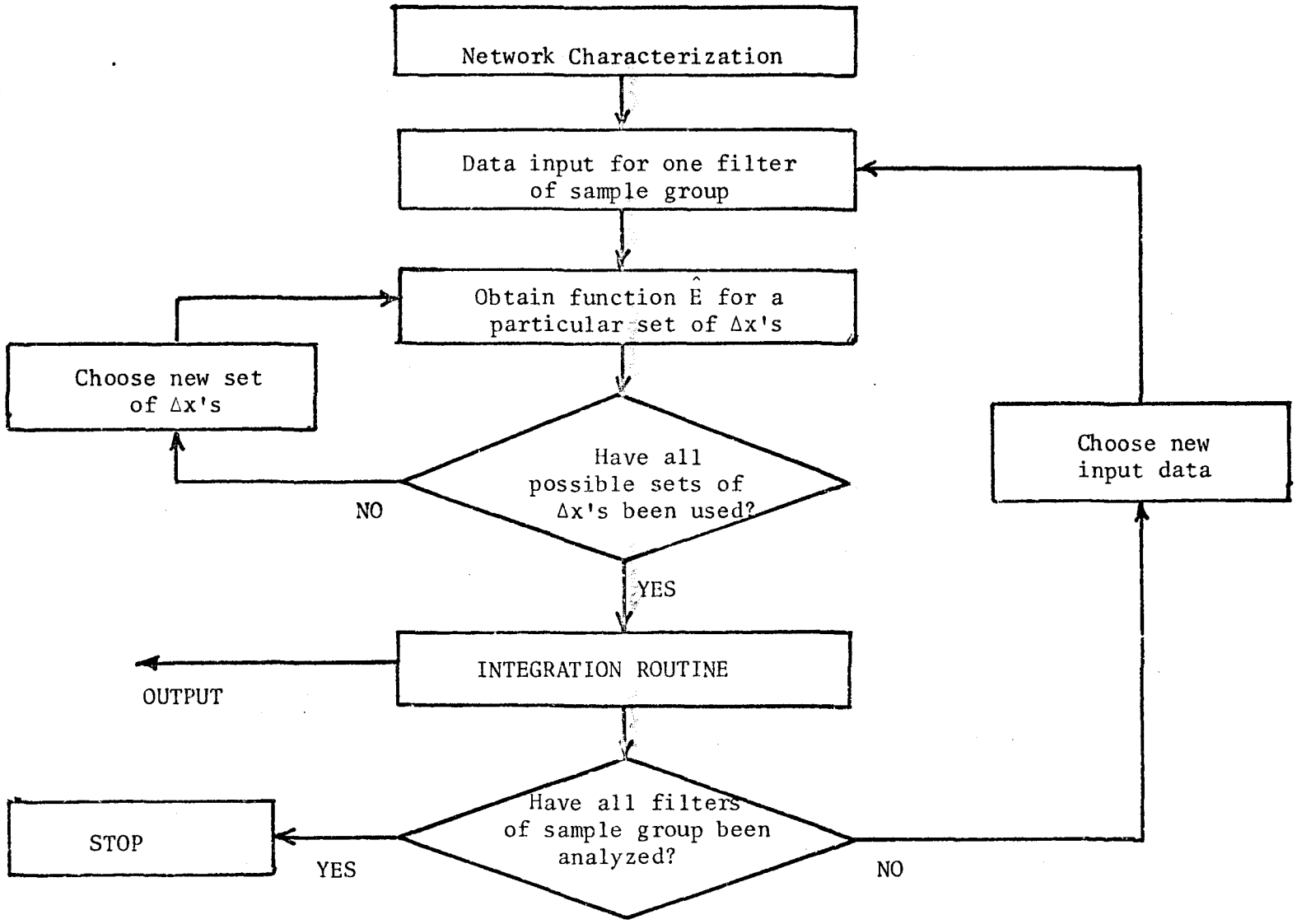

Figure 5.4: Flow-chart representation of procedure used to compute the index P_1

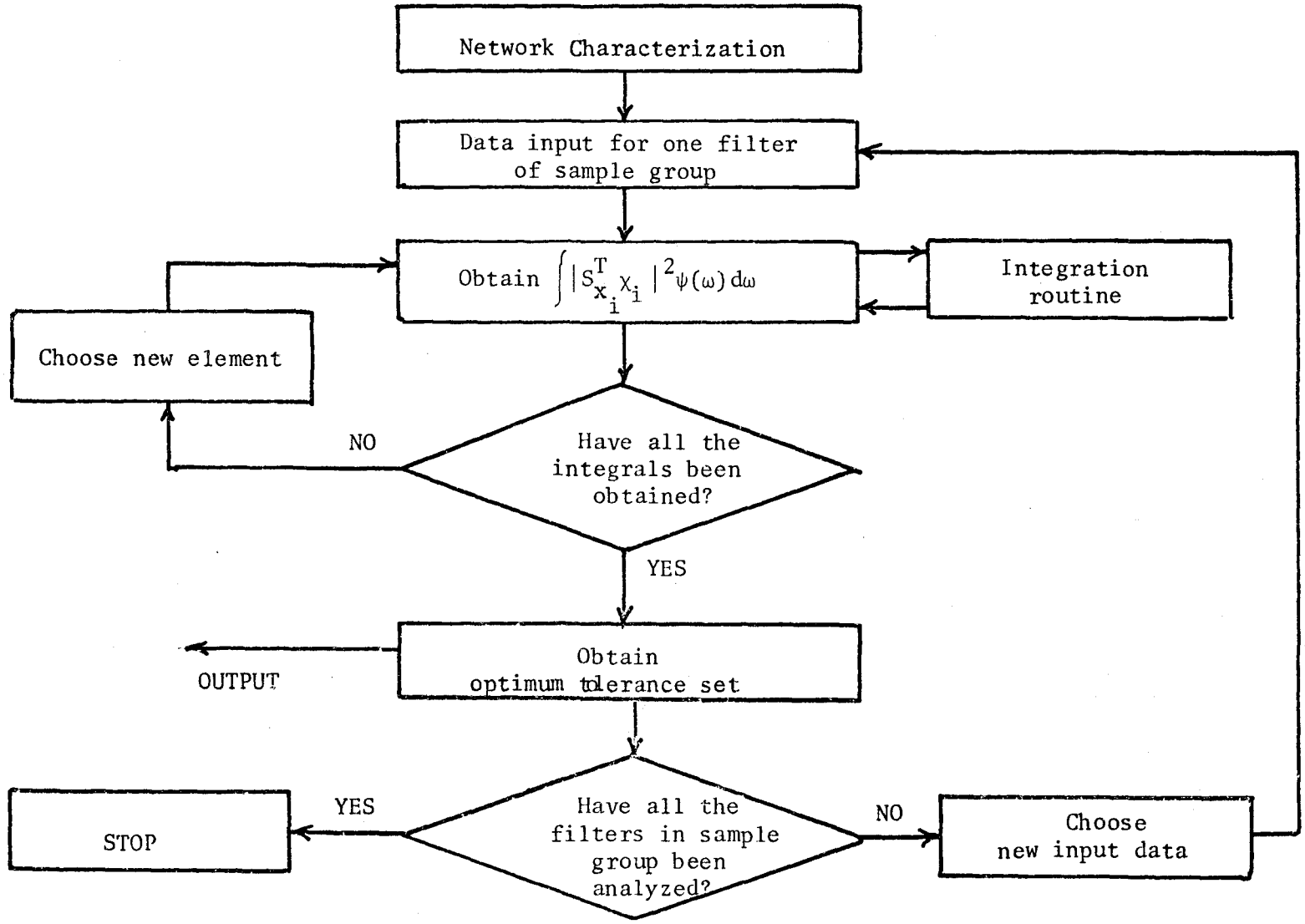

Figure 5.5: Flow-chart representation of procedure used to obtain optimum tolerance sets

5.6 Conclusion:

A new procedure for the computation of sensitivity functions has been described. The procedure is quite general, and can be used to obtain n^{th}-order partial derivatives and corresponding sensitivity functions. Because these sensitivity functions are obtained in analytical form, the procedure is very efficient when the sensitivity functions are required to be computed a great number of times, as is the case, for example, in an optimization procedure. A quantitative comparison of the relative efficiency of this direct method and that of Director and Rohrer has been made for the case of a second-order RC-active filter. For the example considered, it appears that the direct method is considerably more efficient when the number of frequency points at which the index must be computed is large.

CHAPTER VI

A MULTIPARAMETER SENSITIVITY STUDY OF LOW-PASS LC LADDER FILTERS

6.1 Introduction:

A multiparameter sensitivity study of low-pass LC ladder filters was undertaken because the LC ladder filter is one of the most fundamental and most widely used forms of electrical network. Also, as explained in Chapter II, an LC ladder filter may be readily used to derive an equivalent inductorless filter employing gyrators and capacitors only. The most commonly used procedure for the synthesis of a doubly-terminated LC ladder filter is the insertion loss method which was first proposed by Darlington in his classic 1939 paper. From a given specification function ($|Z_{21}(j\omega)|^2$, for example), the squared magnitude of the reflection coefficient, $|\rho(j\omega)|^2$, is determined. By putting $j\omega = s$, the reflection coefficient, $\rho(s)$, is then obtained by choosing its zeros to be those zeros of $|\rho(s)|^2$ which lie in the left half (or right half) of the complex frequency plane. Obviously, for reasons of stability, the poles of $\rho(s)$ must lie in the left half of the s-plane. The driving point impedance function, $Z_{in}(s)$, at the input port (see Figure 6.1), is then determined from

$$Z_{in}(s) = \frac{1 - \rho(s)}{1 + \rho(s)} \tag{6.1}$$

and is synthesized using a suitable driving point synthesis procedure.

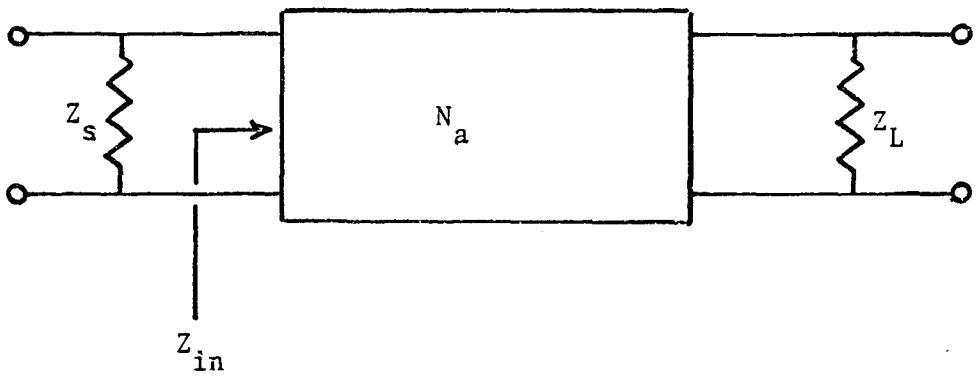

Figure 6.1: Doubly-terminated network

6.2 Standard LC Ladder Filters:

In the design of LC filters, an established method of solving the approximation problem is to make use of different classes of polynomials that are known to possess desirable properties, e.g., Butterworth, Chebyshev and Bessel polynomials. The use of these polynomials, in particular, leads to the realization of filters with maximally-flat magnitude, equi-ripple magnitude, and maximally-flat delay characteristics, respectively. Using the insertion loss technique, tables of element values have been compiled by a number of authors for a wide range of filter networks (see, for example, Weinberg[7]). In this chapter, we limit ourselves to the multi-parameter sensitivity study of low-pass Butterworth and Chebyshev filters. However, the procedures which were used to investigate this group of filters were quite general, and may equally be applied to any other group of filter networks.

6.3 Factors Affecting the Index of Performance:

Using Weinberg's design data, the index P_1 was computed for a wide range of low-pass filters, and the results are tabulated in Tables 6.1 and 6.2. Table 6.1 was obtained when an ideal low-pass window function (with cut-off frequency $\omega = 1$) was used for $\psi(\omega)$, while Table 6.2 was obtained when an ideal bandpass window (centered at $\omega = 1$ and with lower and upper cut-off frequencies of 0.5 and 2.0, respectively) was used for $\psi(\omega)$. The dependence of the index P_1 on the various filter characteristics was evaluated using the results listed in Table 6.2, and is now described:

(a) Order of Complexity: Figure 6.2 shows the effect of increasing the order of complexity of the filter for two Butterworth filters with

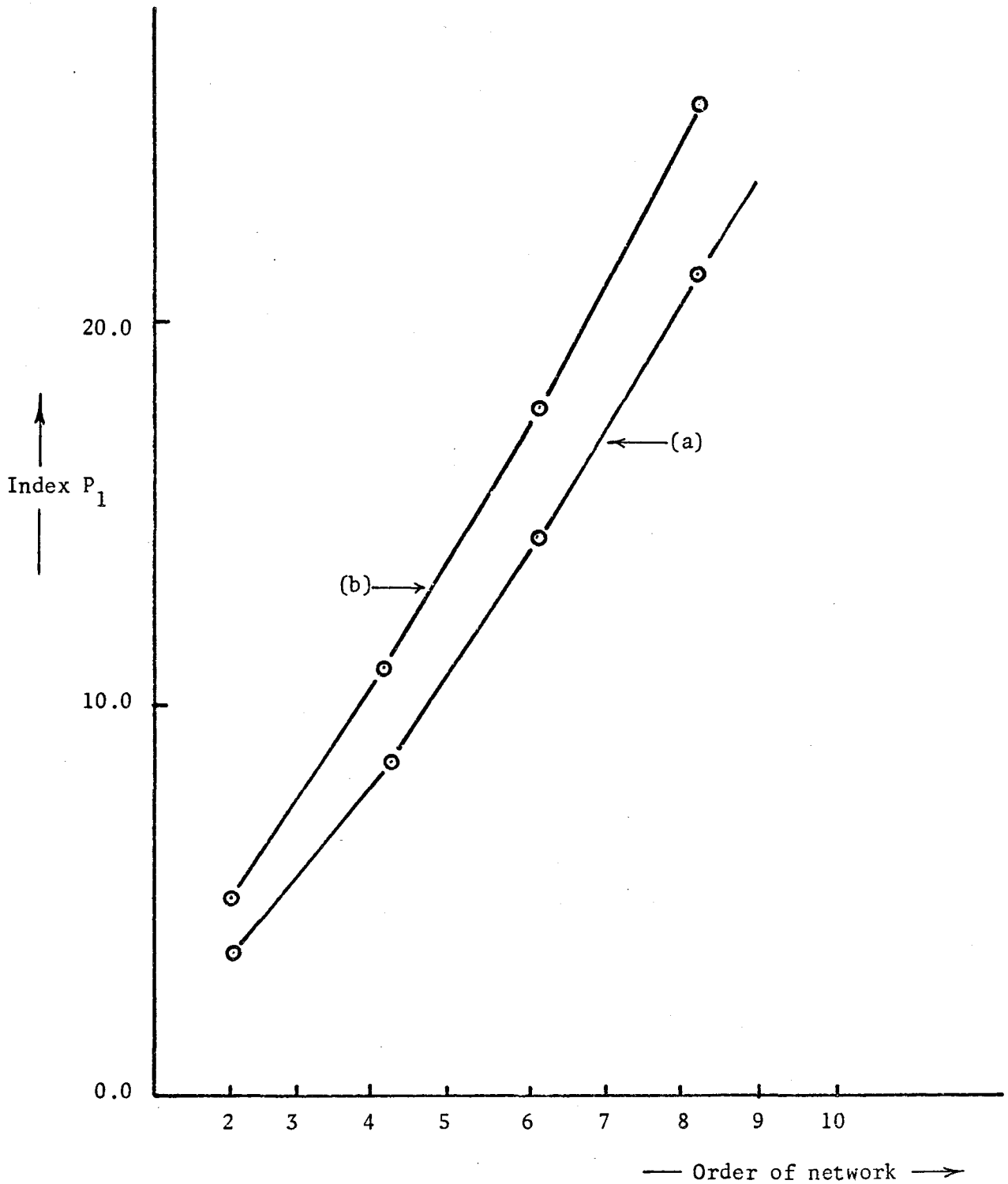

Figure 6.2: Variation of index P_1 with order of filter for

(a) Butterworth filters with source/load resistance ratio, $R_{SL} = 1$

(b) Butterworth filters with $R_{SL} = 1/4$

different values of source/load resistance ratio, R_{SL}. We observe that the sensitivity performance of the network deteriorates as the order of complexity increases.

(b) Magnitude of Passband Ripple : Figure 6.3 shows the effect of increasing passband ripple on the index P_1 for three different filters. We note that the index increases with increasing ripple.

(c) Dissipation: Assuming the dissipation to be uniformly distributed amongst the reactive elements, we have investigated the effect of such dissipation on the sensitivity performance of a fifth-order singly-terminated Butterworth filter. The results, showing the variation of P_1 with the Q of the lossy reactive elements, is shown plotted in Figure 6.4. We note that varying the amount of dissipation has relatively little effect on the index; with increasing dissipation or damping the sensitivity performance improves slightly.

(d) Source/Load Resistance Ratio, R_{SL}: Figures 6.5 and 6.6 show the effect of varying the source/load resistance ratio for a number of odd- and even-ordered Butterworth filters, respectively. We note that the optimum termination occurs for $R_{SL} = 1$, i.e., when load and source resistances are equal. Similar results have been observed for Chebyshev and maximally flat delay filters.

6.4 Optimum Tolerance Sets:

Optimum tolerance sets were obtained for a series of Butterworth filters, doubly terminated with ratio R_{SL} equal to unity. The results are illustrated in Figures 6.7 and 6.8, where we have taken fifth- and ninth-order filters as examples. For this special case, Figure 6.7

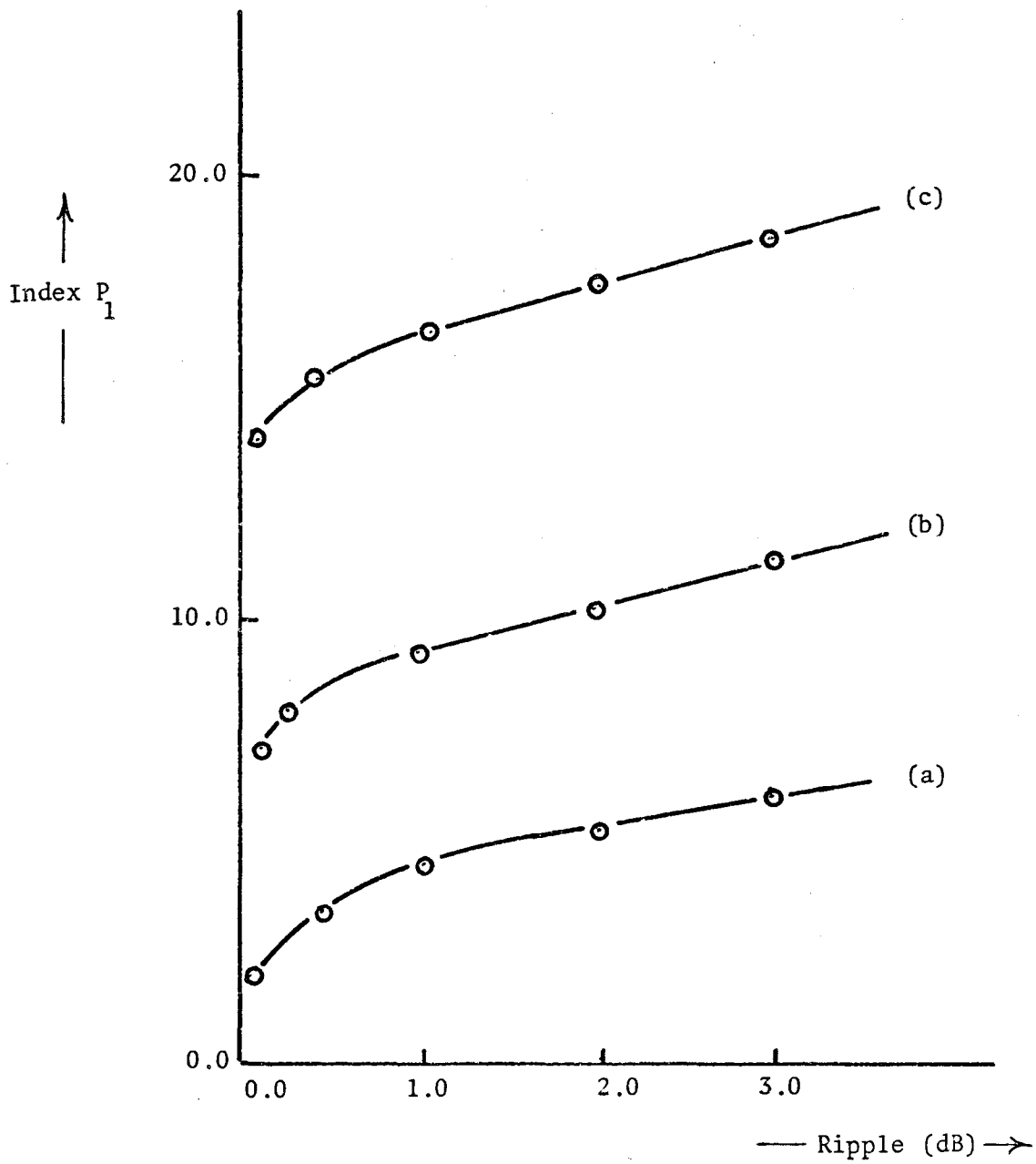

Figure 6.3: Variation of index P_1 with magnitude of passband ripple for

(a) second-order with $R_{SL} = \infty$

(b) third-order with $R_{SL} = 0.125$

(c) fourth-order with $R_{SL} = 8.0$

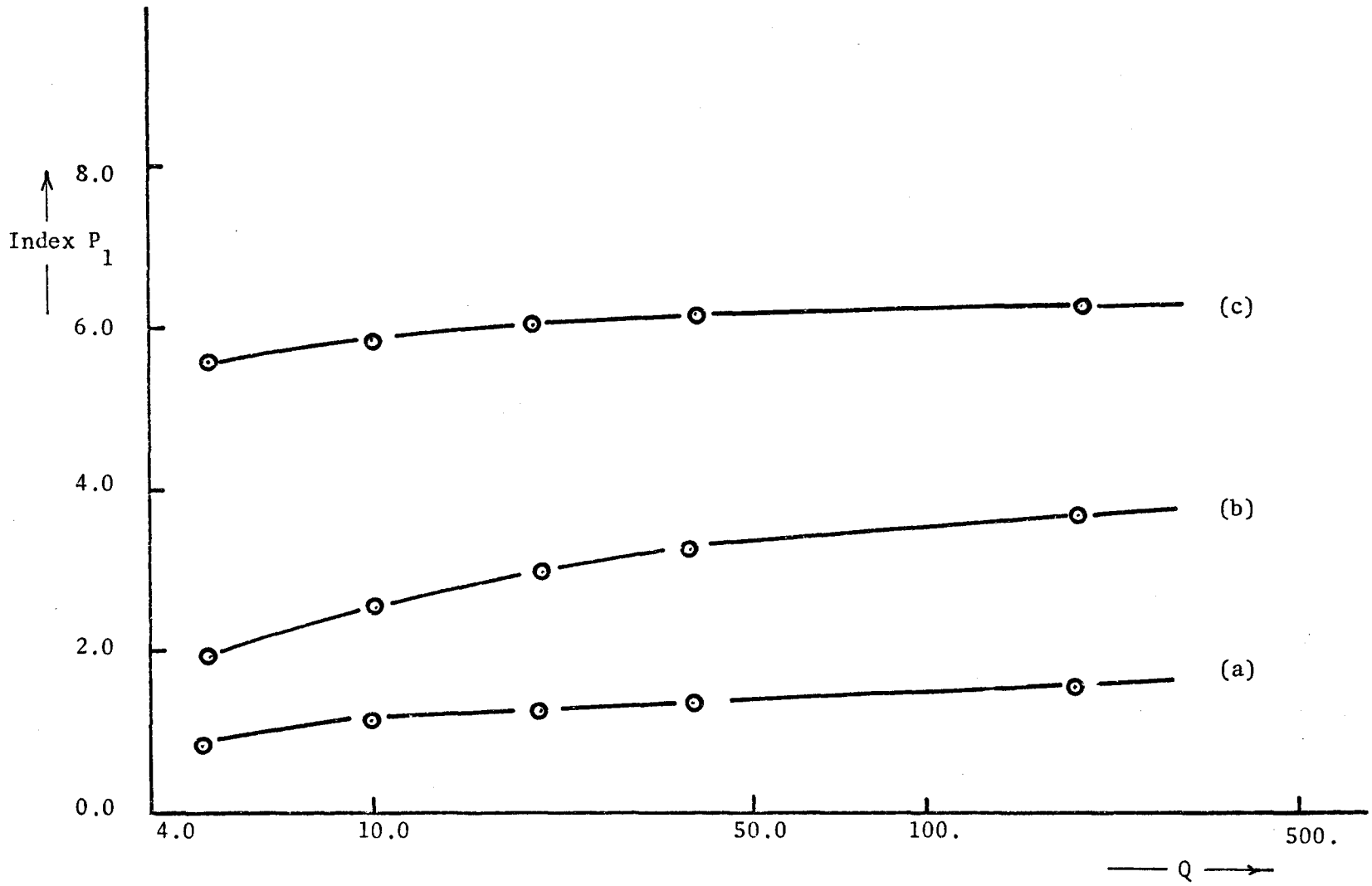

Figure 6.4: Effect of dissipation on index P_1

(a) with $\psi(\omega) = 1$, $0.5 < \omega < 2.0$; $\psi(\omega) = 0$ for all other frequencies

(b) with $\psi(\omega) = 1$, $0 < \omega < 1.0$; $\psi(\omega) = 0$ for all other frequencies

(c) with $\psi(\omega) = 1$, $0 < \omega < 10.0$; $\psi(\omega) = 0$ for all other frequencies

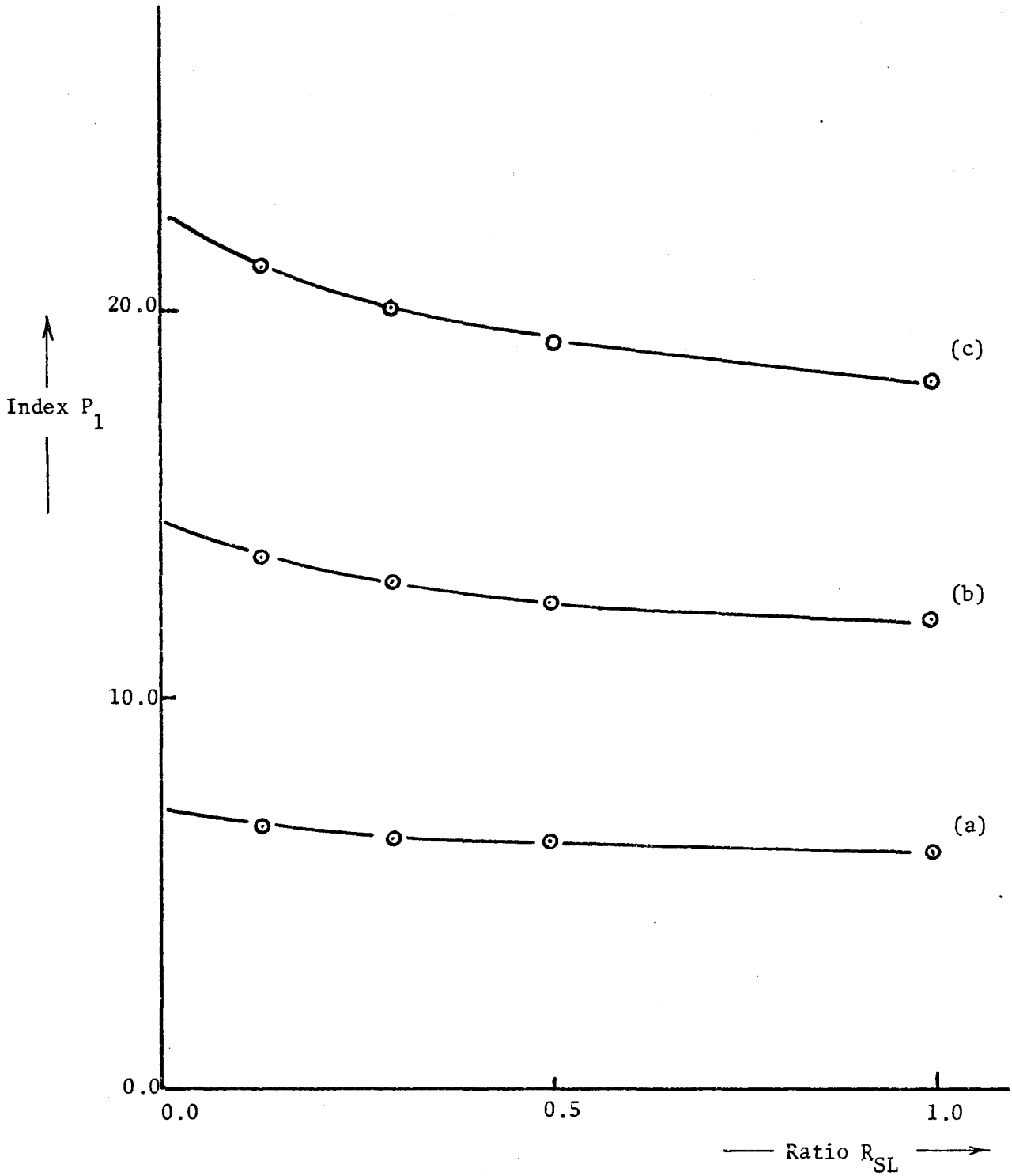

Figure 6.5: Effect of varying source/load resistance ratio on index P_1 for odd-ordered filters

(a) Third-order Butterworth filters

(b) Fifth-order Butterworth filters

(c) Seventh-order Butterworth filters

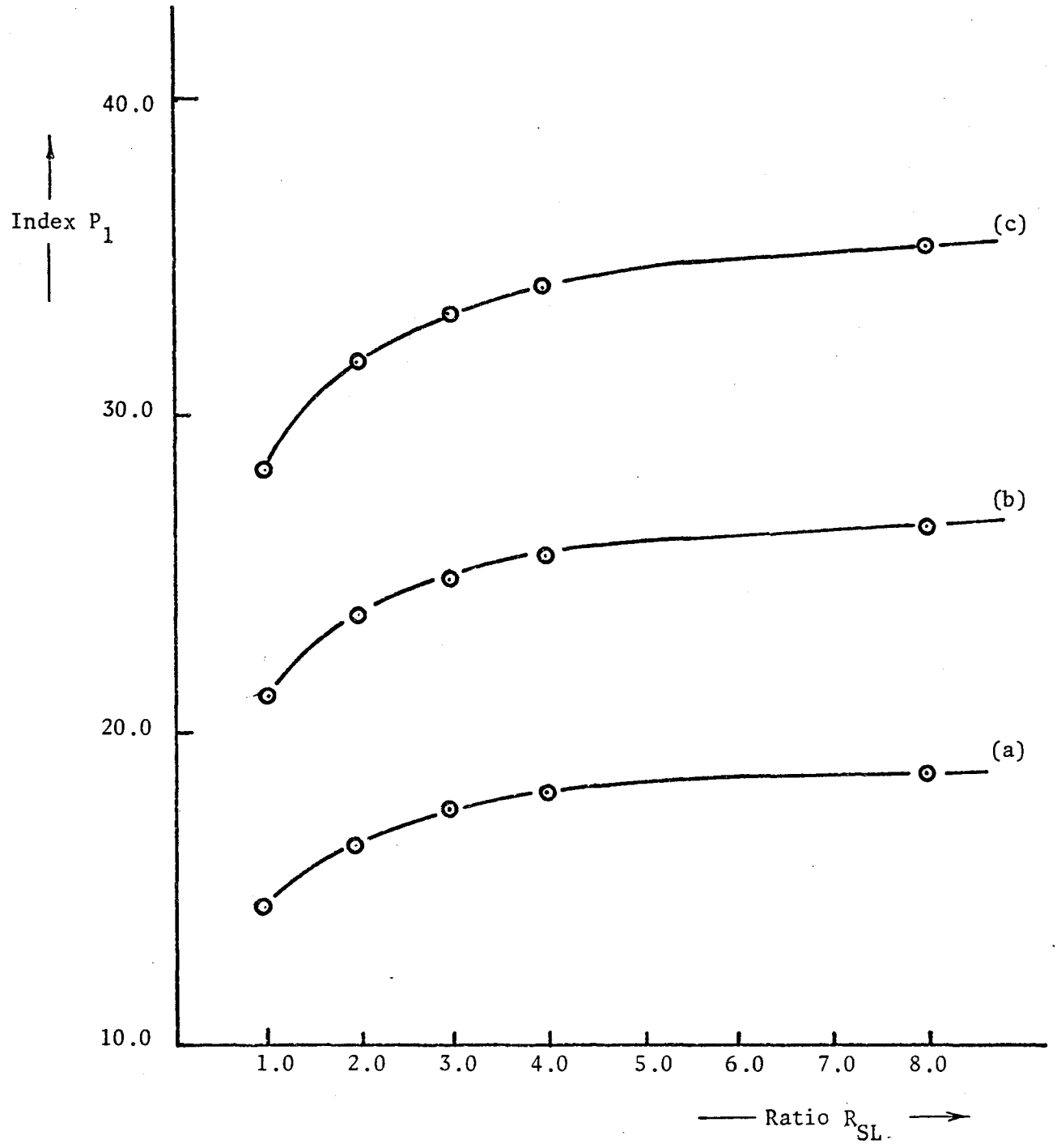

Figure 6.6: Effect of varying source/load resistance ratio for even-ordered filters

(a) Sixth-order Butterworth filters

(b) Eighth-order Butterworth filters

(c) Tenth-order Butterworth filters

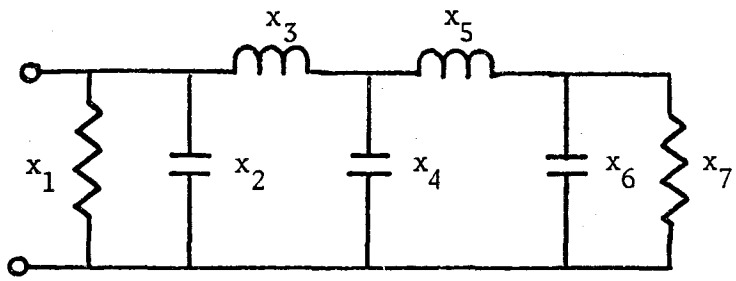

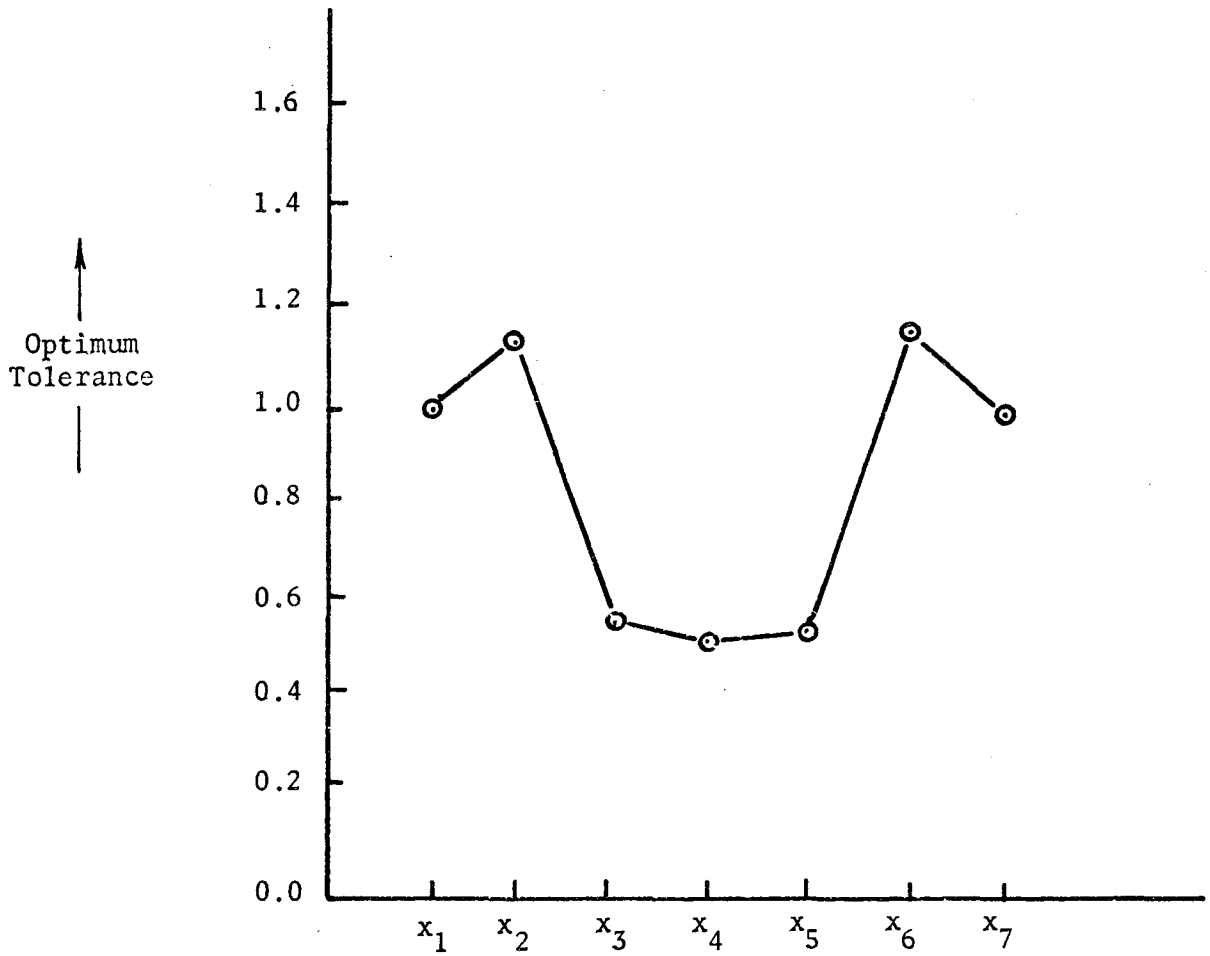

Figure 6.7: Optimum tolerance set for a fifth-order Butterworth filter with $R_{SL} = 1$

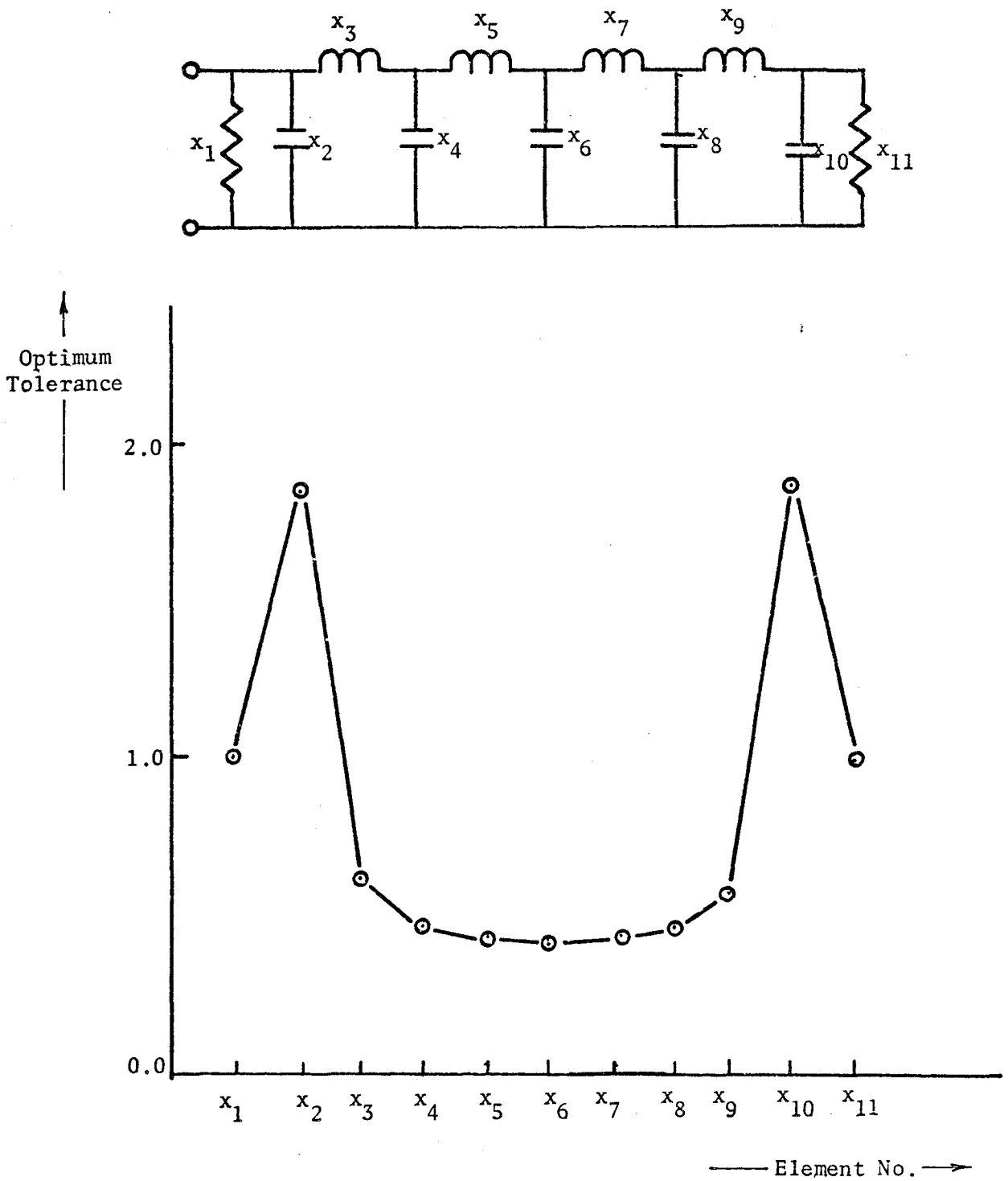

Figure 6.8: Optimum tolerance set for a ninth-order Butterworth filter with $R_{SL} = 1$.

indicates that changes in the inner elements of the filter have a more profound effect upon the overall filter performance, and must therefore be held within closer tolerance limits, than the outer elements of the filter. It should also be noted that the symmetry which occurs in Figure 6.7 is due to the symmetry of the filter itself. If, for example, we were to change the value of R_{SL} then this symmetry would be lost, as illustrated in Figure 6.9.

6.5 Comparison of Sensitivity Performance of Networks with Optimum and Uniform Tolerance Sets:

The sensitivity performance of filters with optimum and uniform tolerance sets were compared; the tolerance of the elements of the latter being made equal to the mean of the optimum tolerance set. Two criteria were used in making this comparison:

(a) Frequency Response in which the bandwidth and the magnitude of the ripple in the passband were used as measures of performance, and

(b) The Index of Performance, P_2 in which the expected value of p_j and its standard deviation were used as measures of performance.

The procedure was essentially the same in all cases; a random sequence of uniformly distributed numbers was used to generate sets of element values (between specified tolerance limits) for filters using both optimum and uniform tolerance sets. The frequency response of both sample groups was then evaluated, with the magnitude of the ripple in the passband and the bandwidth being determined and the respective errors being recorded. The mean square errors for both sample groups were obtained. As a measure of improvement obtained by the use of the optimum tolerance set, we define

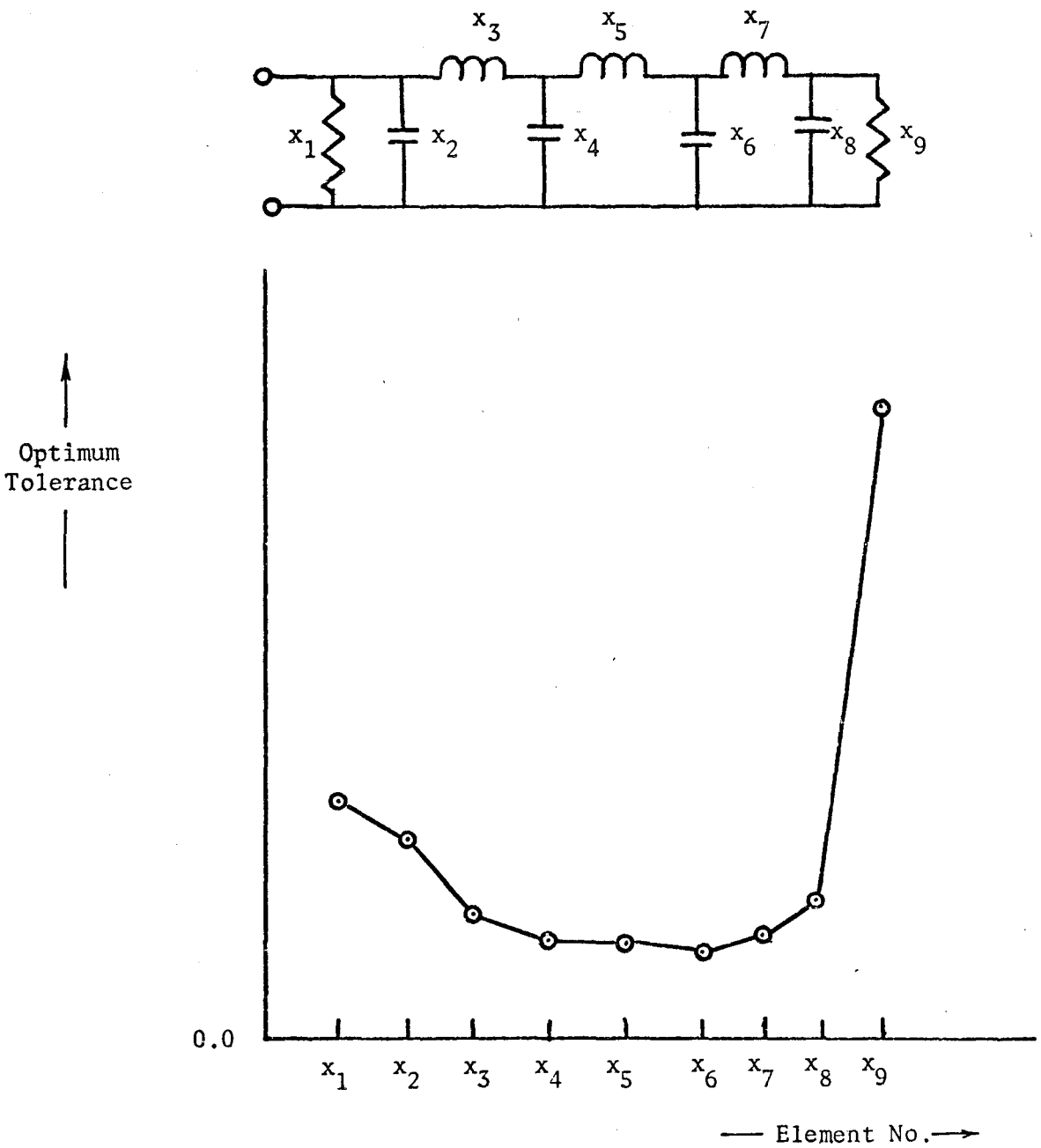

Figure 6.9: Optimum tolerance set for a seventh-order Chebyshev filter, 1/4 dB ripple, with $R_{SL} = 1/3$

improvement factors K_B and K_R, pertaining to the bandwidth and ripple errors, respectively,

$$K_B \triangleq \frac{\text{Mean square bandwidth error for uniform group}}{\text{Mean square bandwidth error for optimum group}}$$

and

$$K_R \triangleq \frac{\text{Mean square ripple error for uniform group}}{\text{Mean square ripple error for optimum group}}$$

In a similar manner, a random sequence of uniformly distributed numbers was used to generate sets of nominal element values between specified tolerance limits for both sample groups. The expected value of p_j (the index P_2) and the standard deviation of p_j was then obtained for both groups, and two additional improvement factors were defined as follows:

$$K_E \triangleq \frac{\text{Expected value of } p_j \text{ for uniform group}}{\text{Expected value of } p_j \text{ for optimum group}}$$

$$K_S \triangleq \frac{\text{Standard deviation of } p_j \text{ for uniform group}}{\text{Standard deviation of } p_j \text{ for optimum group}}$$

Table 6.3 gives these factors for a number of typical filters, where in each case we have used sample groups of at least 100 samples to evaluate the various improvement factors. We see that in all cases substantial improvements in the performance of the filter result from using the optimum tolerance set to define the tolerance limits for the various network parameters.

Table 6.1: Index P_1 using low-pass weighting function

(a) Butterworth filters:

Order of filter	$R_{SL}=0$	$R_{SL}=1/8$	$R_{SL}=1/4$	$R_{SL}=1/3$	$R_{SL}=1/2$	$R_{SL}=1$
2	1.266	1.958	1.756	1.651	1.487	1.076
3	1.947	1.750	1.639	1.595	1.558	1.707
4	2.812	3.278	2.903	2.697	2.399	2.036
5	3.689	3.267	2.996	2.870	2.707	2.589
6	4.519	4.704	4.262	3.999	3.608	3.132
7	5.386	4.734	4.310	4.118	3.873	3.593
8	6.323	6.303	5.594	5.240	4.730	4.224
9	7.266	6.333	5.725	5.440	5.065	4.777
10	8.180	7.897	7.011	6.426	5.956	5.317

(b) Chebyshev filters with 1/10 dB ripple:

Order of filter	$R_{SL}=0$	$R_{SL}=1/8$	$R_{SL}=1/4$	$R_{SL}=1/3$	$R_{SL}=1/2$	$R_{SL}=1$
2	1.036	1.137	0.972	0.891	0.773	-
3	1.291	1.097	0.989	0.948	0.911	0.931
4	2.206	2.721	2.315	2.111	1.813	-
5	3.610	3.068	2.725	2.569	2.373	2.238
6	5.182	5.181	4.463	4.109	3.608	-
7	7.134	6.018	5.307	4.973	4.546	4.204
8	9.292	8.555	7.384	6.818	6.037	-
9	11.690	9.806	8.588	8.028	7.293	6.689
10	14.300	12.680	10.940	10.110	8.978	-

(c) Chebyshev filters with 1/4 dB ripple:

Order of filter	$R_{SL}=0$	$R_{SL}=1/8$	$R_{SL}=1/4$	$R_{SL}=1/3$	$R_{SL}=1/2$	$R_{SL}=1$
2	1.093	1.314	1.121	1.022	0.865	-
3	1.621	1.404	1.279	1.228	1.174	1.154
4	2.914	3.256	2.795	2.549	2.194	-
5	4.457	3.814	3.402	3.212	2.966	2.771
6	6.502	7.289	5.425	4.995	4.377	-
7	8.806	7.489	6.626	6.225	5.687	5.252
8	11.310	10.260	8.859	8.175	7.218	-
9	14.090	11.930	10.500	9.832	8.955	8.209
10	17.070	15.010	12.940	11.950	10.580	-

(d) Chebyshev filters with 1/2 dB ripple:

Order of filter	$R_{SL}=0$	$R_{SL}=1/8$	$R_{SL}=1/4$	$R_{SL}=1/3$	$R_{SL}=1/2$	$R_{SL}=1$
2	1.187	1.504	1.795	1.149	0.898	-
3	2.031	1.784	1.634	1.570	1.492	1.438
4	3.661	3.844	3.297	3.012	2.536	-
5	5.584	4.832	4.345	4.115	3.816	3.564
6	7.883	7.417	6.391	5.784	5.076	-
7	10.500	9.016	8.040	7.581	6.975	6.456
8	13.320	11.960	10.300	9.488	8.281	-
9	16.500	14.080	12.500	11.760	10.770	9.931
10	19.830	17.260	14.880	13.700	12.010	-

(e) Chebyshev filters with 1 dB ripple:

Order of filter	$R_{SL}=0$	$R_{SL}=1/8$	$R_{SL}=1/4$	$R_{SL}=1/3$	$R_{SL}=1/2$	$R_{SL}=1$
2	1.381	1.762	1.464	1.279	-	-
3	2.661	2.374	2.193	2.148	2.007	1.922
4	4.709	4.687	4.001	3.620	-	-
5	7.019	6.170	5.616	5.376	5.015	4.724
6	9.801	8.960	7.674	7.000	-	-
7	12.830	11.190	10.110	9.605	8.936	8.369
8	16.170	14.370	12.170	11.133	-	-
9	19.740	17.100	15.400	14.605	13.540	12.650
10	23.540	20.250	17.320	15.850	-	-

(f) Chebyshev filters with 2 dB ripple:

Order of filter	$R_{SL}=0$	$R_{SL}=1/8$	$R_{SL}=1/4$	$R_{SL}=1/3$	$R_{SL}=1/2$	$R_{SL}=1$
2	1.788	2.131	-	-	-	-
3	3.688	3.357	3.153	3.058	2.933	2.831
4	6.354	5.991	-	-	-	-
5	9.272	8.358	7.769	7.492	7.131	6.832
6	12.770	11.290	-	-	-	-
7	16.410	14.680	13.570	13.040	12.370	11.810
8	20.480	17.580	-	-	-	-
9	24.790	21.980	20.220	19.410	19.100	17.480
10	29.150	24.570	-	-	-	-

(g) Chebyshev filters with 3 dB ripple:

Order of filter	$R_{SL}=0$	$R_{SL}=1/8$	$R_{SL}=1/4$	$R_{SL}=1/3$	$R_{SL}=1/2$	$R_{SL}=1$
2	2.225	2.430	-	-	-	-
3	4.648	4.314	4.099	4.001	3.872	3.768
4	7.903	7.181	-	-	-	-
5	11.380	10.490	9.895	9.628	9.274	8.984
6	15.530	13.430	-	-	-	-
7	19.760	18.080	17.000	16.500	15.860	15.330
8	24.510	20.690	-	-	-	-
9	29.270	26.670	25.000	24.230	23.240	22.410
10	34.440	28.620	-	-	-	-

Table 6.2: Index P_1 using ideal band-pass weighting function

(a) Butterworth filters:

Order of filter	$R_{SL}=0$	$R_{SL}=1/8$	$R_{SL}=1/4$	$R_{SL}=1/3$	$R_{SL}=1/2$	$R_{SL}=1$
2	3.46	5.47	5.15	4.97	4.67	3.72
3	7.09	6.76	6.53	6.42	6.24	5.97
4	10.33	11.81	11.26	10.93	10.41	8.58
5	14.30	13.60	13.08	12.81	12.41	11.89
6	18.60	18.88	18.04	17.58	16.83	14.52
7	22.22	21.11	20.29	19.87	19.21	18.13
8	27.15	26.80	25.67	25.05	24.04	21.10
9	30.85	29.34	28.24	27.67	26.77	24.65
10	35.81	35.47	34.04	33.40	32.00	28.13

(b) Chebyshev filters with 1/10 dB ripple:

Order of filter	$R_{SL}=0$	$R_{SL}=1/8$	$R_{SL}=1/4$	$R_{SL}=1/3$	$R_{SL}=1/2$	$R_{SL}=1$
2	2.39	3.89	3.47	3.25	2.87	-
3	7.58	7.09	6.75	6.58	6.34	6.08
4	13.12	14.24	13.34	12.84	11.99	-
5	19.70	18.42	17.49	17.01	16.28	15.40
6	25.97	26.01	24.51	23.71	22.38	-
7	32.82	30.64	29.06	28.24	27.02	25.57
8	39.53	38.64	36.42	35.24	33.36	-
9	46.79	43.48	41.13	39.94	38.16	36.10
10	54.75	52.61	49.39	47.72	45.16	-

(c) Chebyshev filters with 1/4 dB ripple:

Order of filter	$R_{SL}=0$	$R_{SL}=1/8$	$R_{SL}=1/4$	$R_{SL}=1/3$	$R_{SL}=1/2$	$R_{SL}=1$
2	3.0	4.72	4.26	3.99	3.51	-
3	8.52	7.99	7.62	7.43	7.15	6.87
4	14.08	15.05	13.90	13.56	12.61	-
5	20.57	19.25	18.29	17.79	17.05	16.25
6	27.24	27.01	25.40	24.53	23.07	-
7	34.34	32.02	30.36	29.51	28.26	26.05
8	42.22	40.86	38.34	37.01	34.87	-
9	51.08	47.35	44.69	43.36	41.44	39.44
10	61.60	58.45	54.59	52.58	49.49	-

(d) Chebyshev filters with 1/2 dB ripple:

Order of filter	$R_{SL}=0$	$R_{SL}=1/8$	$R_{SL}=1/4$	$R_{SL}=1/3$	$R_{SL}=1/2$	$R_{SL}=1$
2	3.61	5.29	5.32	4.48	3.76	-
3	9.17	8.63	8.24	8.05	7.77	7.50
4	14.08	15.69	14.66	14.07	12.88	-
5	21.59	20.23	19.25	18.76	18.05	17.36
6	28.76	28.15	26.38	25.41	23.66	-
7	36.55	30.48	32.35	31.48	30.24	29.03
8	46.04	44.17	41.26	39.72	37.08	-
9	56.99	52.87	49.95	48.51	46.46	44.49
10	70.62	66.15	61.57	59.16	55.26	-

(e) Chebyshev filters with 1 dB ripple:

Order of filter	$R_{SL}=0$	$R_{SL}=1/8$	$R_{SL}=1/4$	$R_{SL}=1/3$	$R_{SL}=1/2$	$R_{SL}=1$
2	4.35	5.80	5.22	4.82	-	-
3	9.89	9.35	8.97	8.83	8.52	8.29
4	16.14	16.45	15.29	14.58	-	-
5	22.90	21.54	20.59	20.11	19.46	18.87
6	31.14	29.97	27.93	26.77	-	-
7	40.19	37.64	35.87	35.01	33.81	32.73
8	52.45	48.95	45.93	44.00	-	-
9	66.04	61.56	58.50	57.22	54.93	53.07
10	84.09	77.89	72.16	69.09	-	-

(f) Chebyshev filters with 2 dB ripple:

Order of filter	$R_{SL}=0$	$R_{SL}=1/8$	$R_{SL}=1/4$	$R_{SL}=1/3$	$R_{SL}=1/2$	$R_{SL}=1$
2	5.29	6.30	-	-	-	-
3	10.88	10.37	10.04	9.87	9.65	9.46
4	17.86	17.54	-	-	-	-
5	24.88	23.61	22.75	22.33	21.78	21.30
6	34.61	32.65	-	-	-	-
7	45.54	43.13	41.47	40.69	39.64	38.75
8	61.20	56.83	-	-	-	-
9	77.70	74.26	71.31	69.90	68.44	66.46
10	103.10	94.50	-	-	-	-

(g) Chebyshev filters with 3 dB ripple:

Order of filter	$R_{SL}=0$	$R_{SL}=1/8$	$R_{SL}=1/4$	$R_{SL}=1/3$	$R_{SL}=1/2$	$R_{SL}=1$
2	6.01	6.63	-	-	-	-
3	11.80	11.34	11.03	10.88	10.70	10.54
4	19.33	18.50	-	-	-	-
5	26.41	25.27	24.51	24.15	23.69	23.31
6	37.13	34.54	-	-	-	-
7	49.45	47.24	45.85	45.16	44.28	44.00
8	67.38	61.96	-	-	-	-
9	87.40	83.44	80.52	79.68	78.05	76.71
10	116.89	106.50	-	-	-	-

Table 6.3

Filter						
Order	Ripple (dB)	Ratio† R_{SL}	K_R	K_B	K_E	K_S
4th	1/2	8	2.17	1.55	1.40	1.70
5th	1	1/4	2.18	1.72	5.21	5.66
6th	1	8	3.84	3.89	1.67	1.84
7th	1/4	1/3	5.42	5.79	2.55	3.08

† Note that R_{SL} = source/load resistance ratio.

Improvement Factors Obtained in Evaluating Performance of Optimum Tolerance Sets

6.6 Conclusion:

In investigating the multiparameter sensitivity of low-pass LC ladder filters, some rather interesting results were obtained:

(1) Although it has been suggested by Orchard[3] that the sensitivity performance of LC networks gets worse only by virtue of second-order effects becoming noticeable, nonetheless, it has been observed that increasing the order of complexity of the network has a significant effect on the value of the index P_1.

(2) The optimum terminating conditions exist when the load and source resistances are equal.

(3) Increasing the amount of dissipation improves the sensitivity performance of the network slightly.

(4) The optimum tolerance sets which were obtained for these networks indicate that the sensitive elements tend to be those which are located towards the center of the ladder, and the use of these optimum tolerance sets has been found to improve the sensitivity performance of the network considerably.

CHAPTER VII

EXTENSION TO ACTIVE FILTERS

7.1 Introduction:

In this chapter, we will deal with the extension of the index of performance and the concept of the optimum tolerance set to the case of RC-active filters. As has been pointed out in Chapter II, in the case of highly selective active filters, it is ordinarily preferable to realize the network function as a cascade of second-order sections, each suitably isolated and thereby accounting for a single pair of complex conjugate poles as shown in Figure 7.1. The extent to which variations in the elements of any such section affect the overall response of the network is determined by several factors. For example, the location, in the complex frequency plane, of the particular pole-pair to be realized, and the choice of structure for that section are both factors which influence the sensitivity of the overall response to variations in component parameters.

The choice of structure for such a section is a particularly wide one at the present time, as many suitable networks using NIC's, gyrators, operational and fixed-gain amplifiers are available to the designer. This, naturally, raises the question as to whether an optimum choice of such sections exists for a given filter specification, and if so, then to what extend is the choice of individual section influenced by the coordinates of the pole-pair which it is to realize. In addition, we might also wish

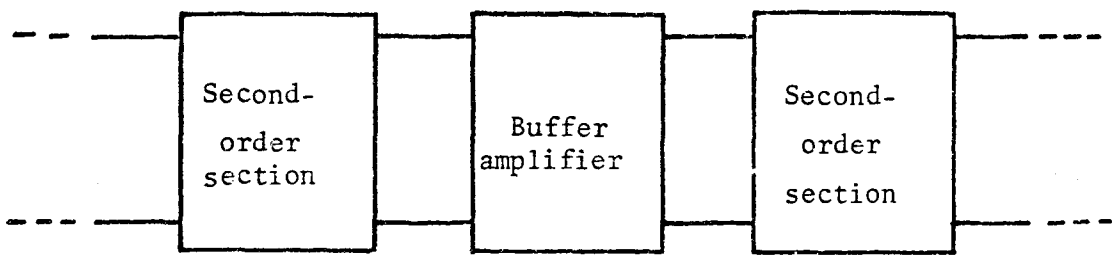

Figure 7.1: Cascade synthesis

to determine the manner in which the various pole and/or zero movements should be controlled, relative to each other, such that the overall effect of such migrations is minimized.

In the following sections, we will consider these questions, and we will show that by extending the use of the index of performance and the concept of the optimum tolerance set to this area, some useful results can be obtained.

7.2 The Pole-Zero Index, P_{pz}:

The first step in the extension of the multiparameter sensitivity index of performance to the case of RC-active filters is to redefine the network parameters of interest to be the coordinates of the pole-zero pattern of the network function of interest. It is rather convenient to define the coordinates of the poles in terms of the relative damping factor, ζ, and the undamped natural frequency of oscillation, ω_n, and to use a similar notation to define the coordinates of the zeros, although it is recognized that in the case of zeros, such parameters do not have the same physical significance. In this thesis, however, consideration of zeros does not arise, as we are concerned with low-pass filters only, the transmission zeros of which are all located at infinite frequency. By redefining the network parameters in this way, it is possible to obtain an index of performance which is defined in terms of small variations in pole-zero locations and which we will denote by P_{pz}.

In the same way that optimum tolerance sets were obtained for the various network elements, we can now obtain optimum tolerance sets for the various ζ_i and ω_{n_i}. The significance of this new optimum tolerance set,

which we will denote by δx_{pz}, is that it defines the limits of pole-zero migrations, such that each such migration contributes equally to the total error in the network response. In other words, we now have a means of obtaining the optimal limits on the movements of one pair of complex-conjugate poles relative to the movement of any other pair. This information becomes particularly useful for the case of RC-active filters of an order greater than two.

7.3 Computational Results:

The index, P_{pz}, and the optimum tolerance set δx_{pz}, have been obtained for a number of low-pass LC-ladder filters. The values obtained for P_{pz} are tabulated in Tables 7.1 and 7.2 where we have used, for the frequency sensitive weighting function $\psi(\omega)$, an ideal low-pass window function with cut-off frequency of 1 radian per second and an ideal band-pass window function with lower and upper cut-off frequencies of 0.5 and 2.0 radians per second, respectively. The values obtained for P_{pz} correlate closely with those obtained for the index P_1, which is to be expected. This correspondence is evidenced in Figures 7.2 and 7.3 where the variations of the index P_{pz} with order of complexity of the network and with magnitude of passband ripple is shown, respectively.

In Figure 7.4, we show the optimum migration areas for a tenth-order, Butterworth filter as defined by the optimum tolerance set, δx_{pz}, for that network. Not unexpectedly, these results show that the optimum tolerable limits on pole migration are less stringent as the pole moves away from the $j\omega$-axis, corresponding to an increased relative damping factor, ζ.

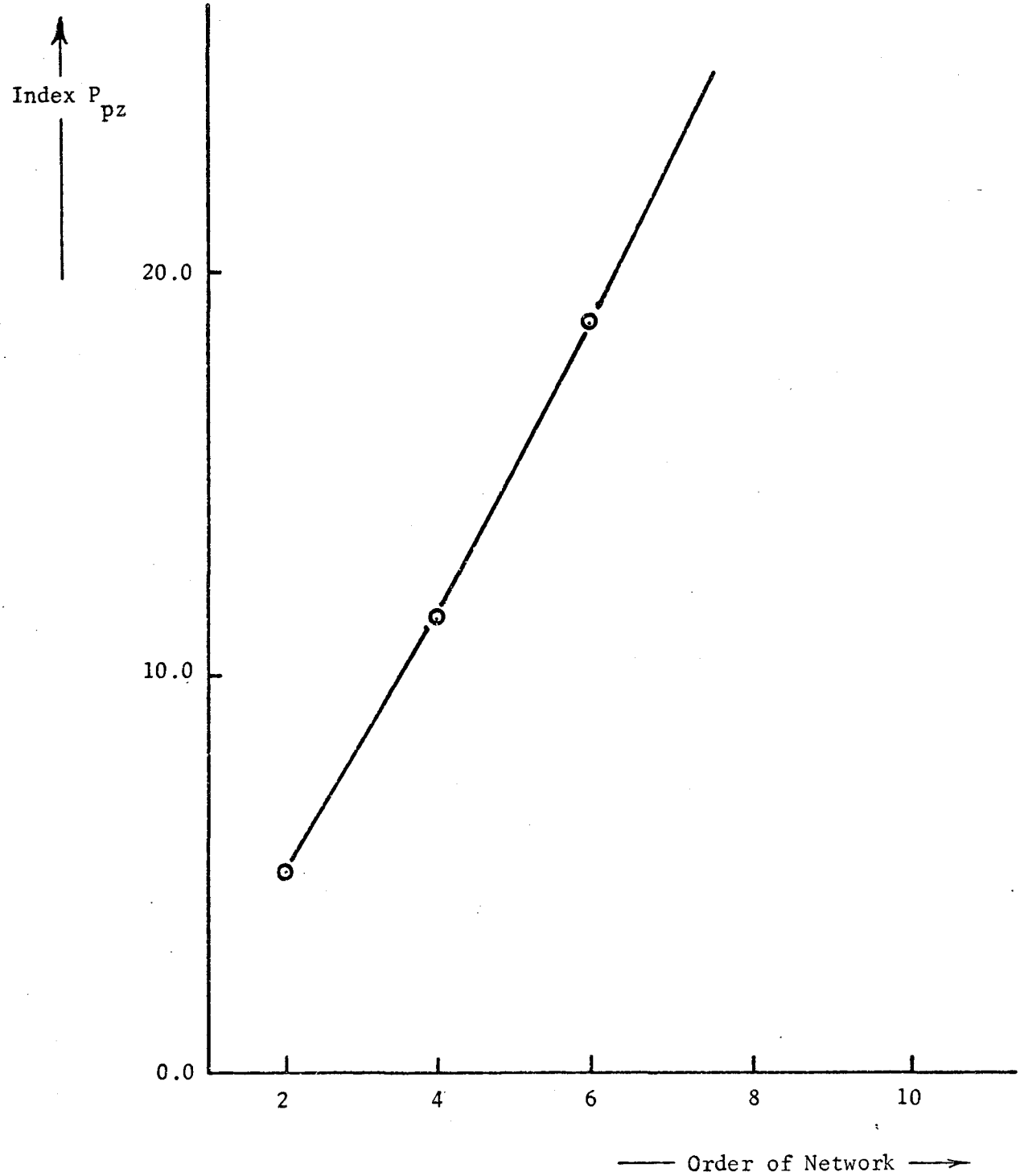

Figure 7.2: Variation of index P_{pz} with order of filter for Butterworth filters

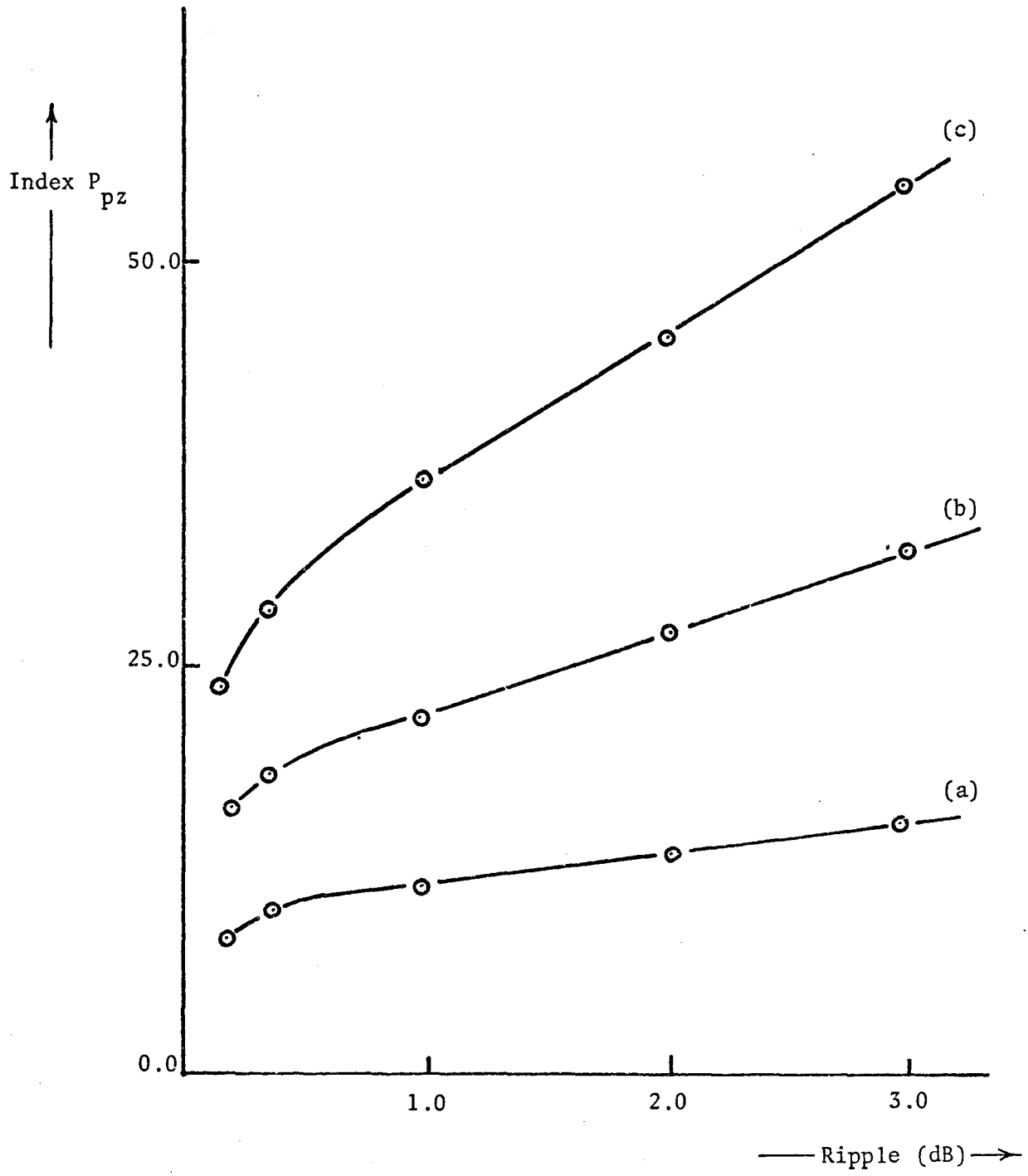

Figure 7.3: Variation of index P_{pz} with magnitude of passband ripple for

(a) third-order filters
(b) fourth-order filters
(c) fifth-order filters

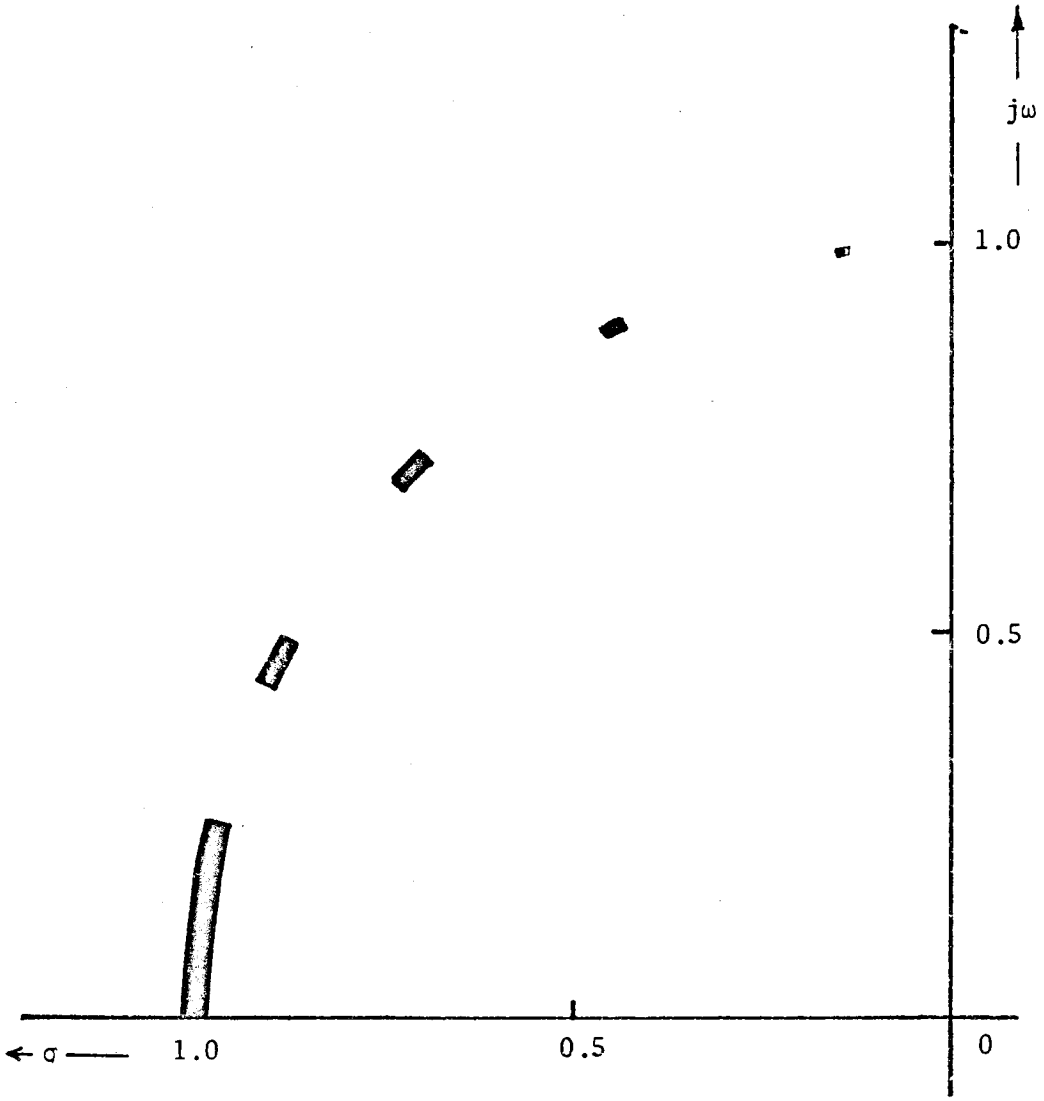

Figure 7.4: Optimum migration areas for a tenth-order Butterworth filter

Order of filter	Butterworth	1/2 dB ripple	1 dB ripple	2 dB ripple	3 dB ripple
2	5.55	4.89	5.29	5.32	6.65
3	6.26	8.13	9.57	12.13	14.68
4	10.40	15.08	18.14	23.63	29.13
5	12.54	22.40	28.09	38.18	48.18
6	17.05	33.67	42.69	58.64	74.41
7	19.24	46.21	59.68	83.31	106.50
8	23.76	62.81	81.52	114.20	146.20
9	26.25	81.29	106.40	150.00	192.40
10	30.91	103.90	136.30	192.10	246.40

Table 7.1(a): Pole-zero index, P_{pz}, for various low-pass LC ladder filters, using ideal low-pass weighting function

Order of Complexity	Butterworth	1/2 dB ripple	1 dB ripple	2 dB ripple	3 dB ripple
2	4.607	6.440	6.004	4.439	5.891
3	6.535	10.720	11.560	13.610	15.930
4	11.410	19.690	22.230	27.150	32.060
5	13.990	31.130	36.930	46.570	54.700
6	19.490	47.930	58.710	75.660	88.990
7	22.340	69.990	89.150	118.500	141.200
8	28.250	101.200	133.300	182.100	219.300
9	31.290	143.400	194.900	272.400	331.000
10	37.230	200.500	290.400	400.900	497.300

Table 7.1(b): Pole-zero index, P_{pz}, for various low-pass ladder LC filters, using ideal band-pass weighting function

7.4 Sensitivity Analysis of Typical RC-active Second-order Sections:

The multiparameter sensitivity performance of five typical RC-active second-order sections involving negative impedance converters, gyrators and operational amplifiers was investigated. These networks, which have been synthesized by classical techniques[46], are shown in Figures 7.5 through 7.9. The element values in each case are given as functions of ζ and ω_n. The multiparameter sensitivity performance of these networks, as defined by the index P_1, was computed for a number of different values of ζ, with the natural frequency of oscillation, ω_n, normalized to unity. The computational results are shown plotted in Figure 7.10. In performing this sensitivity analysis, the conversion factor, k, of the negative impedance converter used in the network of Figure 7.5 and the gyration resistance, r, of the gyrator used in the network of Figure 7.6 were both considered network variables as were the other network elements. The results show quite clearly that in the case of each network considered, the sensitivity performance deteriorates as the value of ζ is decreased. Furthermore, we note that the network of Figure 7.7, employing a single operational amplifier, gives the best overall sensitivity performance of the five networks considered.

7.5 A New RC-active Second-order Section:

As an alternative to the networks discussed in the previous section, a new network, consisting of a single-loop negative feedback system, is now proposed. The new network contains an ideal voltage-controlled voltage source, μV_a, and an RC two-port network driven from a current source, I_1, as shown in Figure 7.11. This structure has a number of advantages when

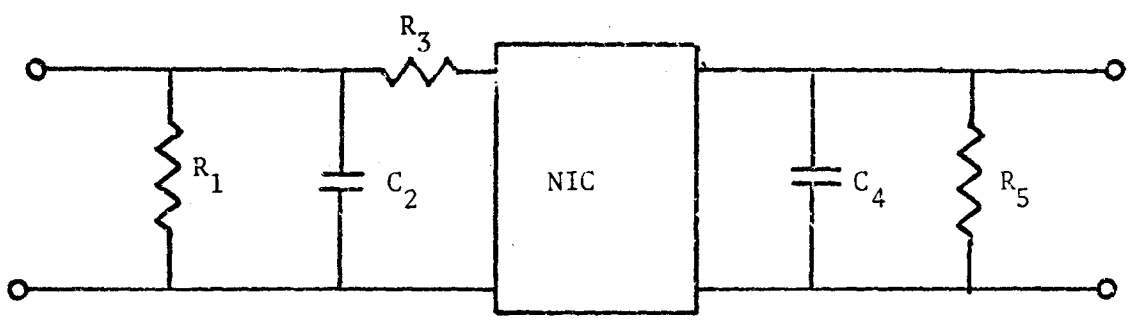

Figure 7.5: RC-NIC second-order low-pass filter

$$R_1 = 11.22 - 2.22\zeta$$
$$R_3 = 1.0$$
$$R_4 = 2.22(1 - \zeta)$$
$$C_2 = \frac{1}{\omega_n(1.122 - 0.222\zeta)}$$
$$C_4 = \frac{1}{2.22\ \omega_n(1 - \zeta)}$$

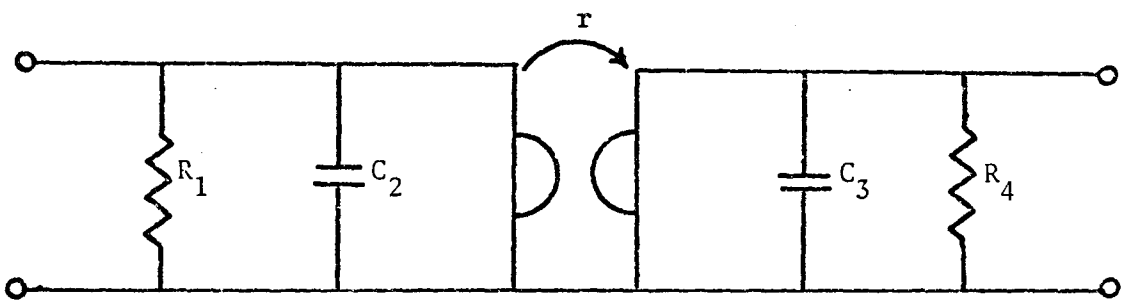

Figure 7.6: RC-gyrator second-order low-pass filter

$$R_1 = \frac{1 - \zeta^2}{\zeta}$$

$$R_4 = \frac{1}{\zeta}$$

$$r = 1$$

$$C_2 = \frac{1}{\omega_n(1 - \zeta^2)}$$

$$C_3 = \frac{1}{\omega_n}$$

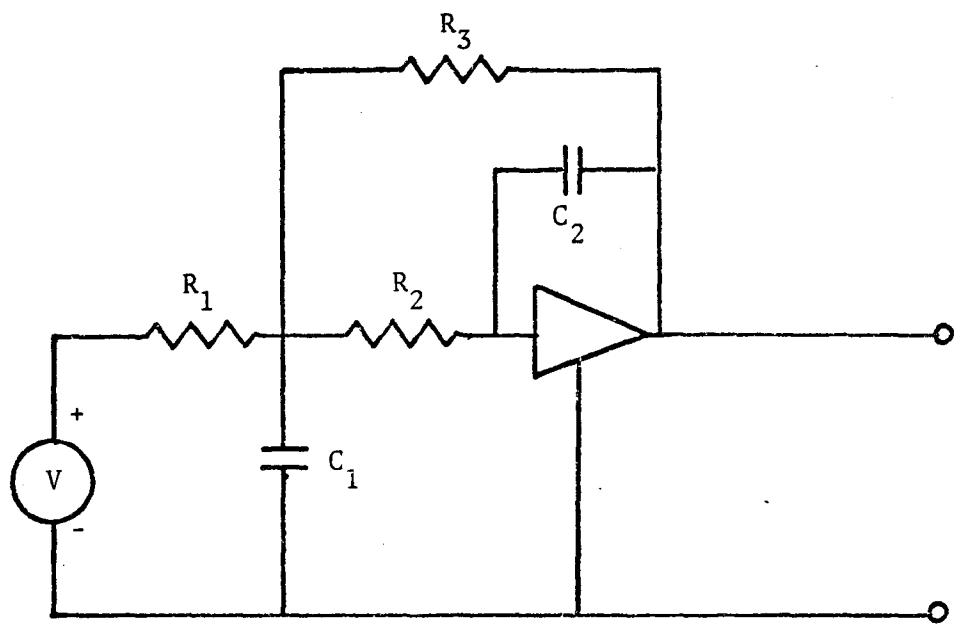

Figure 7.7: RC-active second-order low-pass filter employing one operational amplifier

$$R_1 = 1.0$$
$$R_2 = 0.5$$
$$R_3 = 1.0$$
$$C_1 = \frac{2}{\zeta\omega_n}$$
$$C_2 = \frac{\zeta}{\omega_n}$$

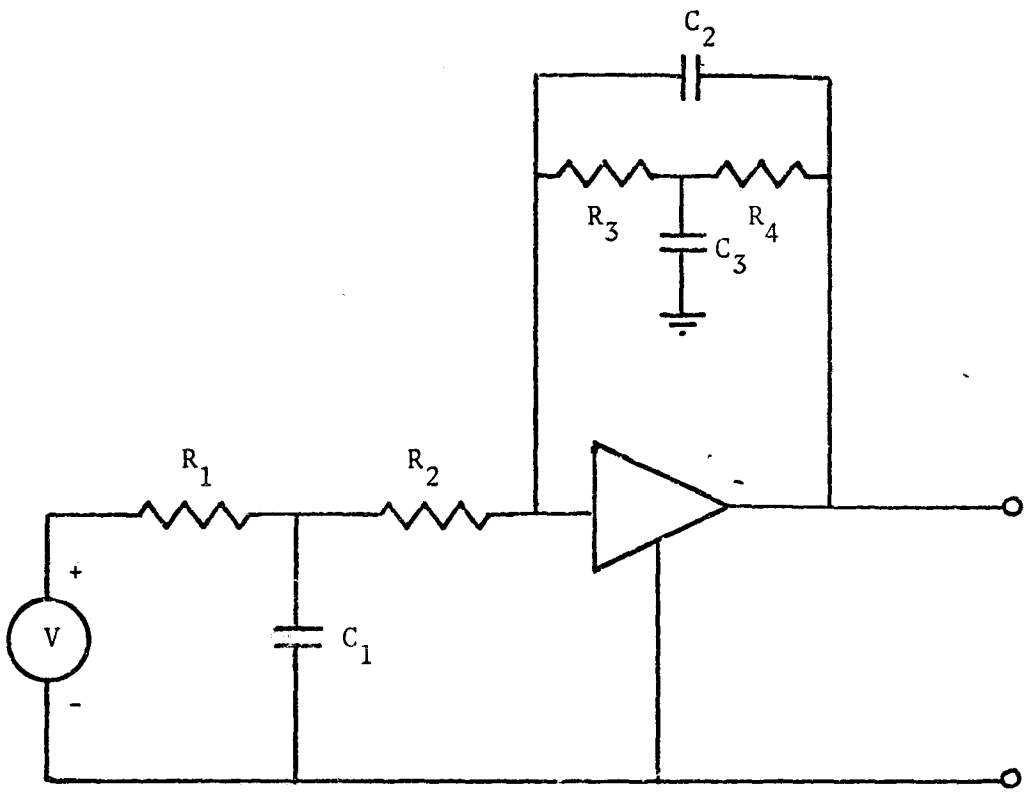

Figure 7.8: RC-active second-order low-pass filter employing one operational amplifier

$R_1 = 1.0$ $\quad$ $C_1 = \frac{1}{\zeta\omega_n}$

$R_2 = 1.0$

$R_3 = 1.0$ $\quad$ $C_2 = \frac{\zeta}{\omega_n}$

$R_4 = 1.0$ $\quad$ $C_3 = \frac{1}{\zeta\omega_n}$

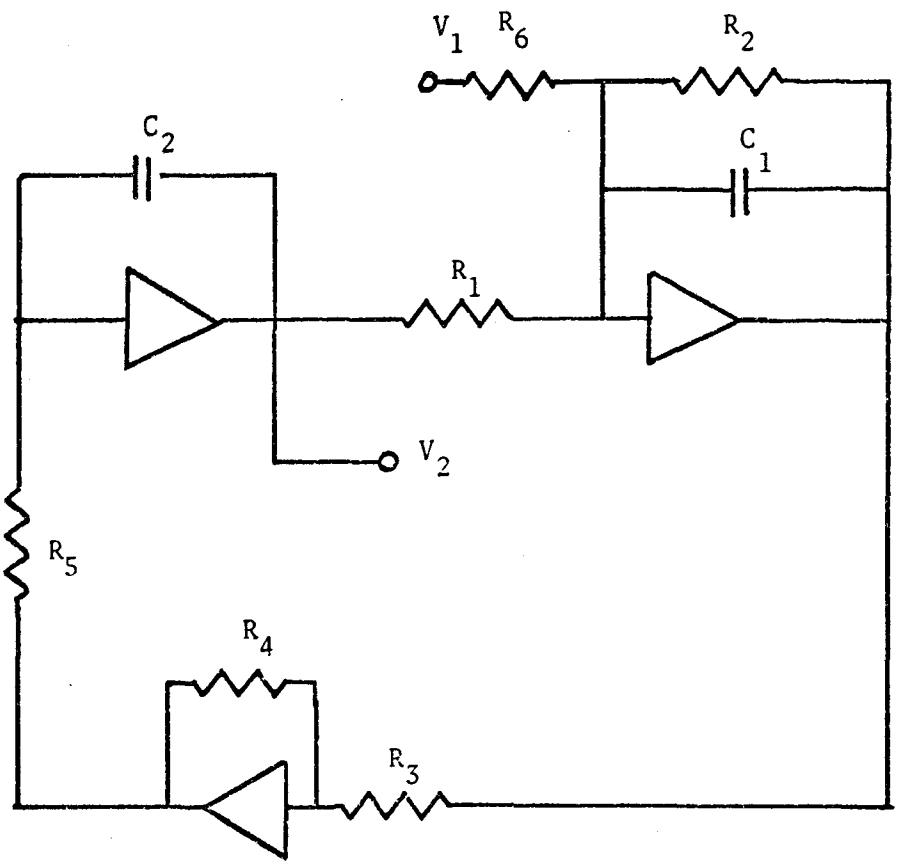

Figure 7.9: RC-active second-order low-pass filter employing three operational amplifiers

$R_1 = 1.0$ $\qquad$ $R_5 = \frac{1}{\omega_n^2}$

$R_2 = \frac{1}{2\zeta\omega_n}$ $\qquad$ $R_6 = 1.0$

$R_3 = 1.0$ $\qquad$ $C_1 = 1.0$

$R_4 = 1.0$ $\qquad$ $C_2 = 1.0$

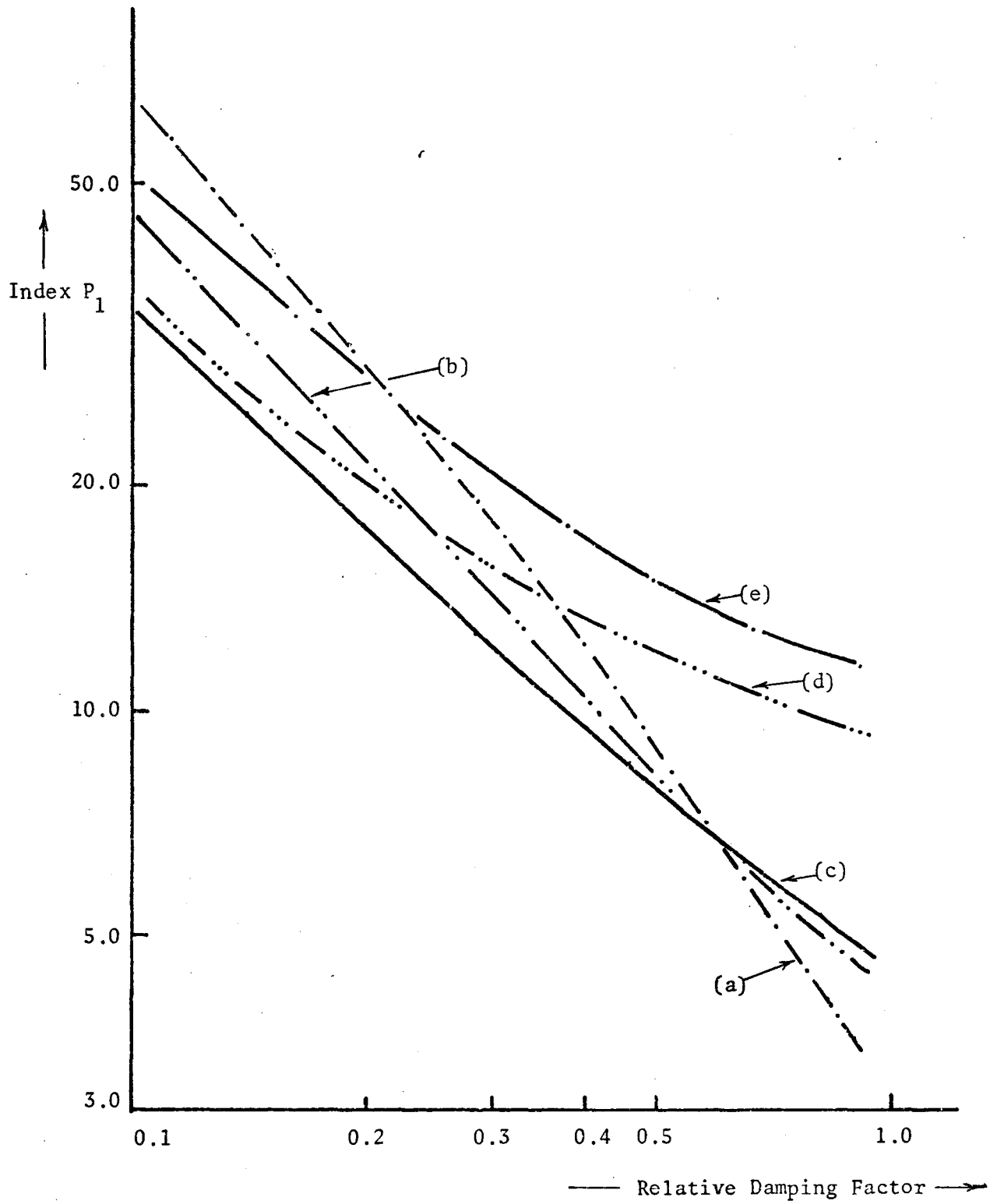

Figure 7.10: Sensitivity performance of various RC-active filters:
(a) RC-NIC structure
(b) RC-gyrator structure
(c) Operational amplifier structure of Figure 7.7
(d) Operational amplifier structure of Figure 7.8
(e) Operational amplifier structure of Figure 7.9

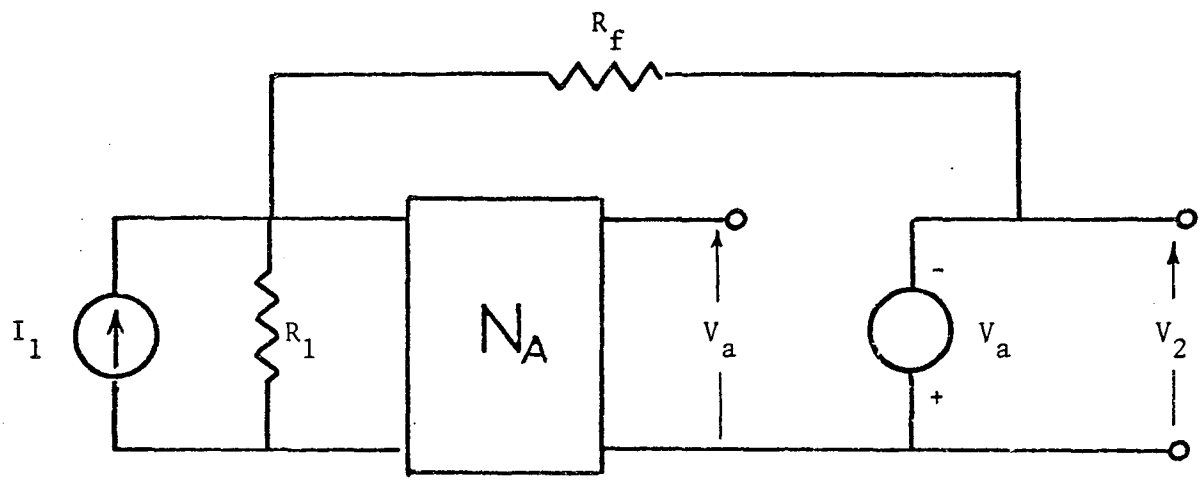

(a)

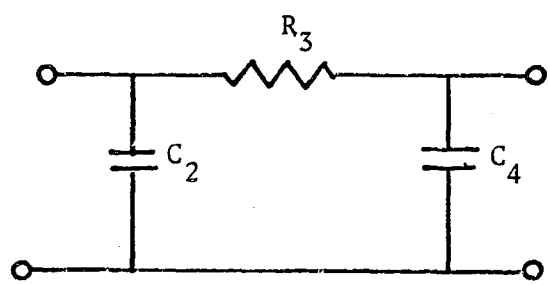

(b)

Figure 7.11: RC-active filter employing a fixed-gain amplifier
(a) General structure
(b) Sub-network N_a for a low-pass realization

applied to the synthesis of RC-active filters:

(1) It can accommodate a finite source resistance in R_1.

(2) It is highly flexible in that the form of the network N_a determines the type of filtering characteristic realized. Thus, to realize a low-pass filtering characteristic, we use a low-pass RC π-section as shown in Figure 7.11(b).

(3) It requires a minimum number of elements to realize a prescribed filtering characteristic.

(4) To realize high-order filters, we may cascade sections without the need for isolation amplifiers.

All of the network components in Figure 7.11 are, in effect, included in the feedback loop. Thus, the sensitivity of the natural frequencies of the network to component parameter variations may be effectively spread over all components, thereby avoiding the need for precise control over any particular parameter. For this reason, together with the fact that the capacitors of network N_a are grounded, it would seem that the structure is well suited for integration.

7.6 Sensitivity Analysis and Optimal Synthesis of the Network:

7.6.1 Analysis of the network

Analysis of the network of Figure 7.11(a) in terms of the z-parameters of the sub-network N_a, yields the following expression for the transfer function:

$$T(s) = \frac{V_2}{I_1} = \frac{-\mu z_{21} R_1 R_f}{R_1 R_f + z_{11}(R_1 + R_f) + \mu z_{21} R_1} \qquad (7.1)$$

If a low-pass filtering characteristic is required, we may use the structure shown in Figure 7.11(b) for N_a obtaining

$$T(s) = \frac{K}{s^2 + 2\zeta\,\omega_n s + \omega_n^2} \tag{7.2}$$

where

$$\omega_n^2 = \frac{R_f + R_1(1 + \mu)}{C_2 C_4 R_1 R_3 R_f} \tag{7.3}$$

$$2\zeta\omega_n = \frac{1}{C_2 R_3} + \frac{1}{C_2 R_1} + \frac{1}{C_4 R_3} + \frac{1}{C_2 R_f} \tag{7.4}$$

and

$$K = \frac{-\mu}{C_2 C_4 R_3} \tag{7.5}$$

7.6.2 Synthesis of the network

The problem now remains to find an acceptable set of parameters (R_1, R_3, C_2, C_4, R_f and μ) such that the constraints imposed by Equations 7.3 and 7.4 are satisfied. To obtain such a set, we can either adopt an approach in which the sensitivity of the network is defined in terms of a single-parameter sensitivity function, e.g., the pole sensitivity with respect to the active parameter μ, or alternatively, we can use some form of optimal search routine to find an optimum set of element values such that the multiparameter sensitivity index of performance, P_1, of the network is minimized.

We will consider both of these techniques in turn. In the first instance, we will obtain a set of element values which are defined in terms of ζ, whereupon we may make a direct multiparameter sensitivity comparison with the five other RC-active filters previously discussed. Following that, we will use optimal search techniques in conjunction with the multiparameter sensitivity index of performance to find an optimum set of element values. We will perform the search routine for a range of different values of ζ, starting the search, in each case, from that point in parameter space which is obtained by the classical procedure. In this way, we shall be able to obtain a quantitative measure of the extent to which the optimal search routine can improve the performance of the filter for various values of ζ.

(a) <u>The approach based on pole-sensitivity considerations</u>: Following the procedure outlined in Appendix A we obtain the following expressions for the various element values which define the dependence of these nominal values on the relative damping factor, ζ.

$$R_1 = 1.667 \qquad C_2 = \frac{2.55}{\zeta\omega_n}$$

$$R_3 = 1.000 \qquad C_4 = \frac{5.10}{\zeta\omega_n}$$

$$R_f = 0.333$$

$$\mu = \frac{4.335}{\zeta^2} - 1.20 \tag{7.5}$$

Using these element values, with the natural frequency of oscillation normalized to unity, the multiparameter sensitivity index, P_1, was computed for a range of different values of ζ. The results, which are

shown plotted in Figure 7.12, indicate, as expected, that the sensitivity performance of the network deteriorates as ζ decreases.

(b) The optimal synthesis procedure: As an alternative to the previous procedure, an optimal synthesis procedure was programmed on the CDC 6400 computer. The procedure uses the steepest-descent method of optimal search to find a set of element values which tends to minimize the index of performance, P_1, while at the same time satisfies the constraint Equations 7.3 and 7.4.

In applying steepest-descent, the index of performance, P_1, is interpreted as a surface in parameter space. The maximum change in P_1 occurs in the direction of the gradient vector, ∇P_1, where

$$\nabla P_1 = \begin{bmatrix} \frac{\partial P_1}{\partial x_1} \\ \frac{\partial P_1}{\partial x_2} \\ \vdots \\ \frac{\partial P_1}{\partial x_n} \end{bmatrix} \tag{7.6}$$

At each iteration of a simple steepest-descent routine, the gradient vector ∇P_1, is computed, and on this basis a corrective change in the

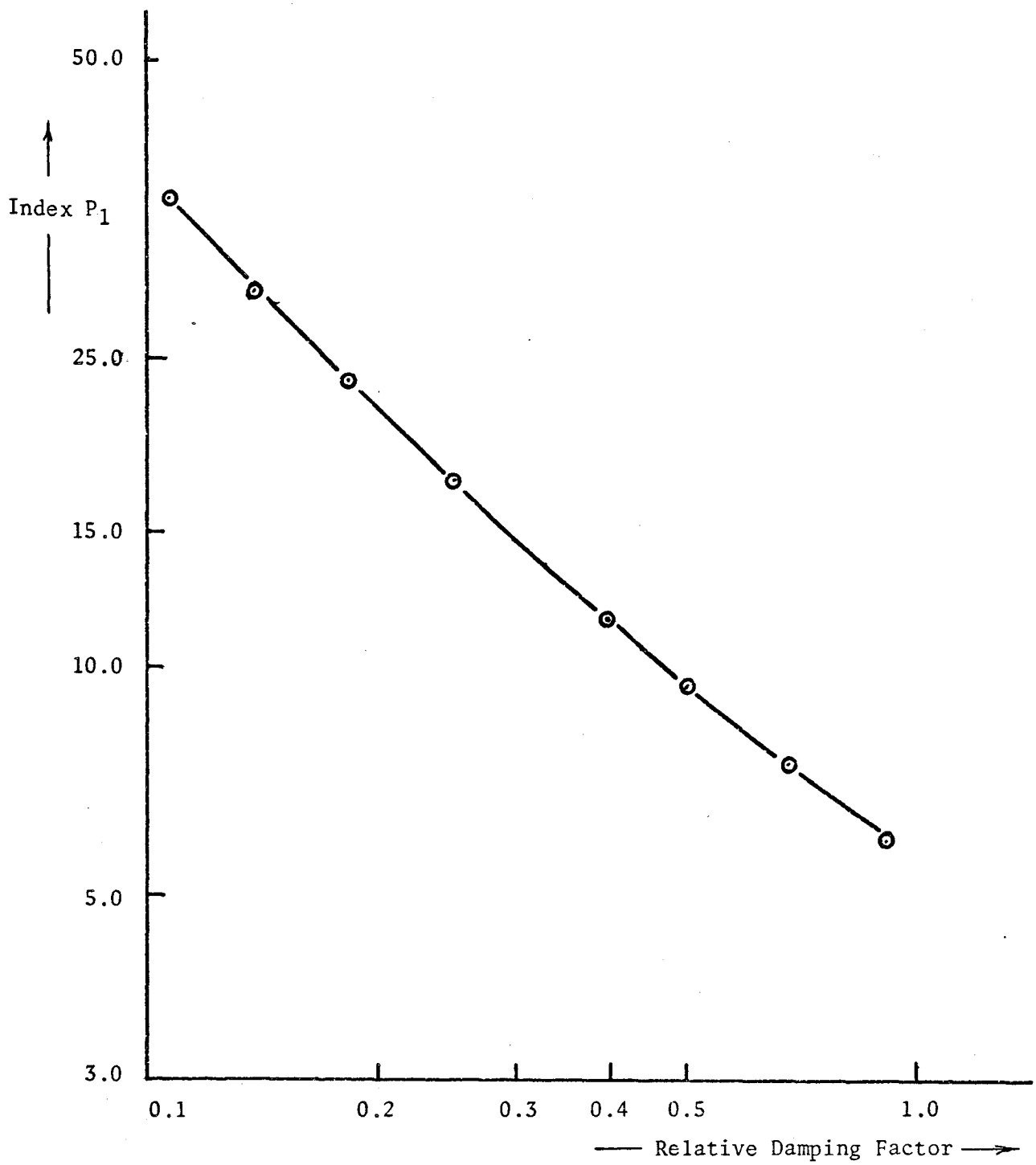

Figure 7.12: Variation of index P_1 with ζ for the network of Figure 7.11

parameter vector $\mathbf{x}$ is made according to the following:

$$\mathbf{x}^{j+1} = \mathbf{x}^{j} - k^{j}\nabla P_1 \tag{7.7}$$

where $\mathbf{x}^j$ is the vector parameter at the jth iteration, and k^j is a gain parameter. The k^j is assumed positive, with a magnitude that is controlled at each iteration to ensure reasonable convergence towards the optimum value of P_1. The computer iterates this procedure until a stopping condition is satisfied.

The problem that we are specifically faced with is one of non-linear programming. That is, we have a non-linear index of performance, $P_1(s,\mathbf{x})$, which we wish to minimize subject to the non-linear equality constraints of Equations 7.3 and 7.4 and to other inequality constraints imposed by the requirement that the element values must fall within some acceptable bounds. In the programs which were written in support of this thesis, bounds were also placed on the value which the ratio, r_x, of any two like elements, could assume, i.e.,

$$\frac{1}{\alpha_r} \leq r_x \leq \alpha_r \tag{7.7}$$

where the parameter α_r is chosen appropriately by the user.

Each constraint defines one or more regions in parameter spaces which are not allowed as solutions. Multiple constraints simply increase the disallowed volume. This principle is illustrated in Figure 7.13 for the two parameter case, with examples of the three types of constraints mentions above.

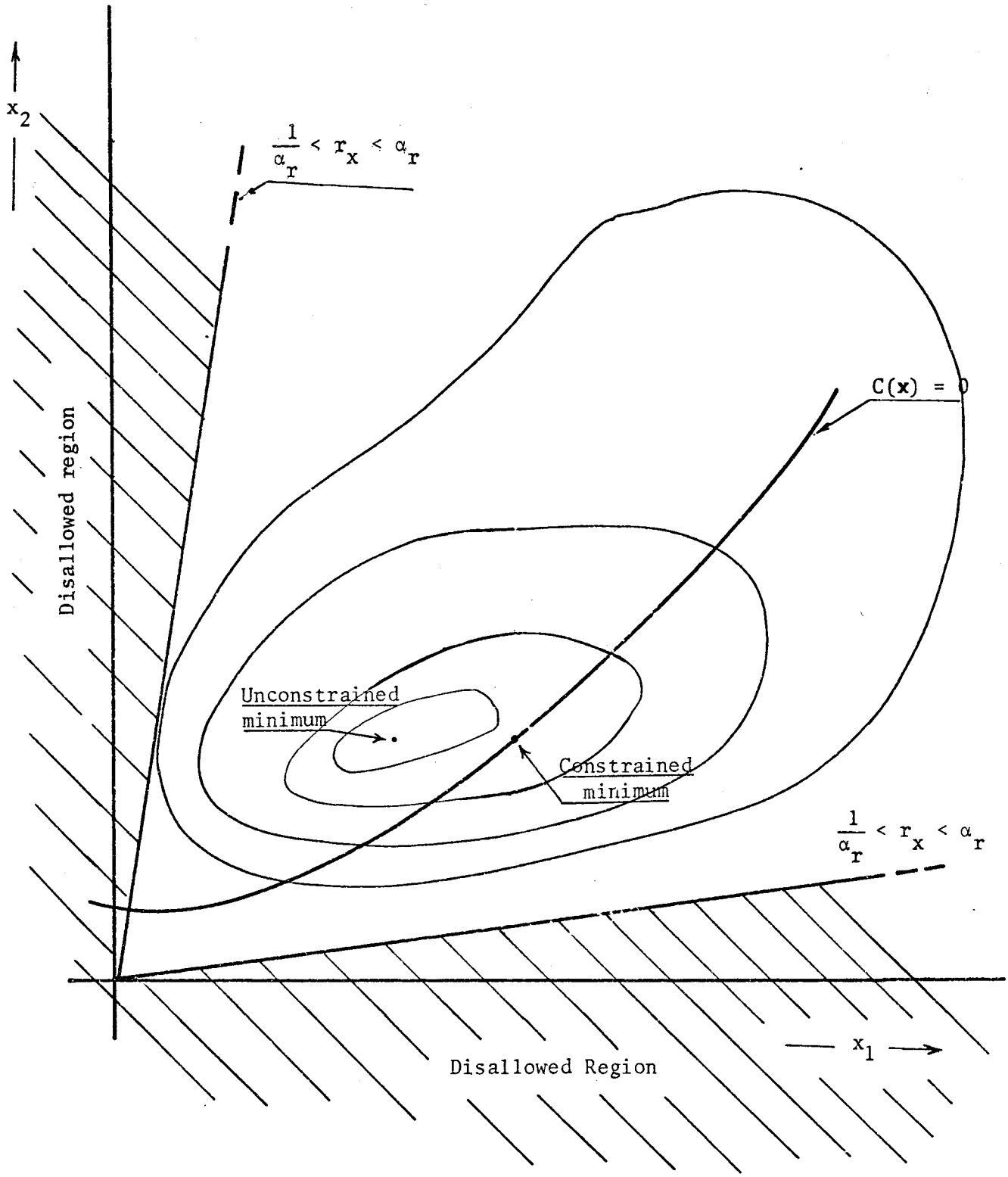

Figure 7.13: Constrained search, two-parameter problem

For the general n-parameter case, an equality constraint of the form $C(\mathbf{x}) = 0$ must be satisfied. One method of solution is to choose an arbitrary starting point in parameter space and adjust this parameter setting in steps (using steepest-descent perhaps) until the constraint is satisfied. The search then procedes along, or close to, the $C(\mathbf{x}) = 0$ contour on the P_1 surface in parameter space until the constrained minimum value of P_1 is reached. This procedure is readily formulated using ∇C (the gradient of C), and ∇P_{1C} (the constrained gradient of P_1), which is defined as that direction in parameter space along which P_1 may be improved without affecting C. The procedure may readily be extended to the case of multiple equality constraints. A more detailed description of the procedure is given elsewhere[47,48,49].

Equality constraints may also be handled by the so-called elimination method, in which one or more of the constraint equations are used to solve for one or more network parameters in terms of the remaining ones. These relationships are then substituted into the objective function. Thus, the number of independent variables, and consequently, the complexity of the problem is reduced. It should be noted that the method is not always applicable, as it requires the initial solution of the constraint equations in closed form.

In the case of the network of Figure 7.11, the elimination method has been used to advantage. The network has a total of six variable parameters, including μ. However, only two equality constraints, imposed by the prescribed pole-pair coordinates in the complex frequency plane, and defined by Equations 7.3 and 7.4 must be satisfied. We therefore have

four degrees of freedom which may be used to reduce the multiparameter sensitivity of the network. The first step in the procedure was to solve Equations 7.3 and 7.4 for the control parameter, μ, and for the feedback resistor, R_f:

$$\mu = \frac{C_4R_3(\omega_n^2 C_2C_4R_1R_3 - 1)}{2\zeta\omega_n C_2C_4R_1R_3 - C_4R_1 - C_4R_3 - C_2R_1} - 1 \tag{7.8}$$

and

$$\frac{1}{R_f} = 2\zeta\omega_n C_2 - \frac{1}{R_3} - \frac{1}{R_1} - \frac{C_2}{C_4R_3} \tag{7.9}$$

These values for μ and R_f were then substituted into the expression for the index P_1. In this way, the problem was transformed into an optimal search of four-dimensional space for that set of C_2, C_4, R_1 and R_3 which (with the corresponding values of μ and R_f as defined by Equations 7.8 and 7.9) minimizes P_1 while realizing the prescribed pole-pair coordinates exactly. A description of the optimal search routine now follows.

7.7 The Optimal Search Routine:

The unconstrained search of the four dimensional space bounded by the acceptable values of the parameters $\mathbf{x}' \triangleq [C_2, C_4, R_1, R_3]^t$ is best described with the aid of a flow-chart (see Figure 7.14)

The computer is programmed with a mathematical model (network characterization block) and instructions for computing the index P_1 and its gradient ∇P_1. An initial parameter setting is read in, and the value of μ and R_f which realize the prescribed pole-pair coordinates in the complex frequency plain are then computed. A corrective adjustment in $\mathbf{x}'$ is then made. The magnitude of this adjustment is controlled by the gain constant

k^j, i.e.,

$$\delta x' = -k^j \nabla P_1 \tag{7.10}$$

The new value of the index P_1 is now computed and the actual change in P_1 is determined, and is compared with its predicted change. The magnitude of the gain constant, k^j, is controlled by the convergence characteristics of the search routine. The steepest-descent procedure extrapolates from the measured P_1-surface slope components, thus approximating the P_1-surface as a plane. The actual P_1-surface, in most cases, is more accurately represented by a quadratic form, so that the planar approximation becomes progressively poorer with increasing distance from the test point. Thus, if k^j is made too large, the actual value of P_1 may be far from the predicted value at the new set point, and the procedure may fail to converge to the optimum solution. We therefore control the magnitude of k^j at each adjustment step to prevent divergence. If the predicted and actual change in P_1 differ appreciably, the magnitude of k^j is decreased appropriately. By the same token, if the predicted and actual change are very close to each other (suggesting that the step size is too small) the value of k^j may be increased to speed up convergence.

The procedure is repeated until a stopping criterion is satisfied. The stopping criterion is usually expressed as $\| \nabla P \| < \varepsilon_p$, where ε_p is a positive constant chosen to terminate the computer run near the optimum value of P_1. In our case, we have an additional stopping criterion, as defined by Equation 7.7, which causes the search to be terminated when any parameter assumes an unacceptable value.

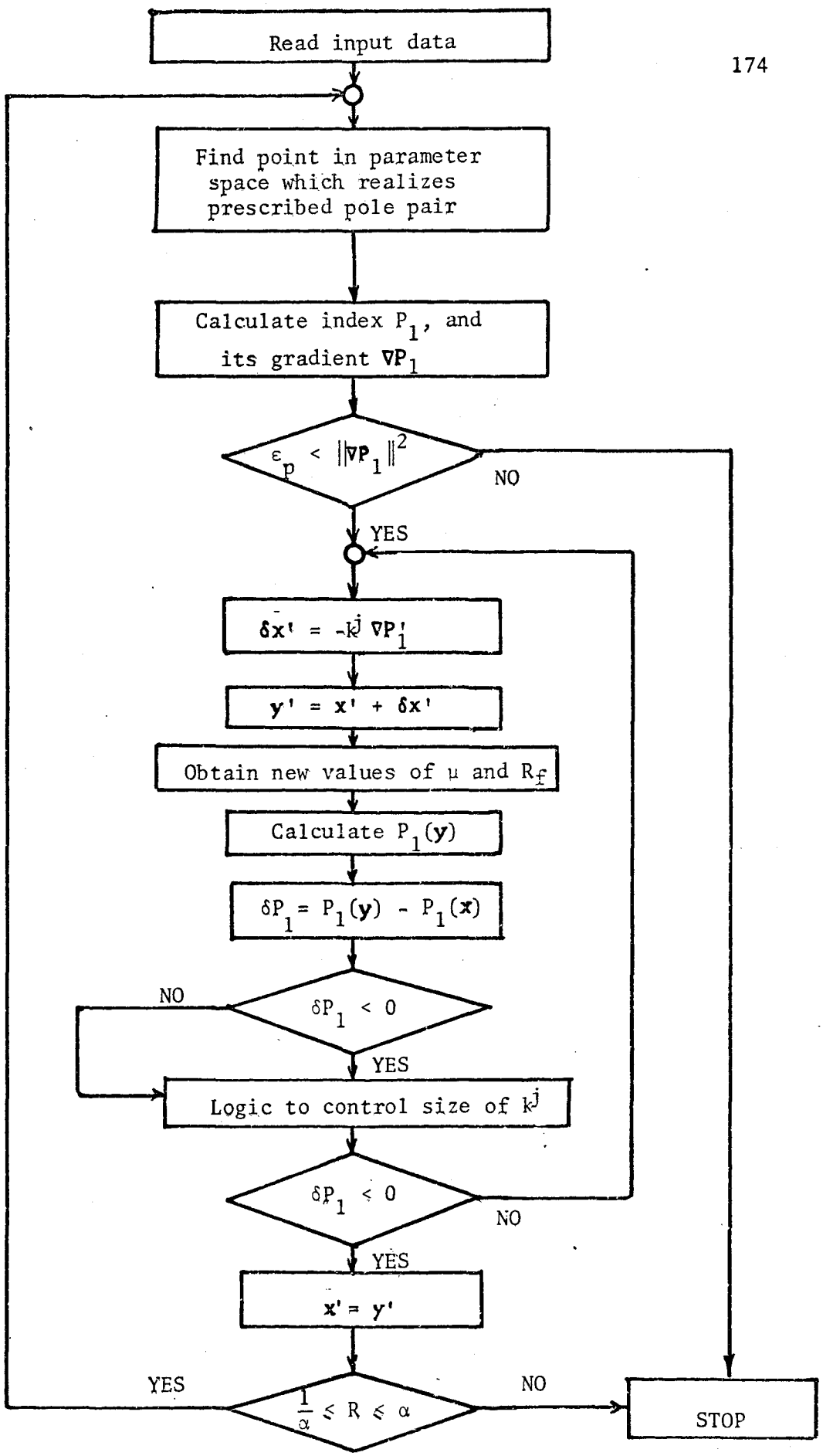

Figure 7.14: Flow chart representation of the optimal search routine

7.8 Sensitivity Performance of Optimized Networks:

The index of performance, P_1, was used in conjunction with a steepest-descent optimal search routine to synthesize a number of RC-active filters using the configuration of Figure 7.11.

7.8.1 Optimization of second-order Butterworth Section

In the synthesis of an optimum second-order low-pass Butterworth section, the magnitude of the index P_1 was reduced by approximately 30% during the first ten iterations of the search routine as is illustrated in Figure 7.15. The sensitivity performance of the original non-optimized version and the resulting optimized version was compared, and typical response curves are shown in Figure 7.16. The following procedure was used to obtain these and other similar curves which follow in Figures 7.18 through 7.20. A random sequence of uniformly distributed numbers was used to generate sets of element values between specified tolerance limits for both versions of the filter. The frequency response of the resulting networks was then evaluated and the error in the response of the optimized version at the cut-off frequency was noted. This procedure was repeated 25 times using different random number sequences. The curves of Figure 7.16 correspond to that set of randomly generated element values (between specified tolerance limits) which resulted in the largest such error. The nominal values of the elements used in both cases and the resulting values of the index P_1 which correspond to the curves of Figure 7.16 are tabulated in Table 7.2.

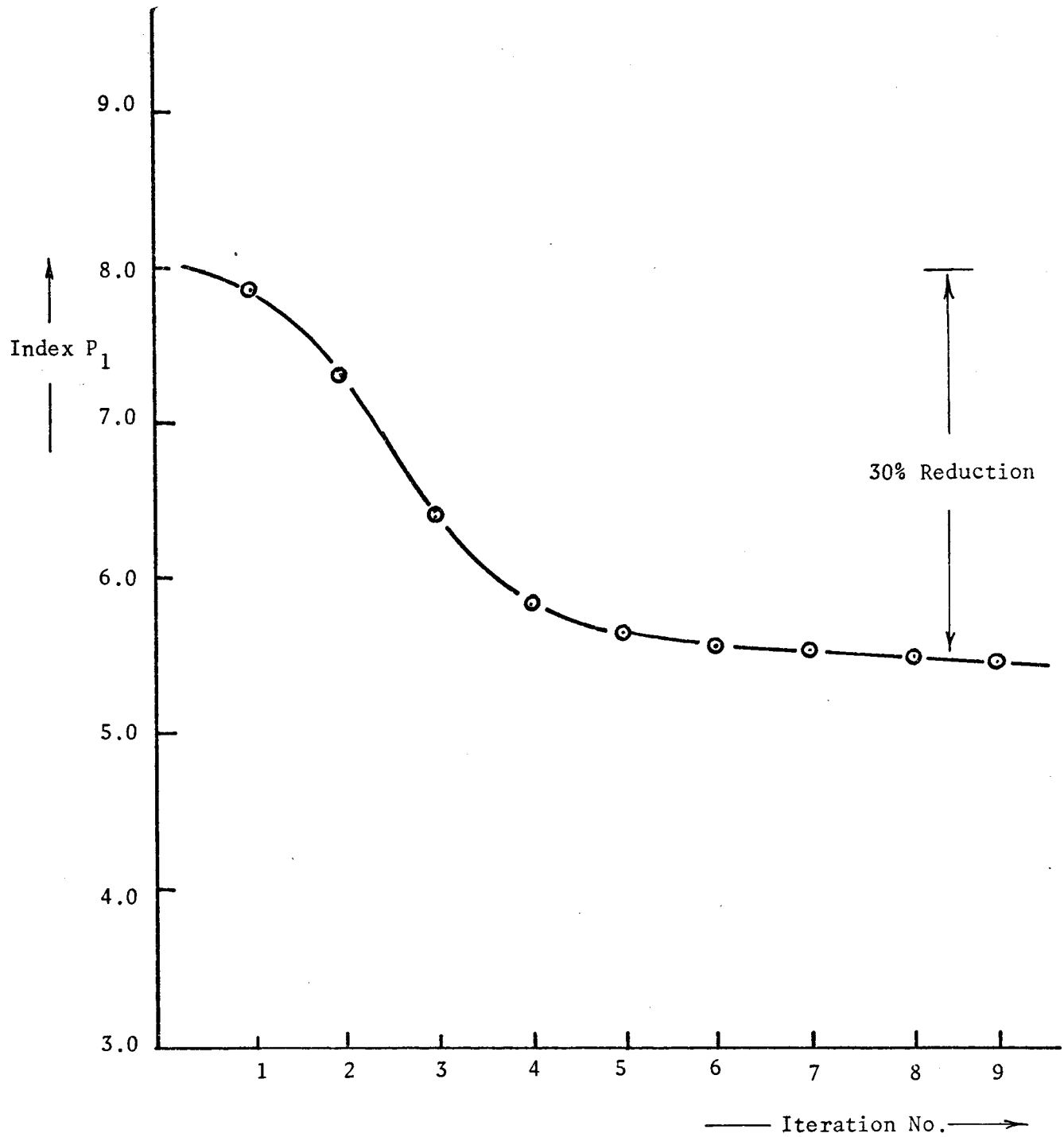

Figure 7.15: Effect of optimization; second-order Butterworth RC-active filter

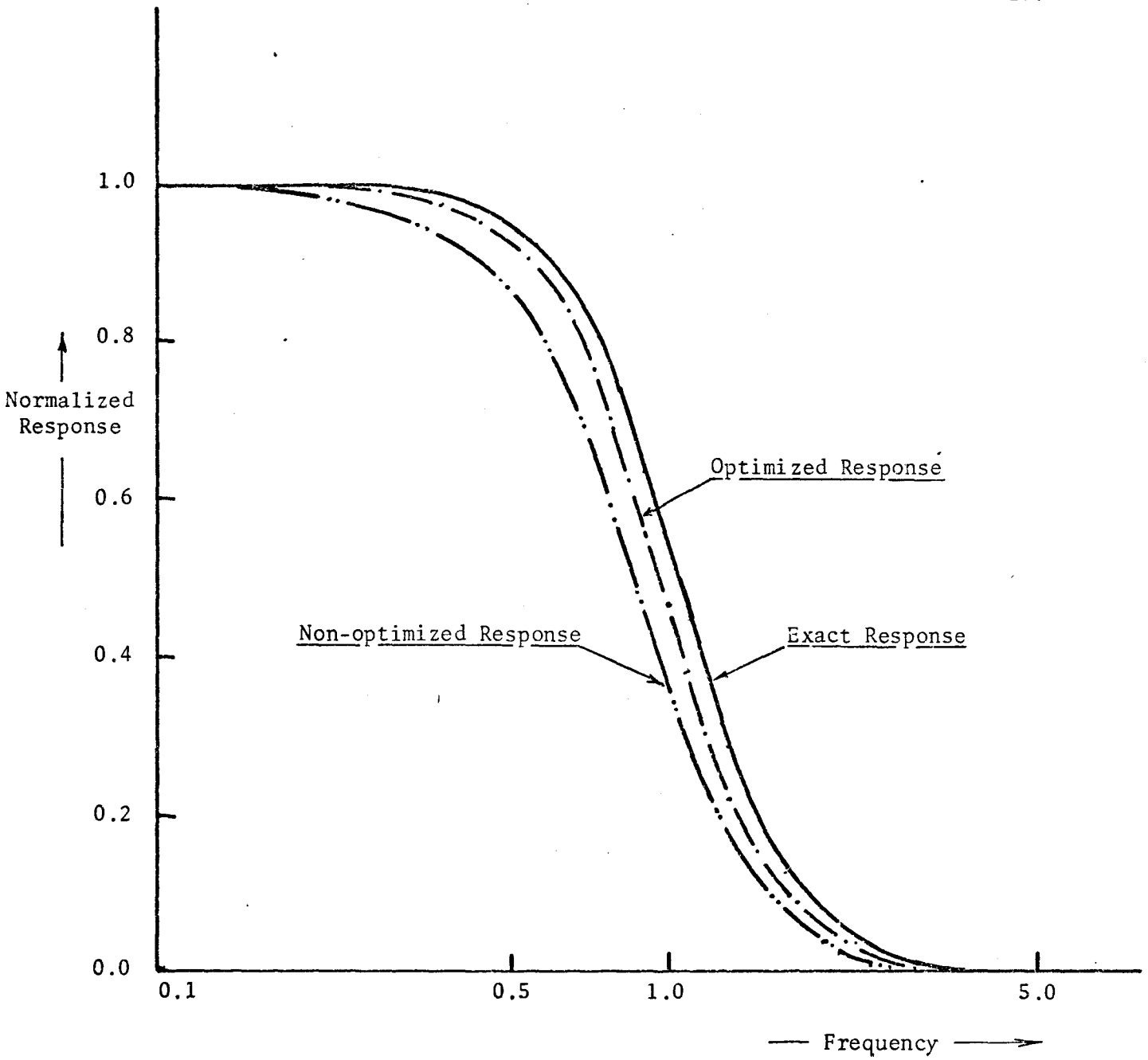

Figure 7.16: Sensitivity performance of optimized and non-optimized versions of RC-active filter with second-order Butterworth response

Network element	Non-optimized structure	Optimized structure
R_1	1.0000	11.6845
C_2	10.0000	10.0045
R_3	10.0000	9.6951
C_4	2.0000	0.1038
R_f	0.0797	0.2488
μ	1.4869	1.4845
Index P_1	7.8220	5.4510

Table 7.2: Element nominal values and corresponding value of the index P_1 for the optimized and non-optimized networks used to obtain the responses shown in Figure 7.16

7.8.2 Statistical analysis of errors of optimized and non-optimized versions of the filter

As a further indication of the improvement in performance of the optimized version of the filter, the errors which occurred in the network response (when the network elements were perturbed) were analyzed for both the optimized and the non-optimized versions of the network described in Table 7.2. These errors were computed for a number of frequency points of interest, and their standard deviation was determined. The results obtained are shown plotted in Figure 7.17. It is noted that in the case of the optimized version of the filter, the standard deviation is considerably less than that of the non-optimized version in the frequency band of interest. Furthermore, these results confirm our earlier conclusion, viz., that the network response is particularly sensitive in the vicinity of the cut-off frequency.

The Chi-squared goodness-of-fit test was also applied to the error data to determine the extent to which the distribution of these errors approximated to a normal or Gaussian distribution. The results of this test are tabulated in Table 7.3, where the value of Chi-squared obtained, and the corresponding probability that the data was generated by a normal process are tabled as a function of frequency. On the basis of these results, which tend to be negative, we may conclude that the errors have probably been generated by a process which is not exactly normal, a conclusion which is implied in Equation 4.3. As each of the δx_i have been given a rectangular distribution, it follows that $\frac{\Delta T}{T}$ will have a distribution which tends towards a normal distribution as the number of parameters, x_i,

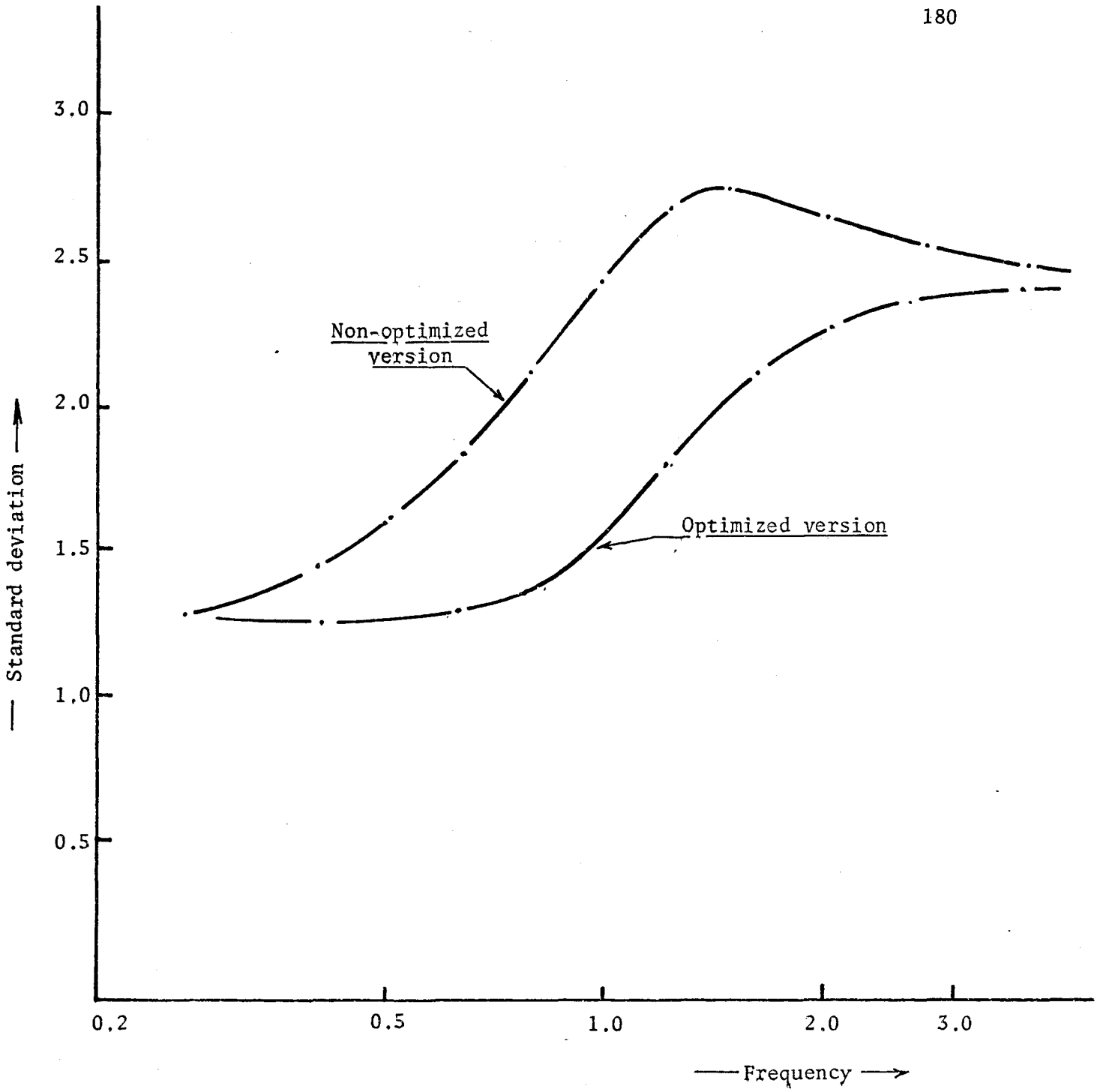

Figure 7.17: Standard deviation of errors in network response

tends to become large. In this particular example, there are but six parameters; we would not, therefore, expect the distribution of $\frac{\Delta T}{T}$ to be particularly close to normal.

The index P_2 was also computed, and the standard deviation of the various p_j was determined, for both versions of the network. The results are tabulated in Table 7.4. The Chi-squared test was again applied to the p_j data (50 samples) and the results were again negative.

7.8.3 Other optimized networks

(a) The synthesis of filters realizing several different values of relative damping factor, ζ, was undertaken. The sensitivity performance of the resulting optimized networks was again compared with that of the non-optimized versions. The results are shown plotted in Figures 7.18, 7.19 and 7.20 for the case of $\zeta = 0.9$, $\zeta = 0.6$ and $\zeta = 0.3$, respectively. The nominal element values for both versions of each filter are tabulated in Table 7.5.

(b) For the case of a Chebyshev filter with 1 dB passband ripple, the sensitivity performance of an optimized network was compared with that of the network synthesized in Appendix "A". The set of element values obtained in Appendix "A" was used as the starting point in parameter space for the optimization procedure. The results of this sensitivity comparison are shown plotted in Figure 7.21, and the nominal element values for both versions of the filter are listed in Table 7.6.

(c) Finally, the nominal element values which are defined in terms of ζ by Equation 7.5 were chosen as starting points in parameter space and optimal search was applied for a number of different values of ζ. The

Non-optimized Version			Optimized Version	
Frequency	Value obtained for Chi-squared	Prob (Norm)	Value obtained for Chi-squared	Prob (Norm)
0.2	9.2	42%	10.0	27%
0.4	6.4	60%	10.0	27%
0.6	10.8	22%	12.0	16%
0.8	9.2	34%	9.6	28%
1.0	16.8	4%	9.2	33%
1.2	10.8	22%	9.2	33%
1.4	12.0	14%	9.6	28%
1.6	12.0	14%	12.0	16%
1.8	10.0	27%	9.2	33%
2.0	6.4	60%	8.0	43%
2.2	6.4	60%	6.0	65%
2.4	5.6	69%	7.6	48%
2.6	5.6	69%	6.0	65%
2.8	5.6	69%	5.2	73%
3.0	6.4	60%	4.8	77%

Table 7.3: Chi-squared goodness-of-fit test

Non-optimized Version		Optimized Version	
Index P_2	$\sigma(p_j)$	Index P_2	$\sigma(p_j)$
0.847	0.747	0.305	0.287

Table 7.4: Index P_2 and standard deviation of p_j

resulting reduction in the value of the index P_1 is shown in Figure 7.22, where it is plotted as a function of ζ. It is noted that the reduction becomes more significant as the value of ζ is increased.

7.9 A "Two-level" Optimization Procedure:

In the synthesis of an RC-active filter, such as that shown in Figure 7.11, optimal search techniques can be used to find the optimum nominal element value set. In addition, the optimum tolerance set for this optimum nominal set can then be obtained, and can be used to further improve the performance of the network.

The effect of such a two-level optimization procedure is illustrated in Figures 7.23 and 7.24 where we compare typical response curves for optimized and non-optimized versions of the network. The corresponding nominal values and tolerances of the elements are listed in Table 7.7. It is noted from these results that the combined effect of the optimal nominal set and the optimum tolerance set results in a truly significant improvement in the performance of the network.

7.10 Design of a Highly Selective RC-active Filter:

We will conclude this chapter with an outline of a procedure for the optimum design of a highly selective RC-active filter. The procedure incorporates many of the concepts and ideas which have already been considered in this thesis, e.g., the index of performance, P_1, the elemental optimum tolerance set, δX_o, the pole-zero optimum tolerance set, δX_{pz}, and the two-level optimization procedure.

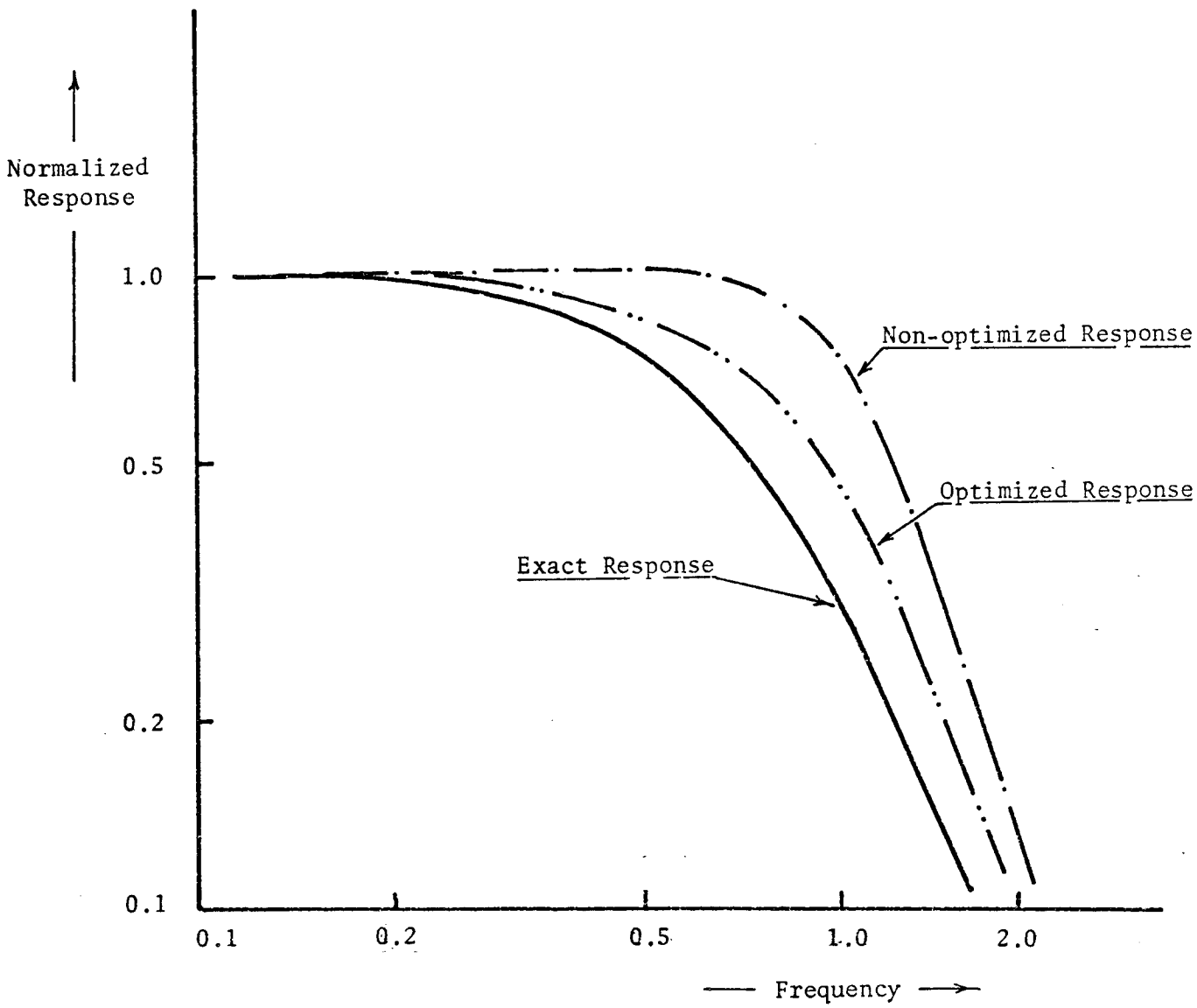

Figure 7.18; Sensitivity performance of RC-active filter with $\zeta = 0.9$ (20% tolerance on all parameters)

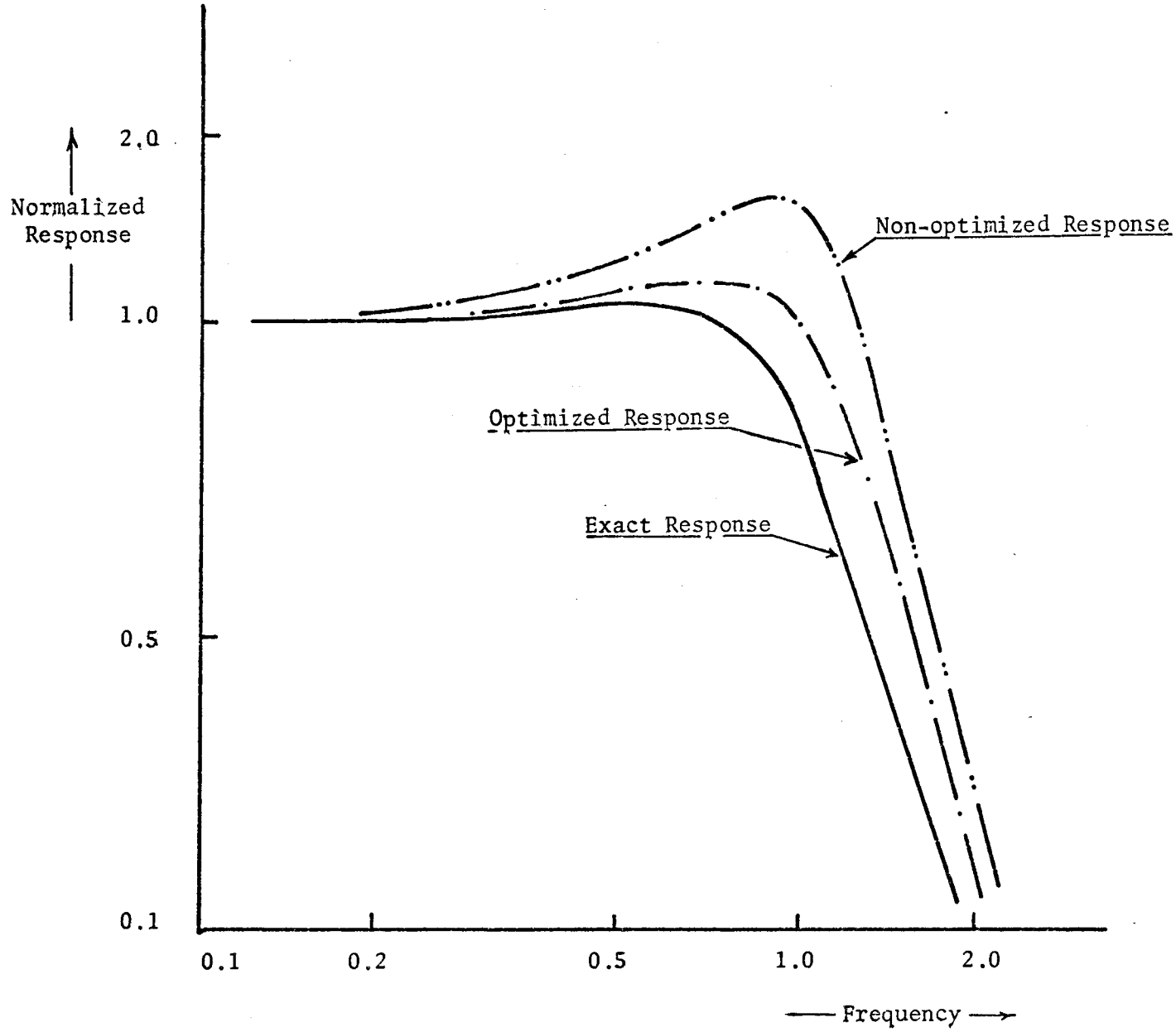

Figure 7.19: Sensitivity performance of optimized RC-active filter with $\zeta = 0.6$ (20% tolerance on all parameters)

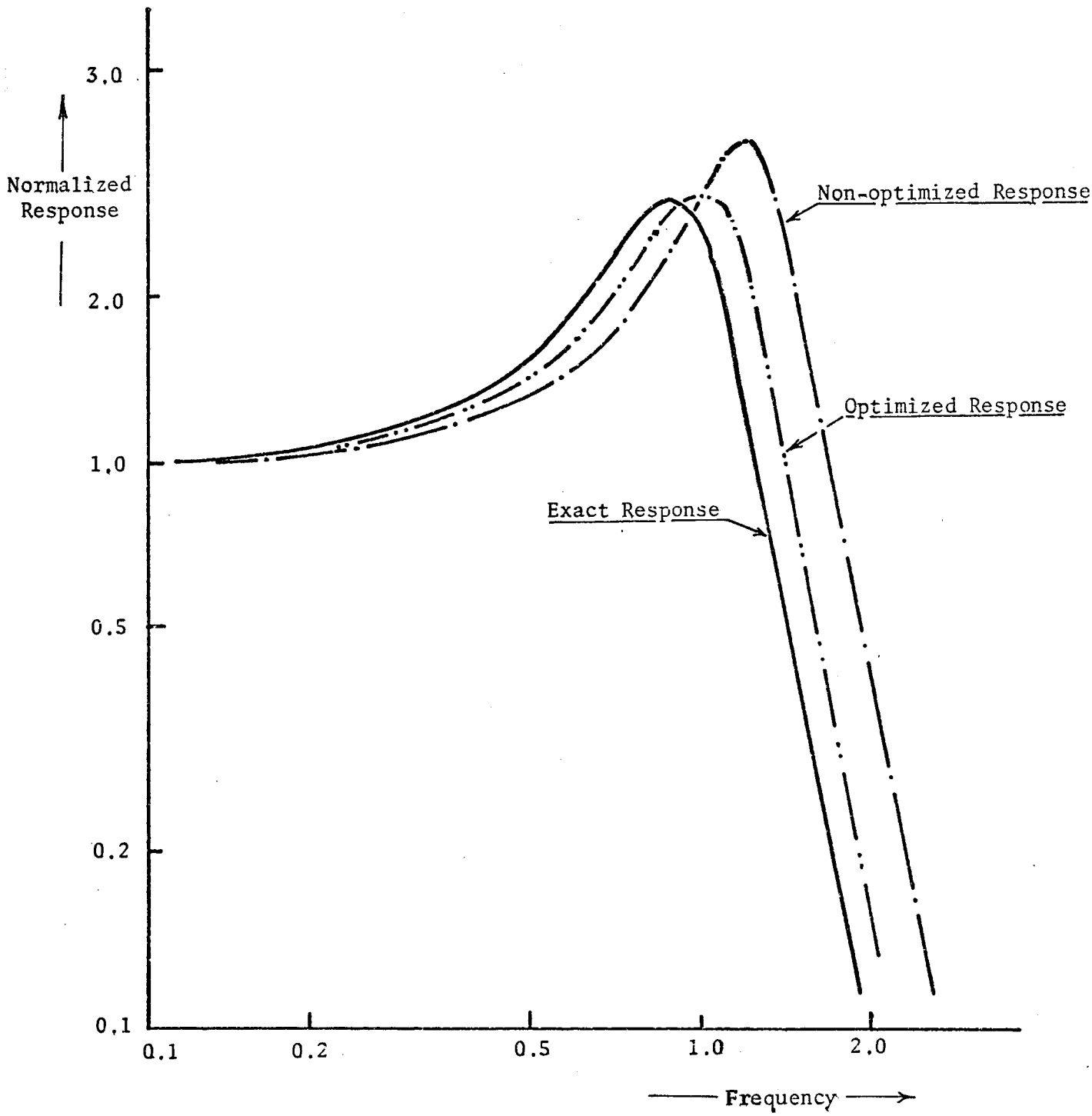

Figure 7.20: Sensitivity performance of RC-active filter with $\zeta = 0.3$ (20% tolerance on all parameters)

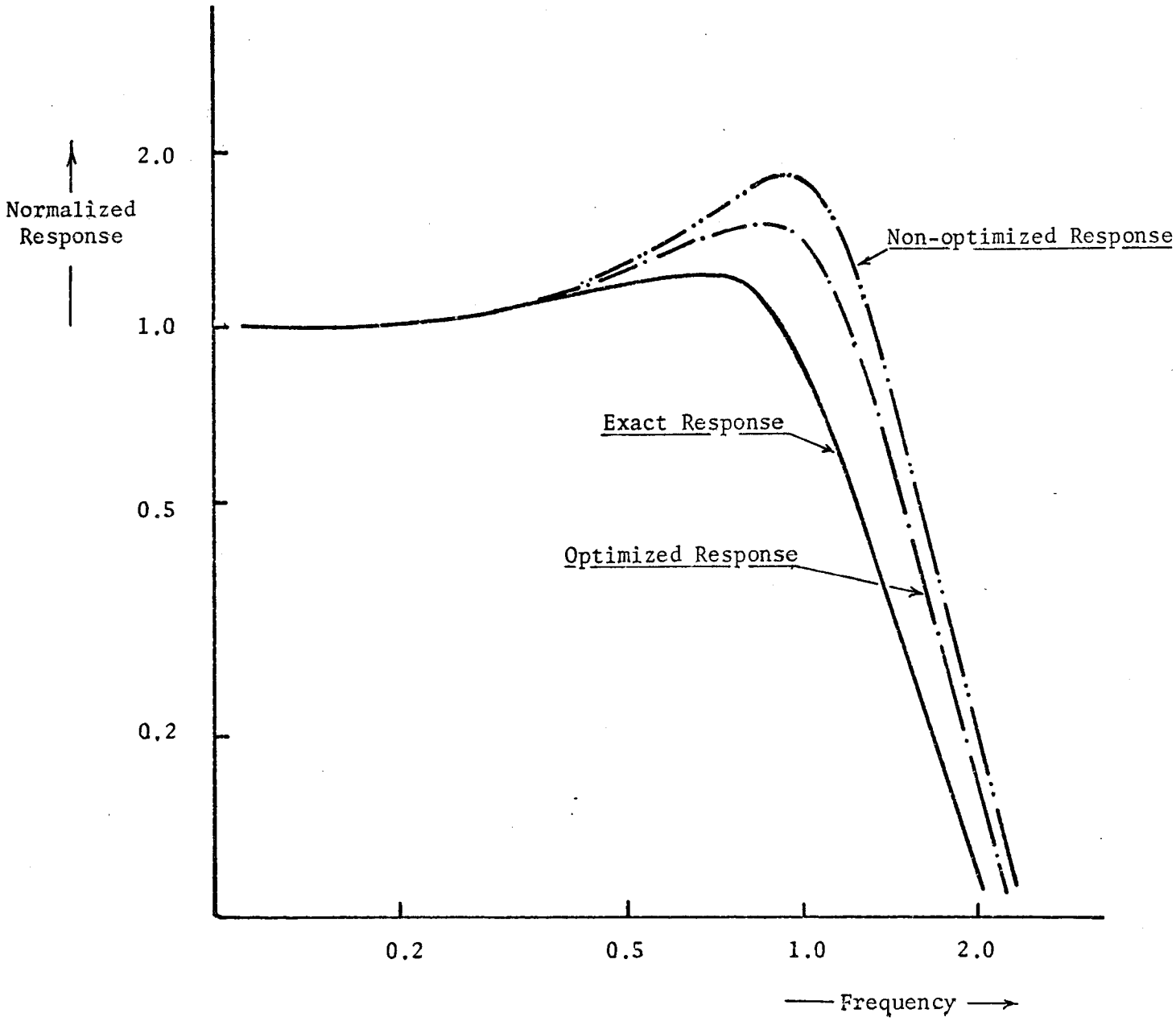

Figure 7.21: Results obtained when optimization routine was applied to network synthesized in Appendix "A"

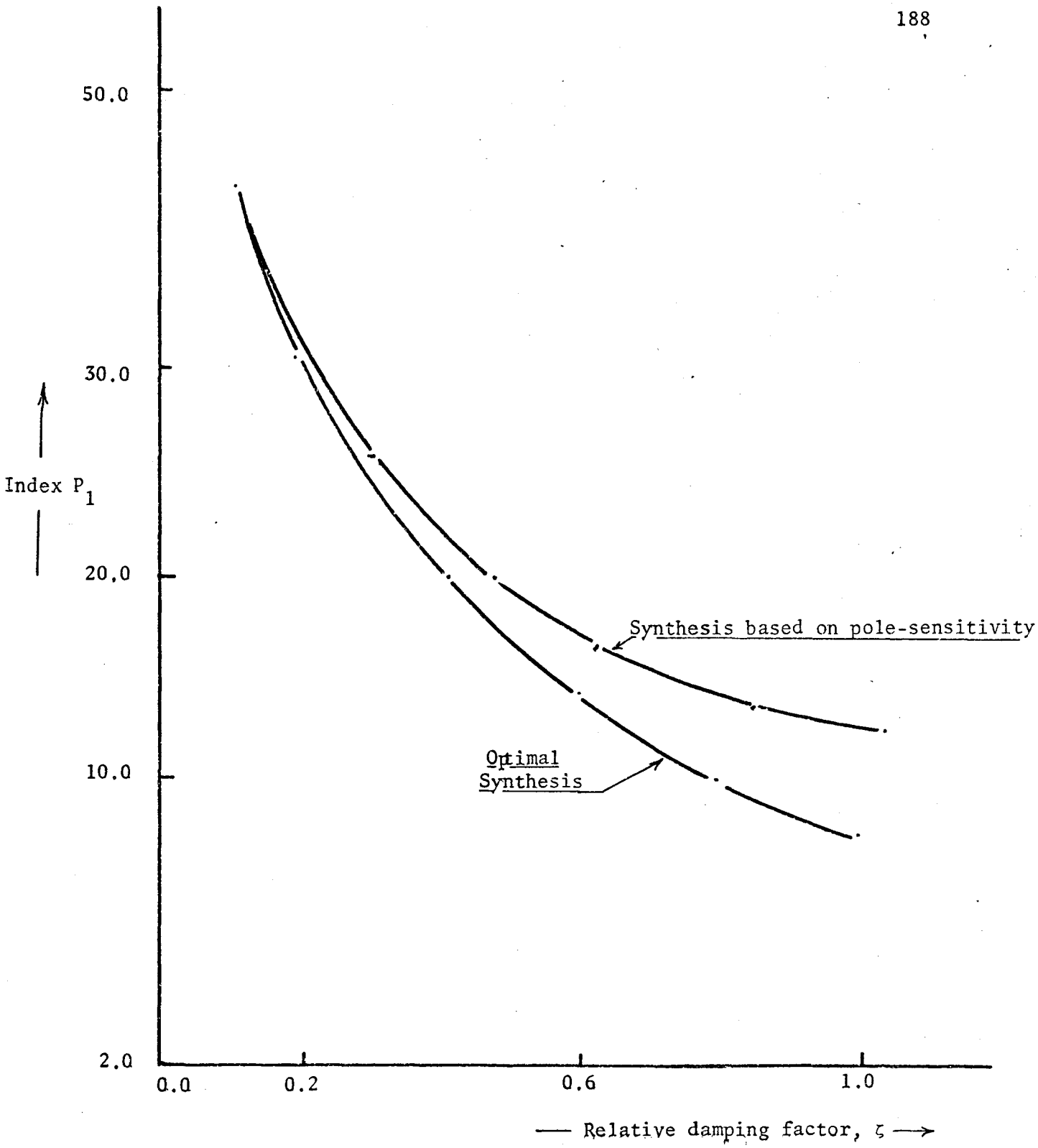

Figure 7.22: Improvement obtained by using optimal synthesis technique for different values of relative damping factor ζ

ζ	Network element	Non-optimized structure	Optimized structure
0.9 (Fig. 7.18)	R_1	2.641×10^{-2}	5.019
	C_2	2.108×10	8.442×10^{-1}
	R_3	3.808×10	9.523×10^{-1}
	C_4	3.129×10	3.289
	R_f	3.201×10	1.397×10^{3}
	μ	8.027×10^{5}	3.415×10^{3}
0.6 (Fig. 7.19)	R_1	5.134×10^{-2}	5.031
	C_2	1.628×10	1.134
	R_3	2.991×10	1.159
	C_4	2.459×10	3.275
	R_f	4.683×10^{2}	3.883×10^{3}
	μ	5.600×10^{6}	1.594×10^{4}
0.3 (Fig. 7.20)	R_1	2.053×10^{2}	2.287×10
	C_2	1.684	4.412
	R_3	1.680×10^{3}	7.381×10^{2}
	C_4	1.997×10^{-1}	3.731×10^{-3}
	R_f	1.000	1.000
	μ	1.158×10^{5}	2.540×10^{2}

Table 7.5: Nominal element values for the optimized and non-optimized networks used to obtain the results shown in Figures 7.18, 7.19 and 7.20

Network element	Non-optimized structure	Optimized structure
R_1	1.0000	6.588
C_2	1.5090	3.253
R_3	3.0000	0.627
C_4	4.5270	3.419
R_f	4.6275	3.271
μ	100.0000	23.640

Table 7.6: Nominal element values used to obtain the results shown in Figure 7.21

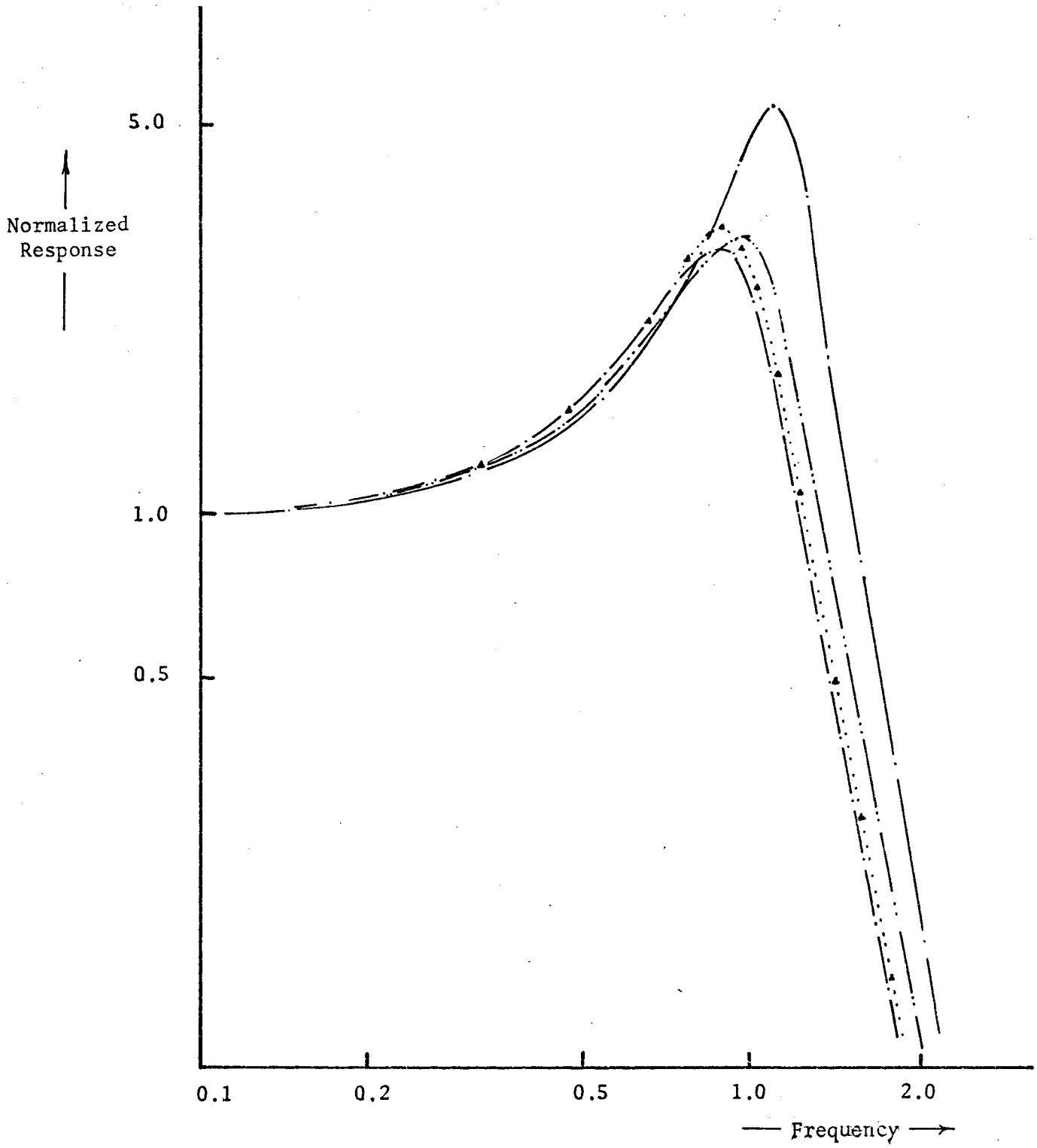

Figure 7.23: Improvement obtained through use of "two-level" optimization procedure:

(a) —·—·—·— Exact response

(b) ——·—— Non-optimized response

(c) ——··—— Optimized nominal element set

(d) ··▲···▲·· Optimized nominal element set with optimum tolerance set

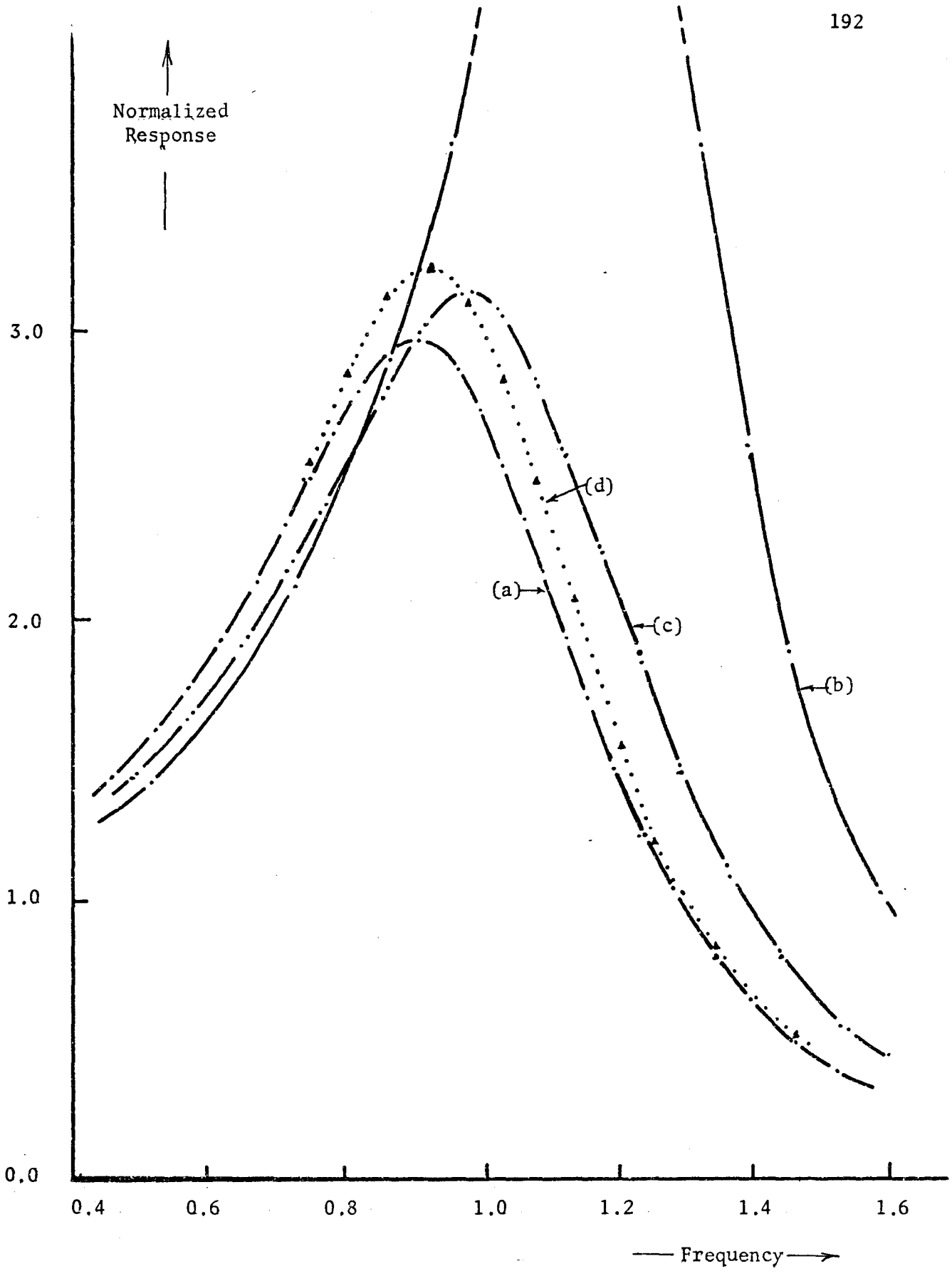

Figure 7.24: Exploded view of Figure 7.23 with linear scales

Element	Non-optimized Nominal values	Optimized Nominal values	Normalized Tolerance Sets	
			Uniform	Optimum
R_1	30.8700	4.961	2.437	9.054
C_2	44.6800	1.402	2.437	1.103
R_3	55.8700	2.193	2.437	1.101
C_4	44.5800	3.662	2.437	1.029
R_5	0.0374	107.900	2.437	1.335
μ	4245.0000	1192.000	2.437	1.000

Table 7.7: Element values and normalized tolerances used to obtain the results shown in Figures 7.23 and 7.24.

The pole-zero optimum tolerance set, δX_{pz}, is particularly useful for the case of active filters which are to be realized as a cascade of second-order sections. This tolerance set, δX_{pz}, defines the optimum tolerable limits on the variations of each pole-pair of the network. These limits may, in turn, be used to obtain the elemental optimum tolerance set, δX_{o_i}, for the ith sub-network element set.

The first step in the design procedure is to obtain δX_{pz}. We must then choose a suitable structure for each of the various sub-sections of the network. The index of performance, P_1, can be computed for each suitable sub-network, and the choice of such sub-network can be based on the resulting sensitivity performance as defined by P_1. In other words, the value of P_1 obtained for a given ζ will determine the structure to be used in the pertinent sub-section.

In the synthesis of such a sub-section, we may either use classical techniques to obtain the nominal element value set, or better, we can use optimal search techniques to obtain an optimum set of nominal values for the elements of the network. The optimum tolerance set, δX_o, for the optimum nominal set thus obtained can then be used to further improve the performance of the network.

Finally, the last step in the design procedure, that of setting tolerance levels of each stage relative to the others, may now be taken. First, we define the ith pole-pair parameters, ζ_i and ω_{n_i}, in terms of the network elements. From the known optimum tolerance set for these elements, δX_{o_i}, we may obtain the standard deviation of ζ_i and ω_{n_i} due to random variations (between specified tolerance limits) of the elements, x_i.

Let these standard deviations be denoted by $\sigma(\zeta_i)$ and $\sigma(\omega_{n_i})$, respectively. The elemental optimum tolerance set is now scaled by a factor that is chosen such that neither $\sigma(\zeta_i)$ nor $\sigma(\omega_{n_i})$ will exceed the optimum tolerance set for ζ_i and ω_{n_i} as obtained earlier. Having completed this step for each section, we now have an optimum tolerance set for all the elements of the network. However, this set must now be assigned an absolute level, which might, for example, be determined by the smallest permissible tolerance in a given practical situation. The procedure is illustrated by means of a numerical example which is given in detail in Appendix "B". In this example, the sensitivity performance of an optimized version of a tenth-order Butterworth low-pass filter, employing an optimum tolerance set, is compared with a non-optimized version of the same filter employing a uniform tolerance set equal to the mean of the tolerance set used in the optimized version. The results of this comparison are illustrated in Figure 7.25, where we observe a considerable improvement in the case of the optimum filter in the region of the cut-off frequency.

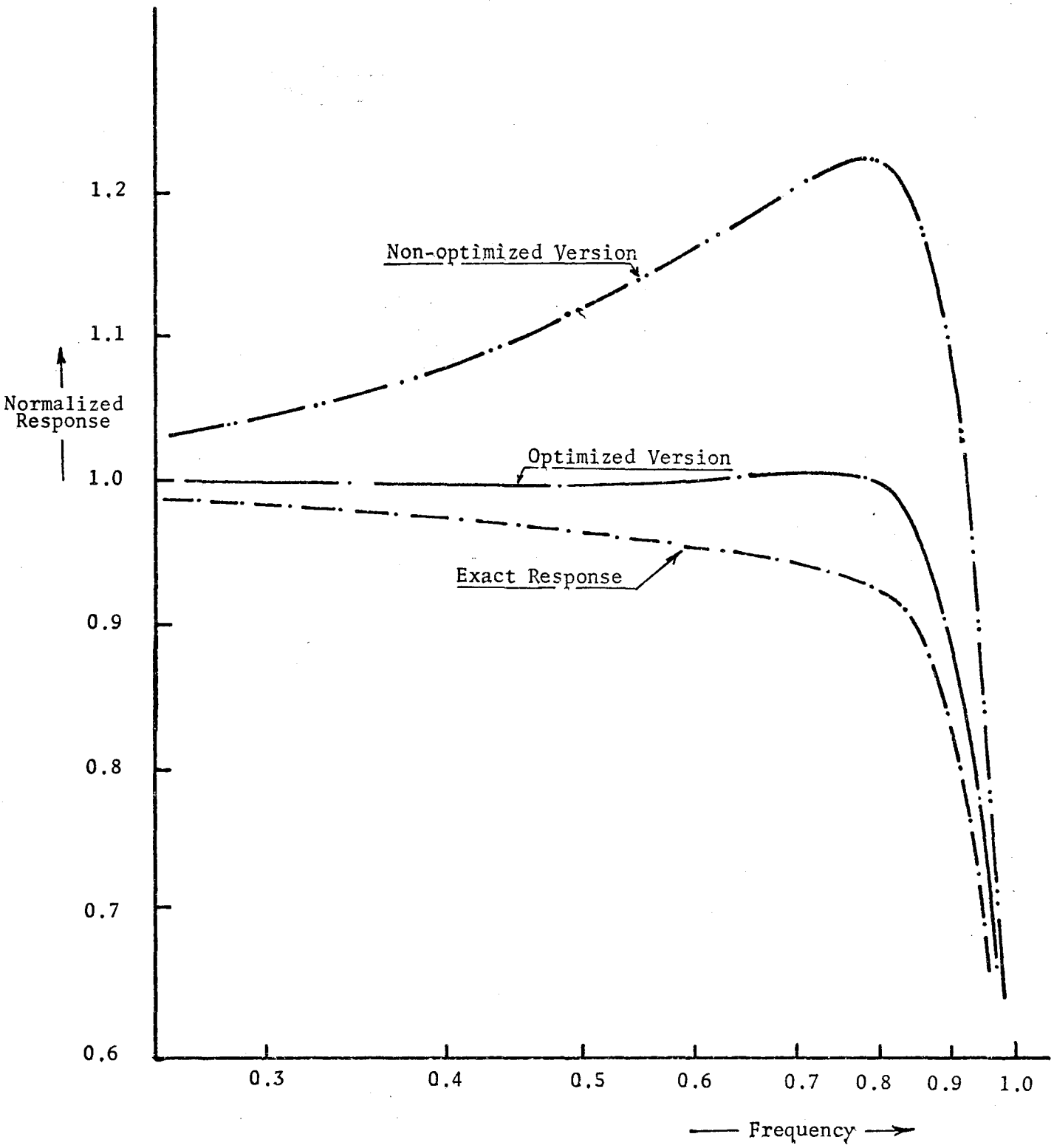

Figure 7.25: Sensitivity performance of tenth-order RC-active filter

CHAPTER VIII

CONCLUSIONS

An investigation of the multiparameter sensitivity of a wide range of linear, time-invariant networks has been undertaken. As a first step in this investigation, the sensitivity of a number of RC-gyrator filters was considered. A procedure for developing gyrator-capacitor equivalent networks for LC-ladder filters was developed. The procedure was used to construct low-pass and bandpass filters with measured responses showing very close agreement with theory. The sensitivity of the response characteristics of these networks, with respect to variations in supply voltages, was measured, and the experimental results obtained indicate that such filters are highly insensitive to such variations.

In the optimum design of a network based on sensitivity considerations, however, we need a sensitivity criterion, or index of performance, which gives a meaningful measure of the multiparameter sensitivity of the network. The indices which have already been proposed in the literature have been critically appraised, and some shortcomings have been pointed out. A new multiparameter sensitivity index of performance has been proposed. The index provides a quantitative measure of the fractional change in the overall response of the network due to simultaneous variations in some or all of the network parameters. The index has been used as the basis of comparing the sensitivity performance of different networks, including LC-ladder and RC-active structures.

The several methods which have been proposed for the computation of sensitivity functions have also been critically reviewed, and a new method, which involves the representation of polynomials in array form, is described. The efficiency of computation of this method has been compared with that of Director and Rohrer's adjoint network procedure, and it is shown that for a class of networks, considerable advantage is to be gained by using the direct approach.

A procedure has been outlined for generating an optimum tolerance set, which, when used to define the tolerance limits of the various elements of a given filter, ensures that the element changes contribute equally to the total change in the filter performance, thereby resulting in a substantial improvement in the overall performance and reliability as compared to the case of uniform tolerances.

The index of performance has been used to evaluate the multi-parameter sensitivity of various second-order RC-active filter sections, thus facilitating the choice of structure to be used for the synthesis of filters involving the cascade of a number of second-order sections. It has also been used, in conjunction with optimal search techniques, to obtain the optimum nominal set of element values for the chosen section. The use of this optimum nominal set may be combined with an optimum tolerance set, resulting in a further improvement in the performance of the filter. In the case of a high-order filter, the optimum tolerance sets for the various sub-sections of the filter are related to each other by the pole-zero optimum tolerance set which defines the optimum migration areas for each complex-conjugate pole-pair of the overall network.

APPENDIX "A"

SENSITIVITY ANALYSIS BASED ON THE POLE-SENSITIVITY FUNCTION

In this Appendix, we first obtain an expression which will define the pole sensitivity of the network with respect to the active parameter, μ, in terms of the network parameters. We next obtain a set of nominal element values for the network, such that a prescribed pole-pair is realized while at the same time the magnitude of the pole-sensitivity is less than some prescribed value. Finally, we obtain the element values as functions of the relative damping factor, ζ.

The first step in the procedure is to obtain an expression for the pole-sensitivity function, $S_{\mu}^{p_i}$. The transfer function of the network is given as

$$T(s) = \frac{\dfrac{-\mu}{C_2C_4R_3}}{s^2 + \left\{\dfrac{1}{C_2R_3} + \dfrac{1}{C_2R_1} + \dfrac{1}{C_4R_3} + \dfrac{1}{C_2R_f}\right\}s + \dfrac{R_f + R_1(1+\mu)}{C_2C_4R_1R_3R_f}} \tag{1}$$

from which

$$2\zeta\omega_n = \frac{1}{C_2R_3} + \frac{1}{C_2R_1} + \frac{1}{C_4R_3} + \frac{1}{C_2R_f} \triangleq \beta_\zeta \tag{2}$$

and

$$\omega_n^2 = \frac{R_f + R_1(1+\mu)}{C_2C_4R_1R_3R_f} \tag{3}$$

Noting that $\zeta\omega_n$ is independent of μ, and that the poles of the network are given by

$$s_i = -\zeta\omega_n \pm j\omega_n \sqrt{1 - \zeta^2} \tag{4}$$

we obtain

$$\frac{ds_1}{d\mu} = -j \left\{ \sqrt{1 - \zeta^2} \frac{d\omega_n}{d\mu} - \frac{\zeta\omega_n}{\sqrt{1-\zeta^2}} \frac{d\zeta}{d\mu} \right\} \tag{5}$$

From Equations 2 and 3, we obtain

$$\frac{d\zeta}{d\mu} = \frac{-\beta_\zeta}{4\omega_n^3 C_2 C_4 R_3 R_f} \tag{6}$$

and

$$\frac{d\omega_n}{d\mu} = \frac{1}{2\omega_n C_2 C_4 R_3 R_f} \tag{7}$$

Substituting Equations 6 and 7 into 5, we obtain

$$\frac{ds_1}{d\mu} = \frac{-j}{2\omega_n C_2 C_4 R_3 R_f \sqrt{1 - \zeta^2}} \tag{8}$$

from which

$$\left| S_\mu^{s_1} \right| \triangleq \left| \frac{ds_1}{d\mu/\mu} \right| = \frac{\mu}{2\omega_n C_2 C_4 R_3 R_f \sqrt{1 - \zeta^2}} \tag{9}$$

Suppose, for example, we wish to synthesize a network which will satisfy the following specifications:

(i) The network is to have a second-order low-pass Chebyshev response with 1 dB ripple in the passband.

(ii) The magnitude of the pole-sensitivity function, $S_{\mu}^{p_i}$, is to be less than unity.

(iii) The maximum value that the ratio, r_x, of any two like elements in the network may assume is 10.0.

Normalizing the impedance level of the network by letting $R_1 = 1$, letting $\mu = 100$, and choosing resistance and capacitance ratios as follows

$$\begin{aligned} C_4 &= 3C_2 \\ R_3 &= 3R_1 \end{aligned} \tag{10}$$

we obtain the following results:

Element	Nominal Value	Design Specifications	Realized Values
R_1	1.000	$\omega_n = 1.05$	$\omega_n = 1.05$
C_2	1.509		
R_3	3.000	$\zeta = 0.5227$	$\zeta = 0.5227$
C_4	4.527		
R_f	4.627	$\lvert S_{\mu}^{p_i}\rvert < 1.0$	$\lvert S_{\mu}^{p_i}\rvert = 0.630$
μ	100.000	$0.1 \leq r_x \leq 10.0$	$0.2 \leq r_x \leq 5.0$

To obtain a set of element values which are defined in terms of the relative damping factor, ζ, we procede as follows: We first normalize the impedance level of the network with respect to R_3, say, whereupon we have

$$2\zeta\omega_n = -\frac{1}{C_2}\{1 + \frac{1}{R_1} + \frac{1}{R_f} + \frac{1}{C_4}\} \tag{11}$$

$$\omega_n^2 = \frac{R_f + R_1(1 + \mu)}{C_2C_4R_1R_f} \tag{12}$$

Choosing

$$\begin{aligned} C_4 &= 2C_2 \\ R_1 &= 5/3\ R_3 \\ R_f &= 1/3\ R_3 \end{aligned} \tag{13}$$

we obtain the following results

Element	Nominal Value
R_1	1.667
C_2	$2.55/\zeta\omega_n$
R_3	1.000
C_4	$5.1/\zeta\omega_n$
R_f	0.333
μ	$4.335/\zeta^2 - 1.20$

APPENDIX "B"

DESIGN OF A TENTH-ORDER BUTTERWORTH LOW-PASS RC-ACTIVE FILTER

Let it be desired to synthesize a tenth-order Butterworth low-pass filter by means of a cascade of five second-order sections. The first step in the design procedure is to obtain the pole-zero optimum tolerance set, δX_{pz}, which is given in Table B1.

Pole-pair Number	Coordinates in the s-plane	Variable parameter	Nominal value	Normalized optimum tolerance (%)
1.	-0.1564 ± j0.9877	$\omega_n(1)$	1.0000	0.2107
		$\zeta(1)$	0.1564	1.7630
2.	-0.4540 ± j0.8910	$\omega_n(2)$	1.0000	0.3230
		$\zeta(2)$	0.4540	1.2180
3.	-0.7071 ± j0.7071	$\omega_n(3)$	1.0000	0.3790
		$\zeta(3)$	0.7071	1.0790
4.	-0.8910 ± j0.4540	$\omega_n(4)$	1.0000	0.4096
		$\zeta(4)$	0.8910	1.0220
5.	-0.9877 ± j0.1564	$\omega_n(5)$	1.0000	0.4235
		$\zeta(5)$	0.9877	1.0000

Table B1

On the basis of the relative sensitivity performance of the six RC-active networks considered in Chapter VII, and on account of the minimal number of components involved, and the fact that no isolation is needed between stages, let us choose the network of Figure 7.11 for each sub-section of the filter. The next step in the procedure is to find an optimum nominal set and corresponding optimum tolerance set for each sub-section of the filter. These sets have been obtained and are listed in Table B2, where a non-optimum set of nominal values is also included.

The elements of each sub-section were next allowed to vary randomly between the pertinent optimum tolerance limits, and the resulting changes in the parameters ζ_i and ω_{n_i} were computed. The standard deviation in each case was determined. The elemental optimum tolerance sets for each section, δX_{o_i}, were then scaled by a factor such that no standard deviation exceeded the pertinent pole-zero optimum tolerance (Table B1). The overall elemental optimum tolerance set, δX_o, was then scaled so that the smallest tolerance limit was acceptable; in our example, this limit was assigned the value of 1%. As for the upper tolerance limit, it must be small enough to justify a first-order sensitivity analysis; in our case, an upper tolerance limit of 20% was adopted. The resulting tolerance set is given in Table B3.

	Element	Pole-Pair No. 1	2	3	4	5	
(a)	R_1	10.000	5.000	0.080	0.080	0.080	Non-optimized version
	C_2	4.000	1.990	16.000	16.000	16.000	
	R_3	6.000	2.981	2.400	2.444	2.400	
	C_4	8.000	3.991	8.000	8.000	8.000	
	R_f	1.109	0.906	0.1127	0.0677	0.056	
	μ	211.900	20.256	32.209	18.963	15.495	
(b)	R_1	10.048	5.041	88.250	60.150	50.292	Optimized Version
	C_2	2.263	1.351	16.408	16.264	16.216	
	R_3	2.556	1.369	0.1834	0.1434	0.1271	
	C_4	6.662	3.323	7.575	7.546	7.575	
	R_f	11.863	734.500	0.1686	0.1438	0.1368	
	μ	455.000	4370	2.943	1.527	1.082	
(c)	R_1	26.224	10.011	2085	1470	1244	Optimum tolerance sets
	C_2	1.033	1.208	1.218	1.294	1.330	
	R_3	1.032	1.218	1.348	1.513	1.612	
	C_4	1.009	1.070	1.229	1.326	1.382	
	R_f	1.157	1.554	1.670	1.882	2.007	
	μ	1.000	1.000	1.000	1.000	1.000	

Table B2

(a) Nominal element values for non-optimized version of filter
(b) Nominal element values for optimized version of filter
(c) Optimum tolerance sets for the optimized version of filter

Element	Pole-Pair No.				
	1	2	3	4	5
R_1	20.00	11.02	20.00	20.00	20.00
C_2	1.03	1.33	1.34	1.43	1.47
R_3	1.03	1.34	1.49	1.67	1.78
C_4	1.01	1.18	1.36	1.46	1.52
R_f	1.00	1.10	1.10	1.10	1.10

Table B3

Optimum tolerance set with lower and upper limits of 1 and 20 per cent, respectively

REFERENCES

1. Calahan, D.A.: "Sensitivity Minimization in Active-RC Synthesis", I.R.E. Trans., CT-9, pp. 38 - 42, 1962.
2. Sipress, J.M.: "Synthesis and Sensitivity of Active-RC Networks", D.E.E. Dissertations, Polytechnic, Brooklyn, 1960.
3. Orchard, H.J.: "Inductorless Filters", Electronics Letters, 2, p. 224, 1966.
4. Haykim, S.S.: "RC-gyrator Low-pass Filter", Proc. I.E.E., 113, pp. 1504 - 1506, 1966.
5. Holmes, W.H., Gruetzmann, S., and Heinlein, W.E.: "High-performance Direct-coupled Gyrators", Electronics Letters, 3, p. 39, 1967.
6. Sheahan, D.F.: "Gyrator-floatation Circuit", Electronics Letters, 3, p. 39, 1967.
7. Weinberg, L.: "Network Analysis and Synthesis", McGraw-Hill, 1962.
8. Haykim, S.S.: "Families of Bandpass Filtering Characteristics", Proc. I.E.E., 113, p. 439, 1966.
9. Bode, H.: "Network Analysis and Feedback Amplifier Design", Van Nostrand, 1945.
10. Mason, S.J.: "Feedback Theory, Some Properties of Signal Flow-Graphs", Proc. I.R.E., 41, pp. 44 - 56, September 1953.
11. Horowitz, I.: "Synthesis of Feedback Systems", Academic Press, New York, 1962.
12. Sandberg, I.W.: "On the Theory of Linear Multiloop Feedback Systems", B.S.T.J., 42, pp. 355 - 382, March 1963.

13. Goldstein, A.J., and Kuo, F.F.: "Multiparameter Sensitivity", I.R.E. Trans., CT-8, 2, pp. 177 - 178, June 1961.

14. Lee, S.C.: "On Multiparameter Sensitivity", Proc. Third Allerton Conference, pp. 407 - 420, 1965.

15. Blostein, M.L.: "Some Bounds on Sensitivity in RLC Networks", Proc. First Allerton Conference, pp. 488 - 501, November 1963.

16. Blostein, M.L.: "Sensitivity Analysis of Parasitic Effects in Resistance-terminated LC Two-ports", I.E.E.E. Trans., CT-14, pp. 21 - 25, March 1967.

17. Leeds, J.V., Jr., and Ugron, G.I.: "Simplified Multiple Parameter Sensitivity Calculation and Continuously Equivalent Networks", I.E.E.E. Trans., CT-14, pp. 188 - 191, June 1967.

18. Holt, A.G.J., and Fidler, J.K.: "Summed Sensitivity of Network Functions", Electronics Letters, 1968, 4, pp. 85 - 87.

19. Kuh, E.S., and Lau, C.G.: "Sensitivity Invariants of Continuously Equivalent Networks", I.E.E.E. Trans., CT-15, pp. 175 - 177, September 1968.

20. Roska, T.: "Summed Sensitivity Invariants and Their Generation", Electronics Letters, 5, p. 398, 1969.

21. Schmidt, G., and Kasper, R.: "On Minimum Sensitivity Networks", I.E.E.E. Trans., CT-14, pp. 438 - 440, December 1967.

22. Holt, A.G.J., and Fidler, J.K.: "Summed Sensitivity of Active Networks", Electronics Letters, 4, p. 385, 1968.

23. Holt, A.G.J., and Lee, M.R.: "Summed Sensitivity of Active-RC Networks", Electronics Letters, 4, pp. 298 - 299, 1968.

24. Kumpel, Z.: "Root-sensitivity Invariants", Electronics Letters, 4, pp. 598 - 599, 1968.

25. Huang, R.Y.: "The Sensitivity of the Poles of a Closed-loop System", Trans. A.I.E.E. (Applic. and Ind.), pp. 182 - 187, September 1958.

26. Schoeffler, J.D.: "Synthesis of Minimum Sensitivity Networks", I.E.E.E. Trans., CT-14, pp. 271 - 276, December 1967.

27. Holt, A.G.J., and Fidler, J.K.: "Optimally Sensitive Networks", Electronics Letters, 4, pp. 176 - 178, 1968.

28. Truxal, J.G.: "Automatic Feedback Control System Synthesis", McGraw-Hill, New York, 1955.

29. Lynch, W.A.: "A Formulation of the Sensitivity Function", I.R.E. Trans., CT-4, p. 289, September 1957.

30. Parker, S.R., Peskin, E., and Chirlian, P.M.: "Application of a Bi-linear Theorem to Network Sensitivity", I.R.E. Trans., CT-12, September 1965, pp. 448 - 450.

31. Sorensen, E.V.: "General Relations Governing Exact Sensitivity of Linear Networks", Proc. I.E.E., 114, pp. 1209 - 1212, September 1967.

32. Leeds, J.V., Jr.: "Transient and Steady-state Sensitivity Analysis", I.E.E.E. Trans., CT-13, pp. 288 - 289, September 1966.

33. Director, S.W., and Rohrer, R.A.: "Automated Network Design, the Frequency Domain Case", I.E.E.E. Trans., CT-16, pp. 330 - 337, August 1969.

34. Director, S.W., and Rohrer, R.A., "The Generalized Adjoint Network and Network Sensitivities", I.E.E.E. Trans., CT-16, pp. 318 - 323, August 1969.

35. Richards, G.A.: "Second Derivative Sensitivity using the Concept of the Adjoint Network", Electronics Letters, 5, p. 398, August 1969.

36. Director, S.W.: "Increased Efficiency of Network Sensitivity Computations by means of the LU Factorization", I.E.E.E. Midwest Symposium on Circuit Theory, Austin, Texas, III-3-1 to III-3-8, April 1969.

37. Isaacson, E., and Keller, H.B.: "Analysis of Numerical Methods", John Wiley and Sons, New York, pp. 26 - 37.

38. Tinney, W.F., and Walker, J.W.: "Direct Solutions of Sparse Network Equations by Optimially Ordered Triangular Factorization", Proc. I.E.E.E., Vol. 55, pp. 1801 - 1809, November 1967.

39. Neill, T.B.M.: "Sensitivity Analysis in Computer-aided Design of Linear Circuits", Electronics Letters, 4, pp. 316 - 317, 1968.

40. Neill, T.B.M.: "Second-order Sensitivity Analysis of a Linear System", Electronics Letters, 5, p. 211, May 1969.

41. Neill, T.B.M.: "Second-order Sensitivity Analysis of a Non-linear Systems", Electronics Letters, 5, p. 212, May 1969.

42. Goddard, P.J., and Spence, R.: "Efficient Method for Calculation of First- and Second-order Network Sensitivities", Electronics Letters, 5, pp. 351 - 352, August 1969.

43. Neill, T.B.M.: "Comment on Efficient Method for the Calculation of First- and Second-order Network Sensitivities", Electronics Letters, 5, pp. 483 - 484, October 1969.

44. Haykim, S.S., and Butler, W.J.: "Multiparameter Sensitivity Index of Performance for Linear Time-invariant Networks", to be published.

45. Temple, V.A.K., and Butler, W.J.: "Program for Obtaining Exact Sensitivity Functions", Electronics Letters, 6, pp. 58 - 60, February 1970.

46. Haykim, S.S.: "Synthesis of RC-active Filters", McGraw-Hill, 1970.

47. Eveleigh, V.W.: "Adaptive Control and Optimization Techniques", McGraw-Hill, 1967.

48. Rosen, J.B.: "The Gradient Projection Method for Non-linear Programming. Part I. Linear Constraints", J. Soc. Ind. Appl. Math., 8, 1, pp. 181 - 217, March 1960.

49. Rosen, J.B.: "The Gradient Projection Method for Non-linear Programming. Part II. Non-linear Constraints", J. Soc. Ind. Appl. Math., 9, 4, pp. 514 - 532, December 1961.